Reliability Impacts of Plug-in Hybrid Electric Vehicles on Power Systems

A Thesis

Submitted to the College of Graduate Studies and Research

In Partial Fulfillment of the Requirements

For the Degree of Master of Science

In the Department of Electrical and Computer Engineering

University of Saskatchewan

Saskatoon, Saskatchewan

By

Xue Wang

PERMISSON TO USE

I agree that the Library, University of Saskatchewan, may make this thesis freely available for inspection. I further agree that permission for copying of this thesis for scholarly purpose may be granted to the professor or professors who supervised the thesis work recorded herein or, in their absence, by the Head of the Department or the Dean of the College in which the thesis work was done. It is understood that due recognition will be given to me and to the University of Saskatchewan in any use of the material in this thesis. Copying or publication or any other use of this thesis for financial gain without approval by the University of Saskatchewan and my written permission is prohibited.

Request for permission to copy or to make any other use of the material in this thesis in whole or part should be addressed to:

Head of the Department of Electrical and Computer Engineering
57 Campus Drive
University of Saskatchewan
Saskatoon, Saskatchewan S7N 5A9

ABSTRACT

Modern power system aims to provide reliable, economic, as well as environmental friendly power supply to its customers. In the past few decades, power systems are going through considerable changes to both the power consumption side as well as the power generation side. The power system planners are faced with growing challenges in maintaining acceptable level of system reliability as new types of loads and generation introduce increased uncertainty in power system planning and operation.

New types of electric devices or loads are often introduced in the market to provide customers more convenience and energy efficiency of utilizing electric power. Electric Vehicle provides an alternative to conventional transport vehicles that burn petroleum fuel and release harmful greenhouse gas emissions. Plug-in hybrid electric vehicle (PHEV) is a relatively new model of EV with more flexibility, and is considered in this research to assess the impacts of charging behavior on the overall power system reliability. PHEV load is different from other types of electric loads as it introduces high variability and uncertainty, and therefore, requires proper modeling of its special characteristics. Different charging scenarios significantly influence power system reliability. This thesis provides a PHEV modeling methodology that incorporates the uncertainty in charging and driving behaviors using Monte Carlo Simulation (MCS) method.

As PHEV sales are increased in response to environmental support, their impacts to system reliability will also increase. A range of reliability studies are carried out in the IEEE Reliability Test System (IEEE-RTS) to investigate the impacts of PHEV charging on system reliability. The system reliability degrades significantly with increase in PHEV penetration if PHEV owners charge their vehicles as soon as they arrive home from work. This effect can be mitigated by introducing a policy for delayed charging. Access to public charging will increase as PHEV increase in the future. The results show that a policy to manage public charging will be important to maintain power system reliability within acceptable limits. As the growth of PHEV is mainly driven by perceived environmental benefits, this research also explores the

interactions between PHEV load and wind energy, and their combined impact of power system reliability. Based on the analysis of the results from case studies performed on the IEEE-RTS, this research provides valuable input for future power systems that are expected to support more PHEV and renewable energy.

ACKNOWLEDGMENTS

My sincerest gratitude would be expressed to my supervisor, Dr. Rajesh Karki, for his immense knowledge, invaluable guidance, patience, continuous encouragement and support in the process of doing my research and the preparation of this thesis. I also would like to give my sincere appreciation to my co-supervisor Dr. Roy Billinton for his professional insights, consistent support and guidance. I am proud of being their master student and I would never complete this thesis without their help and concern all the time through my research.

I would like to acknowledge Dr. Sherif O. Faried and Dr. Ramakrishna Gokaraju for strengthening my knowledge on electric power systems, which is very helpful for building solid foundation for my research. I am also pleased to thank all the professors from the Department of Electrical and Computer Engineering who supervised my courses. I appreciate the Advisory Committee members.

Financial support provided by Department of Electrical and Computer Engineering in University of Saskatchewan, Mr. George Carter and the Natural Science and Engineering Research Council (NSERC) of Canada is gratefully acknowledged.

DEDICATED TO

MY BELOVED HUSBAND *HANBING LI*

TABLE OF CONTENTS

PERMISSON TO USE ..... **i**

ABSTRACT ..... **ii**

ACKNOWLEDGMENTS ..... **iv**

TABLE OF CONTENTS ..... **vi**

LIST OF TABLES ..... **viii**

LIST OF FIGURES ..... **ix**

LIST OF ABBREVIATIONS ..... **xiii**

1 INTRODUCTION **1**

1.1 POWER SYSTEM RELIABILITY 1

1.2 ELECTRIC VEHICLES IN POWER SYSTEMS 3

1.3 APPLICATION OF WIND ENERGY IN POWER SYSTEMS 4

1.4 PROBLEM STATEMENT AND RESEARCH OBJECTIVE 5

1.5 OVERVIEW OF THE THESIS 8

2 BASIC CONCEPTS IN POWER SYSTEM RELIABILITY EVALUATION **10**

2.1 INTRODUCTION 10

2.2 INTRODUCTION OF THE IEEE-RELIABILITY TEST SYSTEM 11

2.3 ANALYTICAL METHOD 12

2.3.1 THE GENERATION SYSTEM MODEL 13

2.3.2 DEVELOPMENT OF WIND GENERATION MODEL 14

2.3.3 LOAD MODEL AND LOSS OF LOAD INDICES 22

2.4 SOFTWARE USED FOR THE HL-I AND HL-II STUDIES 25

2.5 SUMMARY 26

3 DEVELOPMENT OF PHEV MODEL FOR RELIABILITY ANALYSIS **27**

3.1 INTRODUCTION 27

3.2 INTRODUCTION OF PHEV-30 28

3.3 PHEV Charging Scenarios 30
3.4 Important PHEV Characteristics for Model Development 31
3.4.1 Daily Driving Distance 31
3.4.2 Battery Performance during Driving 32
3.4.3 Battery Performance during Charging 33
3.4.4 Charging Start Time 36
3.5 Individual PHEV Modeling 38
3.6 PHEV Fleet Modeling 40
3.7 System Load Model Modification Incorporating PHEV Load 44
3.8 Summary 46
4 GENERATION SYSTEM RELIABILITY EVALUATION INCORPORATING PHEV 48
4.1 Introduction 48
4.2 Development of the Overall Load Model Incorporating PHEV 48
4.3 Impacts of PHEV Charging Scenarios on System Reliability 55
4.4 Reliability Analysis Considering Controlled PHEV Charging 65
4.4.1 Controlling Charging Start Time 65
4.4.2 Determining Public Charging Percentage for Optimal Reliability Benefit 76
4.5 Summary 79
5 BULK SYSTEM RELIABILITY EVALUATION INCORPORATION PHEV LOAD 80
5.1 Introduction 80
5.2 Reliability Studies on HL-II of PHEV in the IEEE-RTS 80
5.3 Reliability Studies of PHEV and WECS in the IEEE-RTS 97
5.4 Summary 99
6 SUMMARY AND CONCLUSIONS 101
7 REFERENCES 105

LIST OF TABLES

TABLE 2.1: COPT OF A WTG UNIT USING 20 YEARS OF HISTORICAL WIND SPEED DATA FOR SWIFT CURRENT 19

TABLE 2.2: COPT OF A WTG UNIT USING 2000 YEARS OF SIMULATED WIND DATA 20

TABLE 2.3: 5-STATE COPT MODEL OF THE WECS 21

TABLE 3.1: PARAMETERS OF PHEV-30 29

TABLE 4.1: SAMPLE STATES OF THE IEEE-RTS LDC INCORPORATING 25% PHEV PENETRATION (2850 MW IS 1.0 PER UNIT) 53

TABLE 4.2: SAMPLE STATES OF LDC UNDER 25% PHEV PENETRATION (3128 MW IS EQUIVALENT TO 1.0 PER UNIT) 54

TABLE 4.3: SYSTEM LOLE AND LOEE WITH INCREASING PHEV PENETRATION IN THE HOME CHARGING SCENARIO 55

TABLE 4.4: SYSTEM RELIABILITY INDICES FOR "PUBLIC/HOME CHARGING" SCENARIO CONSIDERING VARIABLE PUBLIC CHARGING PERCENTAGES AND PHEV PENETRATION LEVELS 64

TABLE 4.5: SYSTEM RELIABILITY INDICES WITH DIFFERENT HOME CHARGING START TIME 73

TABLE 5.1: DATA OF SIX BUSES IN IEEE-RTS 82

TABLE 5.2: BUS IEAR VALUES AND PRIORITY ORDER IN THE IEEE-RTS 83

LIST OF FIGURES

FIGURE 1.1: POWER SYSTEM HIERARCHICAL LEVELS 2

FIGURE 1.2: GLOBAL CUMULATIVE INSTALLED WIND CAPACITY (1996-2014) [14] 5

FIGURE 2.1: SINGLE LINE DIAGRAM OF THE IEEE-RTS 12

FIGURE 2.2: CONCEPTUAL TASKS IN GENERATION CAPACITY RELIABILITY EVALUATION 13

FIGURE 2.3: HOURLY MEAN WIND SPEED DATA OF 20 YEARS ACTUAL WIND DATA IN SWIFT CURRENT 16

FIGURE 2.4: SIMULATED HOURLY MEAN WIND SPEED DATA OF 2000 YEARS 16

FIGURE 2.5: WTG POWER CURVE 17

FIGURE 2.6: CAPACITY OUTAGE LEVEL FOR A WTG UNIT USING HISTORICAL WIND DATA OF 20 YEARS 19

FIGURE 2.7: CAPACITY OUTAGE LEVEL FOR A WTG UNIT USING SIMULATED WIND DATA OF 2000 YEARS 21

FIGURE 2.8: THE IEEE-RTS CHRONOLOGICAL HOURLY LOADS FOR ONE YEAR 22

FIGURE 2.9: LDC OF IEEE-RTS LOAD MODEL 23

FIGURE 2.10: THE IEEE-RTS DAILY LOAD CURVES WITH THE HIGHEST AND LOWEST ANNUAL LOADS 24

FIGURE 3.1: PROBABILITY DISTRIBUTION OF DAILY DRIVING DISTANCE 32

FIGURE 3.2: BATTERY SOC AS A FUNCTION OF DRIVING DISTANCE 33

FIGURE 3.3: BATTERY SOC DURING THE CHARGING PROCESS 34

FIGURE 3.4: POWER DEMAND OF A PHEV DURING THE CHARGING PROCESS 35

FIGURE 3.5: COMPARISON OF THE POWER DEMAND AND CHARGING TIME OF THE NORMAL AND FAST CHARGING METHODS 36

FIGURE 3.6: PROBABILITY DISTRIBUTION OF CHARGING START TIME FOR HOME CHARGING 37

FIGURE 3.7: INDIVIDUAL PHEV LOAD MODEL DEVELOPMENT FOR ONE CHARGING CYCLE 39

FIGURE 3.8: A SAMPLE RUN OF THE PHEV CHARGING CYCLE METHODOLOGY 42

FIGURE 3.9: PHEV FLEET MODELING PROCEDURE 42

FIGURE 3.10: "HOME CHARGING" SCENARIO DAILY LOAD MODEL OF INDIVIDUAL PHEV AND OF THE ENTIRE FLEET 43

FIGURE 3.11: "PUBLIC/HOME CHARGING" SCENARIO DAILY LOAD MODEL OF INDIVIDUAL PHEV AND OF THE ENTIRE FLEET 44

FIGURE 3.12: SUMMER DAILY LOAD MODELS WITH AND WITHOUT PHEV 45

FIGURE 3.13: WINTER DAILY LOAD MODELS WITH AND WITHOUT PHEV 45

FIGURE 4.1: THE IMPACT OF PHEV PENETRATION ON THE SUMMER DAILY LOAD MODELS 49

FIGURE 4.2: THE IMPACT OF PHEV PENETRATION ON THE WINTER DAILY LOAD MODELS 50
FIGURE 4.3: WINTER LDC WITH VARYING PHEV PENETRATION LEVELS 51
FIGURE 4.4: SUMMER LDC WITH VARYING PHEV PENETRATION LEVELS 51
FIGURE 4.5: SYSTEM ANNUAL LDC WITH VARYING PHEV PENETRATION LEVELS 52
FIGURE 4.6: LOAD MODEL OF 10,000 PHEV IN "PUBLIC/HOME CHARGING" SCENARIO WHEN DIFFERENT PUBLIC CHARGING PERCENTAGE IS APPLIED 56
FIGURE 4.7: 24-HOUR SUMMER LOAD CURVE WITH 20% PHEV PUBLIC CHARGING PERCENTAGE IN DIFFERENT PENETRATION LEVELS 57
FIGURE 4.8: 24-HOUR WINTER LOAD CURVE WITH 20% PHEV PUBLIC CHARGING PERCENTAGE IN DIFFERENT PENETRATION LEVELS 58
FIGURE 4.9: 24-HOUR SUMMER LOAD CURVE WITH 40% PHEV PUBLIC CHARGING PERCENTAGE IN DIFFERENT PENETRATION LEVELS 58
FIGURE 4.10: 24-HOUR WINTER LOAD CURVE WITH 40% PHEV PUBLIC CHARGING PERCENTAGE IN DIFFERENT PENETRATION LEVELS 59
FIGURE 4.11: 24-HOUR SUMMER LOAD CURVE WITH 60% PHEV PUBLIC CHARGING PERCENTAGE IN DIFFERENT PENETRATION LEVELS 59
FIGURE 4.12: 24-HOUR WINTER LOAD CURVE WITH 60% PHEV PUBLIC CHARGING PERCENTAGE IN DIFFERENT PENETRATION LEVELS 60
FIGURE 4.13: 24-HOUR SUMMER LOAD CURVE WITH 80% PHEV PUBLIC CHARGING PERCENTAGE IN DIFFERENT PENETRATION LEVELS 60
FIGURE 4.14: 24-HOUR WINTER LOAD CURVE WITH 80% PHEV PUBLIC CHARGING PERCENTAGE IN DIFFERENT PENETRATION LEVELS 61
FIGURE 4.15: SYSTEM ANNUAL LDC WITH 20% PHEV PUBLIC CHARGING PERCENTAGE IN DIFFERENT PENETRATION LEVELS 62
FIGURE 4.16: SYSTEM ANNUAL LDC WITH 40% PHEV PUBLIC CHARGING PERCENTAGE IN DIFFERENT PENETRATION LEVELS 62
FIGURE 4.17: SYSTEM ANNUAL LDC WITH 60% PHEV PUBLIC CHARGING PERCENTAGE IN DIFFERENT PENETRATION LEVELS 63

FIGURE 4.18: SYSTEM ANNUAL LDC WITH 80% PHEV PUBLIC CHARGING PERCENTAGE IN DIFFERENT PENETRATION LEVELS 63
FIGURE 4.19: LOAD MODEL OF 10,000 PHEV IN "PUBLIC/HOME CHARGING" SCENARIO WITH DIFFERENT "CHARGING START TIME" 66
FIGURE 4.20: 24-HOUR SUMMER LOAD CURVE WHEN HOME CHARGING STARTS AT 19:00 WITH 40% PHEV PUBLIC CHARGING PERCENTAGE IN DIFFERENT PENETRATION LEVELS 67
FIGURE 4.21: 24-HOUR WINTER LOAD CURVE WHEN HOME CHARGING STARTS AT 19:00 WITH 40% PHEV PUBLIC CHARGING PERCENTAGE IN DIFFERENT PENETRATION LEVELS 67
FIGURE 4.22: 24-HOUR SUMMER LOAD CURVE WHEN HOME CHARGING STARTS AT 22:00 WITH 40% PHEV PUBLIC CHARGING PERCENTAGE IN DIFFERENT PENETRATION LEVELS 68
FIGURE 4.23: 24-HOUR WINTER LOAD CURVE WHEN HOME CHARGING STARTS AT 22:00 WITH 40% PHEV PUBLIC CHARGING PERCENTAGE IN DIFFERENT PENETRATION LEVELS 68
FIGURE 4.24: 24-HOUR SUMMER LOAD CURVE WHEN HOME CHARGING STARTS AT 23:00 WITH 40% PHEV PUBLIC CHARGING PERCENTAGE IN DIFFERENT PENETRATION LEVELS 69
FIGURE 4.25: 24-HOUR WINTER LOAD CURVE WHEN HOME CHARGING STARTS AT 23:00 WITH 40% PHEV PUBLIC CHARGING PERCENTAGE IN DIFFERENT PENETRATION LEVELS 69
FIGURE 4.26: 24-HOUR SUMMER LOAD CURVE WHEN HOME CHARGING STARTS AT 00:00 WITH 40% PHEV PUBLIC CHARGING PERCENTAGE IN DIFFERENT PENETRATION LEVELS 70
FIGURE 4.27: 24-HOUR WINTER LOAD CURVE WHEN HOME CHARGING STARTS AT 00:00 WITH 40% PHEV PUBLIC CHARGING PERCENTAGE IN DIFFERENT PENETRATION LEVELS 70
FIGURE 4.28: SYSTEM ANNUAL LDC WHEN HOME CHARGING STARTS AT 19:00 WITH 40% PHEV PUBLIC CHARGING PERCENTAGE IN DIFFERENT PENETRATION LEVELS 71
FIGURE 4.29: SYSTEM ANNUAL LDC WHEN HOME CHARGING STARTS AT 22:00 WITH 40% PHEV PUBLIC CHARGING PERCENTAGE IN DIFFERENT PENETRATION LEVELS 71
FIGURE 4.30: SYSTEM ANNUAL LDC WHEN HOME CHARGING STARTS AT 23:00 WITH 40% PHEV PUBLIC CHARGING PERCENTAGE IN DIFFERENT PENETRATION LEVELS 72
FIGURE 4.31: SYSTEM ANNUAL LDC WHEN HOME CHARGING STARTS AT 00:00 WITH 40% PHEV PUBLIC CHARGING PERCENTAGE IN DIFFERENT PENETRATION LEVELS 72
FIGURE 4.32: SYSTEM LOLE OF DIFFERENT CHARGING START TIME IN DIFFERENT PHEV PENETRATION LEVELS 74

FIGURE 4.33: SYSTEM LOEE OF DIFFERENT CHARGING START TIME IN DIFFERENT PHEV PENETRATION LEVELS 74
FIGURE 4.34: CRM OF SUMMER PERIOD FOR DIFFERENT CHARGING START TIME 75
FIGURE 4.35: CRM OF WINTER PERIOD FOR DIFFERENT CHARGING START TIME 76
FIGURE 4.36: SYSTEM LOLE WHEN DIFFERENT PUBLIC CHARGING PERCENTAGES APPLIED TO DIFFERENT PHEV PENETRATION LEVELS 77
FIGURE 4.37: SYSTEM LOEE WHEN DIFFERENT PUBLIC CHARGING PERCENTAGES APPLIED TO DIFFERENT PHEV PENETRATION LEVELS 78
FIGURE 5.1: SINGLE LINE DIAGRAM OF THE IEEE-RTS HIGHLIGHTING SELECTED BUSES FOR HL-II STUDIES 81
FIGURE 5.2: SYSTEM EDLC WHEN PHEV FLEET IS CONNECTED TO BUS 1 85
FIGURE 5.3: SYSTEM EENS WHEN PHEV FLEET IS CONNECTED TO BUS 1 86
FIGURE 5.4: SYSTEM EDLC WHEN PHEV FLEET IS CONNECTED TO BUS 7 86
FIGURE 5.5: SYSTEM EENS WHEN PHEV FLEET IS CONNECTED TO BUS 7 87
FIGURE 5.6: SYSTEM EDLC WHEN PHEV FLEET IS CONNECTED TO BUS 15 88
FIGURE 5.7: SYSTEM EENS WHEN PHEV FLEET IS CONNECTED TO BUS 15 88
FIGURE 5.8: SYSTEM EDLC WHEN PHEV FLEET IS CONNECTED TO BUS 9 89
FIGURE 5.9: SYSTEM EENS WHEN PHEV FLEET IS CONNECTED TO BUS 9 90
FIGURE 5.10: SYSTEM EDLC WHEN PHEV FLEET IS CONNECTED TO BUS 14 91
FIGURE 5.11: SYSTEM EENS WHEN PHEV FLEET IS CONNECTED TO BUS 14 91
FIGURE 5.12: SYSTEM EDLC WHEN PHEV FLEET IS CONNECTED TO BUS 19 92
FIGURE 5.13: SYSTEM EENS WHEN PHEV FLEET IS CONNECTED TO BUS 19 92
FIGURE 5.14: SYSTEM EDLC WHEN PHEV FLEET IS ADDED TO A PARTICULAR GENERATOR BUS 93
FIGURE 5.15: SYSTEM EDLC WHEN PHEV FLEET IS ADDED TO A PARTICULAR NON-GENERATOR BUS 94
FIGURE 5.16: SYSTEM AND BUS EENS WHEN PHEV FLEET IS CONNECTED TO BUS 9 UNDER THE "H" SCENARIO 95
FIGURE 5.17: SYSTEM AND BUS EENS WHEN PHEV FLEET IS CONNECTED TO BUS 9 UNDER THE "HP" SCENARIO 95
FIGURE 5.18: SYSTEM AND BUS EENS WHEN PHEV FLEET IS CONNECTED TO BUS 9 UNDER THE "HPD" SCENARIO 96
FIGURE 5.19: SYSTEM EDLC WHEN PHEV FLEET AND WECS IS CONNECTED TO BUS 15 98
FIGURE 5.20: SYSTEM EDLC WHEN PHEV FLEET AND WECS IS CONNECTED TO BUS 19 98

LIST OF ABBREVIATIONS

A	Availability
ADVISOR	Advanced Vehicle Simulator
ARMA	Auto-Regressive and Moving Average
COPT	Capacity Outage Probability Table
CRM	Capacity Reserve Margin
DPLVC	Daily Peak Load Variation Curve
EDLC	Expected Duration of Load Curtailment
EENS	Expected Energy Not Supplied
FOR	Forced Outage Rate
hrs	Hours
HL-I	Hierarchical Level-I
HL-II	Hierarchical Level-II
HL-III	Hierarchical Level-III
IEEE	Institute of Electrical and Electronics Engineers
IEEE-RTS	IEEE Reliability Test System
IEAR	Interrupted Energy Assessment Rate
kWh	Kilowatt-hour
LDC	Load Duration Curve
LOLE	Loss of Load Expectation
LOEE	Loss of Energy Expectation
MCS	Monte Carlo Simulation
MECORE	Monte Carlo Simulation and Enumeration Composite System Reliability Evaluation Program
MW	Megawatt
MWh	Megawatt-hours
NHTS	National Household Travel Survey
p.u.	Per Unit

PLC	Probability of Load Curtailment
SIPSREL	Small Isolated Power System Reliability
SOC	State of Charge
U	Unavailability
WECS	Wind Energy Conversion System
WTG	Wind Turbine Generator
yr	Year

1 INTRODUCTION

1.1 Power System Reliability

Modern electric power systems are developed to provide reliable and economic power supply to a wide range of customers with varying requirements. Power outages will lead to severe social and economic effects. The reliability of electric power supply is therefore considered to be an important issue in modern power system planning, design and operation.

System reliability can be improved by increasing spare or redundant capacities in generation and network facilities, which will result in increased associated component cost. Power system evaluation should be routinely conducted to ensure adequacy and acceptable continuity of supply in the event of system failures, load or generation uncertainties and regular maintenance. The level of system reliability should be commensurate with the customer requirements and should be achieved as economically as possible. The proper balance between reliability and economy can lead to difficult managerial decisions in power system planning and operating phases [1]. Power system reliability evaluation should therefore focus on meeting customer requirements of supply continuity in an economical way.

Power system reliability in general includes two aspects: system adequacy and system security. System adequacy is considered to be the existence of sufficient facilities within the power system to satisfy the consumer demand. These facilities include those necessary to generate sufficient energy and the associated transmission and distribution networks required to transport the energy to the actual consumer load points. System security studies deal with the ability of the system to respond to disturbances arising within the system, such as sudden changes in state of generation and transmission facilities [1, 2]. Research work presented in this thesis is restricted to power systems adequacy studies.

An overall power system can be divided into three functional zones of generation, transmission and distribution. Power system reliability evaluation can be carried out at three hierarchical levels that are created by combining the functional zones shown in Fig. 1.1.

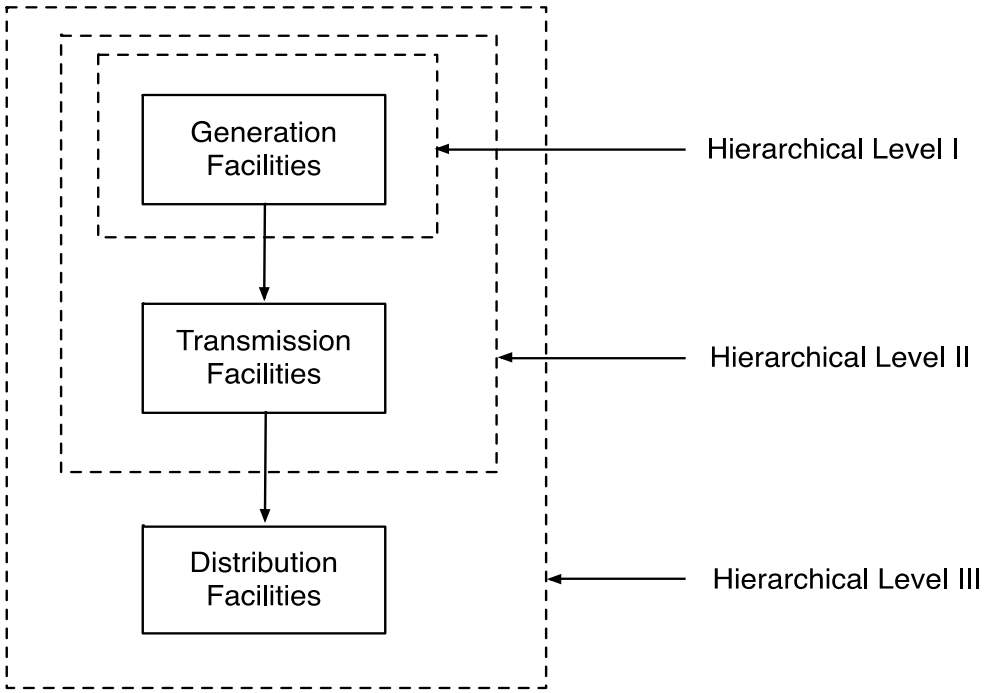

Figure 1.1: Power system hierarchical levels

Reliability assessment at hierarchical level I (HL-I) only considers generation facilities and their ability on a pooled basis to satisfy the pooled system demand. Assessment at hierarchical level II (HL-II) includes both generation and transmission system and its ability to generate and deliver energy to the bulk supply points. Reliability evaluation at HL-III takes the complete system into consideration including distribution and its ability to satisfy the capacity and energy demands of individual consumers [1]. Although evaluation at HL-III is often done to assess past performance, it is not done in predictive reliability assessment due to the complexity of the system at this hierarchical level. The research described in this thesis is conducted at both HL-I and HL-II.

As indicated earlier the primary objective of a power system is to provide reliable and economic electrical energy to its customers. Power systems around the world are experiencing significant changes due to applications of new technologies to address environmental concerns

raised by the public. Rapid growth of wind energy has had substantial impacts on modern power systems. It is expected that more people will use electric vehicles in the near future in response to environmental concerns. The growth of EV will further affect the performance of power systems. These changes caused by expected growth of renewable energy generated and EV energy demand will have profound impact on the reliability of an electric power grid. The impact of these changes in modern and future power systems is included in reliability evaluation presented in this thesis.

1.2 Electric Vehicles in Power Systems

Electric vehicles provide a means of transportation that utilizes electric energy, and could utilize batteries to store electric energy that can be generated from sustainable energy sources, such as wind and photovoltaic. This provides an alternative to conventional transport vehicles that burn petroleum fuel and release harmful greenhouse gas emissions. Electric vehicles can significantly reduce greenhouse gas emissions in the transport sector that are believed to contribute to global warming [3]. There are different types of electric vehicles, such as hybrid electric vehicle (HEV), battery electric vehicle (BEV) and plug-in hybrid electric vehicle (PHEV). The PHEV is a potentially significant technology for reducing vehicle emissions and reliance on petroleum for transportation [4]. It takes the concept of HEV a step further with a larger battery and isn't dependent on electric outlets completely like BEV. Among all the other electric vehicle alternatives, PHEV has received increasing attention in the transportation industry as the technology that can considerably lower emissions and oil dependency. Moreover, the fuel-switching capability in PHEV provides increased flexibility on driving range and economic electric propulsion [5]. A PHEV can store sufficient energy in its battery for daily commute and recharge the battery from the electric grid. It can use internal combustion engines when the battery energy is depleted, and therefore increase the near-term marketability of PHEV compared to other types of electric vehicles [6].

Many countries have plans to substantially increase the number of PHEV on the road by the next decade [7] [8]. The advancement in PHEV technology has gradually established these

vehicles as affordable and efficient option capable of competing with traditional internal combustion engine vehicles. There is ongoing research [9] [10] in new types of energy storage technology, which provide increased compatibility with PHEV. Many researchers in academia and electric vehicle industry have focused on improving efficiency and reliability of the PHEV technology. An equally important area is to develop methodology to evaluate the efficiency and reliability of the overall energy system that generates and delivers energy to the electric transportation system. There is a need to develop appropriate evaluation models that recognize PHEV behavior, the power system to which the PHEV are connected, and the interaction between the two PHEV and system models.

1.3 Application of Wind Energy in Power Systems

In recent years, enhanced global environmental concerns and uncertainty in the cost of conventional energy derived from fossil and nuclear fuels have created an increased interest in the development and utilization of renewable energy [11]. Enormous effort has been put on the development and application of green energy sources in many countries. Wind energy is currently one of the fastest growing energy sources and has the potential to be a major power source in future power systems. This source of energy technology and its application have undergone significant research and development over the past decade. As a result, many modern power systems include a significant portion of power generation from wind energy sources [12]. Figure 1.2 shows the global cumulative installed wind capacity from the year 1996 to 2014. The wind capacity has increased rapidly from 6.1 GW in 1996 to 365.4 GW in 2014. It can be clearly observed from this figure that global wind capacity has been steadily growing in last two decades, and is also increasing at an impressive rate in recent years. This indicates that wind power installations are expected to grow substantially in the next decade to produce clean energy in power systems. Improvements in wind generation technologies will continue to encourage the use of wind energy in both grid-connected and stand-alone systems. Wind energy will likely become economically competitive with other conventional sources in the near future [3].

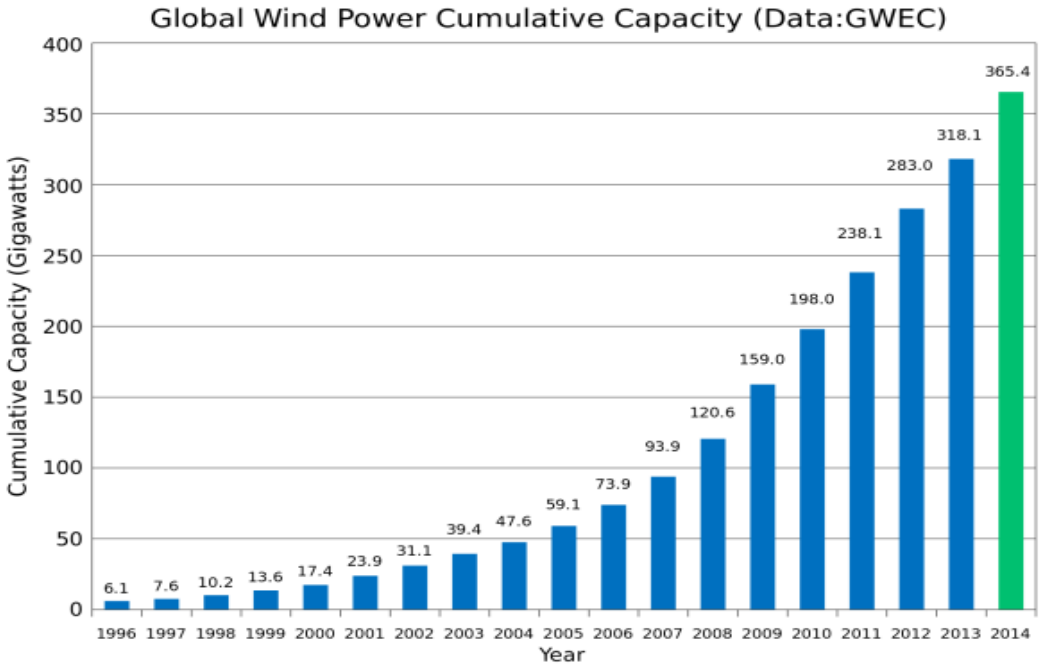

Figure 1.2: Global cumulative installed wind capacity (1996-2014) [13]

A wind turbine generator (WTG) converts wind energy into electric energy. Wind energy is a type of highly variable, site specific and terrain specific energy source [14]. Due to these natural characteristics, the operation of WTG is remarkably different than conventional electric energy sources. The output power of a WTG can randomly vary between zero and its rated capacity value. The variation and uncertainty of the power output could cause significant challenges for power system engineers to plan and operate the system to continuously meet system demand with an acceptable level of reliability [14]. As the penetration of wind energy increases significantly in power systems, it will be increasingly important to evaluate system reliability incorporating various system factors in modern electric power systems.

1.4 Problem Statement and Research Objective

Rapid development of electric vehicles brings new changes to the load profile of power systems. Power system reliability is very sensitive to changing load levels and its characteristics. As the number of electric vehicles connected to power systems increases, the effect on load profile will greatly influence system reliability. On the other hand, rapid growth

of renewable energy sources such as wind power brings considerable changes in the generation side of a power system. The uncertainty and variability of renewable power output can cause challenges in maintaining system reliability. Therefore, it is important to study the impacts of the changes in power systems from both the load and generation sides on the system reliability.

PHEV is a new type of transportation that takes energy from a power system to provide electric propulsion energy to the vehicle. From this perspective, PHEV can be considered as a part of the power system load. The characteristic of a PHEV however depends on the customer's preference. There are many uncertainties associated with charging voltages, modes, locations, driving time and distance that create challenges in appropriately modeling the PHEV for reliability evaluation. Moreover, the rapid development of battery technology and vehicle control methodologies continuously improve performances of PHEV and make it possible to use PHEV in a more intelligent and energy efficient way. This also brings challenges to power systems planning and operation when accommodating large number of PHEV that need to be appropriately modeled and integrated with the overall power system model. Complex evaluation models are not readily accepted in the real world. Therefore, it is important to develop a relatively simple and reasonably accurate model of PHEV suitable for power system reliability evaluation.

The load profile of PHEV is different from other conventional load types, and its unique characteristics should be included in the modeling process. On the other hand, the variation in charging and driving behaviors between different PHEV will also influence the overall impacts on system reliability. Different potential charging scenario should also be taken into account when developing the PHEV model. The impact of PHEV on system reliability is not significant in current power systems that have only a small penetration of electric vehicles. The system reliability, however, will be greatly affected when there are large number of vehicles injected to power systems as expected in the next decade. Therefore, in order to meet system demand with an acceptable level of reliability, PHEV impacts on power systems need to be evaluated incorporating different behavioral perspectives and characteristics of PHEV. It will be necessary to plan and implement suitable policies and remedial measures if PHEV cause

highly adverse impacts on system reliability. It is important to carry out investigative reliability studies to develop suitable policies and control methodologies to maintain acceptable system reliability.

As previously mentioned, PHEV integration can largely modify the system load characteristics, whereas, the injection of wind power can significantly change the generation characteristics of a power system. As the growth of both the PHEV and wind energy is expected to increase in the near future, it will be important to analyze the impact of both technologies on the overall system reliability. Wind energy is highly variable and uncertain depending on the wind characteristics at a geographic site. Potential interactions between wind power and PHEV deployment need to be investigated to determine optimum use of intermittent wind power for maximum benefits of power systems. It is possible to use WTG to reduce adverse effects of PHEV charging when PHEV load is injected at different load points. The reliability implications of the coordination between PHEV and wind energy should be evaluated.

The research carried out in this thesis has the following objectives to address some of the problems noted above:

- To develop a reliability model for PHEV.

  The PHEV reliability model is to be developed to recognize its impact on the power system reliability influenced by the time and amount of electric energy consumed from the power system during its charging behavior. Therefore, the model is greatly affected by driving behavior, charging mode, time, and scenario. The objective is to provide a methodology to develop individual PHEV model considering various PHEV characteristics. The individual PHEV models will be aggregated using a probabilistic technique to develop a relatively simple and reasonable accurate PHEV fleet model suitable for power system reliability evaluation.

- To modify the power system reliability model incorporating PHEV.

The next objective of the research work is to develop an appropriate reliability model of a power system by modifying the system load model incorporating the PHEV models developed in the previous stage considering different PHEV penetration levels. A methodology will be developed that is capable of incorporating the impacts of different PHEV characteristics in the modified power system load model.

- To evaluate the impacts of different PHEV characteristics on power system reliability.

  Another objective of this research is to carry out appropriate case studies to assess the impacts of various PHEV charging and driving behaviors on system reliability. Studies will also be conducted to determine suitable policies and remedial measures to maintain acceptable system reliability when PHEV causes adverse reliability impacts.

- To evaluate the impacts of PHEV and wind energy on bulk power system reliability.

  The objective of the research is also to develop appropriate models to assess the impacts of PHEV and wind energy on the bulk system reliability. Different scenarios of PHEV and wind energy sources connected to various network locations are taken into account to determine appropriate use of wind power and PHEV for maximum reliability benefits of power systems.

1.5 Overview of the thesis

This thesis is organized into six chapters:

Chapter 1 introduces basic concepts regarding power system reliability. Electric vehicle is described as a new type of system load. Wind energy that is widely incorporated in modern power system is also introduced in this chapter. It also outlines the problems and research objectives when incorporating PHEV and wind energy in power systems. The scope of this thesis is also described.

Chapter 2 provides basic concepts and test system related to power system reliability evaluation. Two types of assessment methods are introduced and relevant reliability indices are

presented. Different software programs are used in the analysis at HL-I and HL-II and they are briefly introduced in this chapter. The modeling method of WTG is also introduced in this chapter.

Chapter 3 proposes the development of a reliability model of PHEV and a methodology to evaluate the reliability of a power system considering important PHEV characteristics and charging scenarios. The key parameters are identified and utilized to create the individual PHEV model, which is then combined with other PHEV units to create a model for an entire PHEV fleet that consists of a number of PHEV with different charging and driving behaviors.

Chapter 4 presents HL-I studies to illustrate the impact of PHEV fleet on the power system reliability. The methods of augmenting system reliability through controlled PHEV charging are presented based on the reliability indices obtained in various case studies.

Chapter 5 investigates the interaction between wind energy and PHEV in a test system. System reliability is evaluated at the HL-II level and the results are compared with those obtained from studies at HL-I. The presented studies provide a broader perspective of PHEV impacts on power systems reliability. PHEV charging and wind power deployment are also discussed in detail through the analysis of reliability indices under different charging scenarios and locations. Different penetration levels of PHEV are considered in this process.

Chapter 6 summarizes the research work presented in this thesis and highlights the conclusions.

2 BASIC CONCEPTS IN POWER SYSTEM RELIABILITY EVALUATION

2.1 Introduction

Probabilistic techniques are widely used in reliability evaluation to recognize stochastic nature of system behavior. Quantitative power system reliability is usually expressed in the form of indices that can be used to reflect system capability and adequacy to meet the system load. When renewable energy and electric vehicle are considered in a power system, the impacts of these new types of generation and load on system reliability can be quantified using appropriate reliability indices. Probabilistic evaluation can be carried out for reliability analysis through analytical techniques and simulation methods as two general approaches. They both have advantages and disadvantages, because of which they can be complementary in system analysis.

Analytical techniques assess system adequacy by building analytical models and evaluating adequacy indices from these models using mathematical solutions. The analytical approach can provide results in relatively short calculation time. Analytical techniques are widely used in HL-I and HL-II studies. Monte Carlo Simulation (MCS) methods are more flexible than analytical methods for evaluating systems with complex operating conditions [15]. In this thesis, both the analytical technique and MCS method are described and used in reliability analysis.

Power system reliability studies are often carried out to obtain results with satisfactory accuracy and speed using software tools. There are different types of software that have been developed using either analytical techniques or simulation methods for system reliability evaluation. SIPSREL and MECORE are the two reliability analysis tools used in my research, which were both developed by reliability research group at the University of Saskatchewan. MECORE was later further developed by BC Hydro.

This chapter describes a test system that is widely used for reliability evaluation research. The principles of analytical method and MCS method used in reliability evaluation are explained. The most widely used probabilistic indices for reliability evaluation are introduced. The methodology used for wind speed modeling is also provided in this chapter.

2.2 Introduction of the IEEE-Reliability Test System

The test system used in this thesis is the IEEE Reliability Test System (IEEE-RTS). It was developed by an IEEE Task Force to provide a practical representative bulk power system for research and comparative study purposes. The generating system contains 32 generators with capacities ranging from 12 to 400 MW. The transmission system has 24 buses, which include 10 generating buses, 10 load buses, and 4 connection buses, connected by 33 lines and 5 autotransformers at two voltage levels: 138 kV and 230 kV. The total installed capacity of the IEEE-RTS is 3405 MW and the system peak load is 2850 MW [16]. The single line diagram of IEEE-RTS is shown in Fig. 2.1.

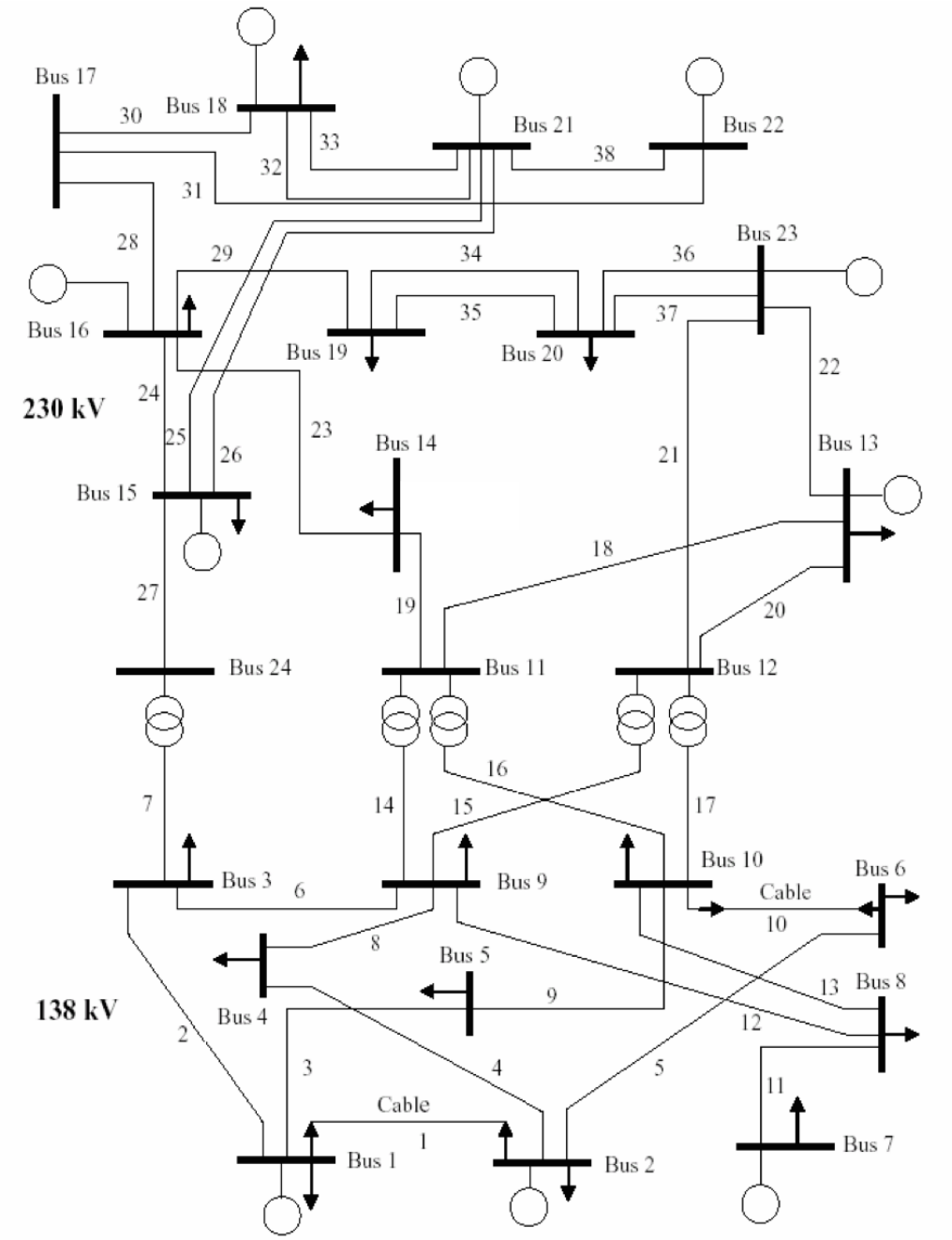

Figure 2.1: Single line diagram of the IEEE-RTS [16]

2.3 Analytical Method

As noted previously, analytical techniques represent the system by analytical models and evaluate the system risk indices from these models using mathematical solutions. Analytical method can be used to obtain expected value of probabilistic indices in relatively short calculation time. However, it usually requires some assumptions to simplify the solutions. This

is particularly the case when complex systems and operating procedures have to be modeled [16]. The resulting analysis may therefore lose some of its significance if adequate considerations are not incorporated in the analytical model of the system. An analytical method is applied in HL-I studies described in this thesis.

The system modeling approach in an HL-I analysis is shown in Fig. 2.2. The generating model and the load model are combined to produce the risk model. The risk indices obtained are the overall system adequacy indices, and do not include transmission constraints in the evaluation [16].

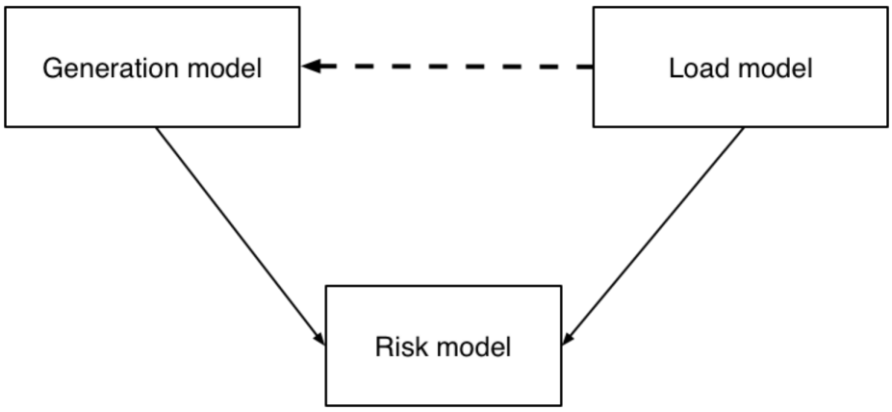

Figure 2.2: Conceptual tasks in generation capacity reliability evaluation

2.3.1 The Generation System Model

The probability of a generating unit being in an outage state is an important parameter in modeling a conventional generation unit. The probability of a generating unit being in a forced outage rate is called the forced outage rate (FOR) or the unavailability (U) of the generation unit. Reciprocally, the probability of a generating unit not being in an outage state is called the availability (A) of the generating unit. The unavailability and availability of a generating unit can be calculated using Equation (2.1) and (2.2) respectively.

$$Unavilability(FOR) = U = \frac{\sum DownTime}{\sum UpTime + \sum DownTime} \tag{2.1}$$

$$Avilability = A = 1 - U = \frac{\sum UpTime}{\sum UpTime + \sum DownTime} \quad (2.2)$$

Each generating unit in the system is represented by either a two-state or a multi-state Markov model. In the two-state model, the generation unit is considered to be either fully available (up) or out of service (down). A multi-state generation model is used to describe a generation unit that can reside in one or more de-rated states. The generation unit can be represented by a discrete probability distribution of multiple capacity states and their corresponding probabilities.

In most analytical techniques, generation model is normally in the form of an array of capacity levels and their associated probabilities. This representation is known as a capacity outage probability table (COPT). The COPT can be constructed using a recursive technique. This technique can be used to build a COPT of a generating system by adding one generating unit to the system at a time [1].

2.3.2 Development of Wind Generation Model

Wind is a highly variable energy source depending on specific terrain and time. An accurate wind generation model for reliability evaluation usually requires a large number of wind power data. However, comprehensive historical wind data is not easy to obtain for most locations of interest. Many researchers have been involved in developing reasonable methods to predict future wind data based on limited wind data records.

Research work on wind generation modeling are reported using both analytical and Monte Carlo simulation methods. The most obvious disadvantage of analytical methods is that the chronological characteristics of wind velocity and their effects on the system behavior cannot be considered. On the other hand, sequential Monte Carlo simulation method can incorporate these considerations and be used to recognize the correlation between the wind speed and the system load and other diurnal and seasonal characteristics of the system. A time series model

has been presented in [13] to predict future wind speed data based on historical wind speeds of a specific site.

The long term wind characteristics of a specific site can be represented by an Auto-Regressive and Moving Average (ARMA) time series model as shown in Equation (2.3).

$$y_t = f_1 y_{t-1} + f_2 y_{t-2} + \ldots + f_n y_{t-n} + a_t - q_1 a_{t-1} - q_2 a_{t-2} - \ldots - q_m a_{t-m} \quad (2.3)$$

where $f_i (i = 1, 2, \ldots, n)$ and $q_j (j = 1, 2, \ldots, m)$ is auto-regressive and moving average parameters of the model, respectively. $\{a_t\}$ is a normal white noise process with zero mean and variance of s_a^2, i.e., $a_t \hat{I} NID(0, s_a^2)$, where NID denotes Normally Independently Distributed. According to Equation (2.3), y_t can be calculated by using randomly generated white noise a_t and previous values of y_{t-i}. Simulated hourly wind speeds SW_t can be obtained by using data series set y_t in Equation (2.4).

$$SW_t = m_t + s_t \times y_t \quad (2.4)$$

Where:

SW_t = Simulated wind speed for Hour t.

m_t = Mean wind speed at Hour t.

s_t = Standard deviation at Hour t.

Wind speed data of a site in Swift Current located in the province of Saskatchewan, Canada were obtained from Environment Canada and used to build ARMA time series models. The hourly wind speed data collected between 1984 and 2003 for the site are used in this research. The ARMA (4, 3) model [17] is presented in Equation (2.5) is the optimal time series model for the Swift Current site.

$$
\begin{aligned}
y_t &= 1.1772 y_{t-1} + 0.1001 y_{t-2} - 0.3572 y_{t-3} + 0.0379 y_{t-4} \\
&+ a_t - 0.5030 a_{t-1} - 0.20924 a_{t-2} + 0.1317 a_{t-3} \\
a_t &\sim NID(0, 0.524760^2)
\end{aligned} \tag{2.5}
$$

Fig. 2.3 shows the chronological hourly mean wind speed data obtained from 20 years of actual data. Fig. 2.4 shows the chronological profile of mean wind speed data from 2000 years of synthetic data obtained from the ARMA (4, 3) model.

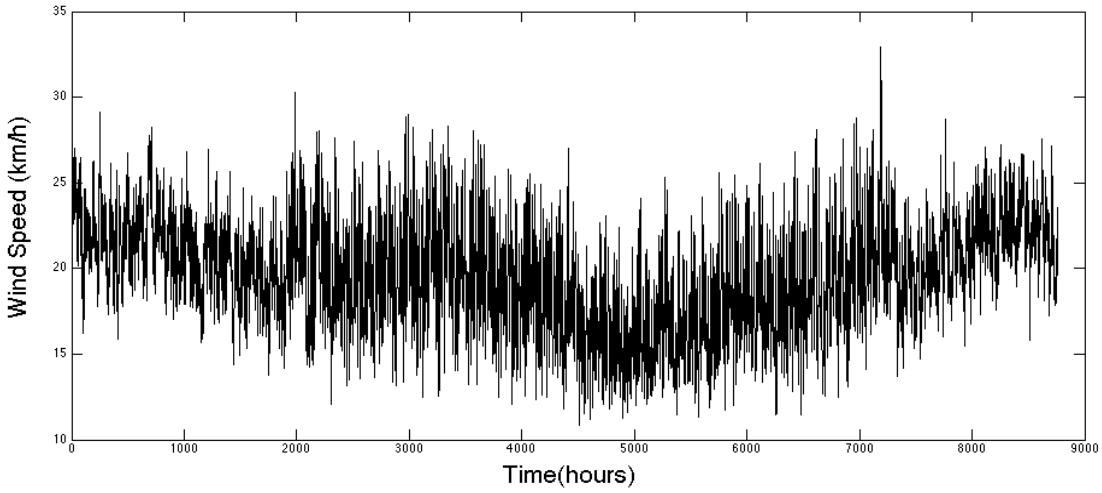

Figure 2.3: Hourly mean wind speed data of 20 years actual wind data in Swift Current

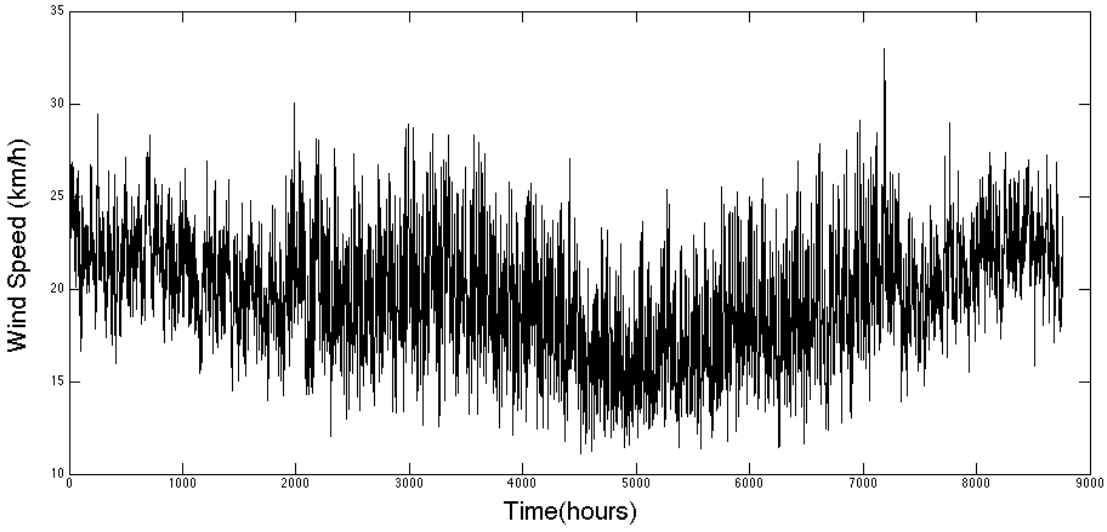

Figure 2.4: Simulated hourly mean wind speed data of 2000 years

The power output of a WTG strongly depends on the wind speed at the specific time and location, and is therefore different from conventional generating units.

Fig. 2.5 shows the relation of the wind power output with the wind speed, and the graph is also known as the "Power Curve". The figure shows that the WTG characteristics are determined by V_{ci} (cut-in wind speed), V_r (rated wind speed), V_{co} (cut-out wind speed) and P_r (rated power output). V_{ci} is the minimum wind speed for a WTG to generate power output, V_{co} is the maximum wind speed that the WTG could be safely operated, and V_r is the minimum wind speed required by the WTG to generate rated capacity. The values of V_{ci}, V_r, V_{co} used in this study are 14.4 km/h, 36 km/h and 80 km/h, respectively [16].

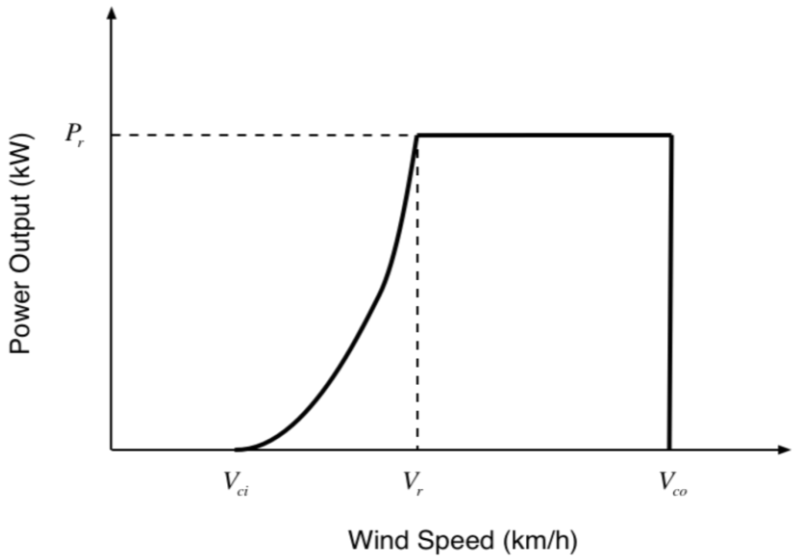

Figure 2.5: WTG power curve

The power curve relation illustrated in Fig. 2.5 can also be expressed by Equation (2.6). The constants A, B and C can be found as functions of V_{ci} and V_r by using the following Equation (2.7) [18].

$$P(SW_t) = \begin{cases} 0 & 0 \le SW_t < V_{ci} \\ (A + B \cdot SW_t + C \cdot SW_t^2) \cdot P_r & V_{ci} \le SW_t < V_r \\ P_r & V_r \le SW_t < V_{co} \\ 0 & SW_t \ge V_{co} \end{cases} \tag{2.6}$$

$$A = \frac{1}{(V_{ci} - V_r)^2}[V_{ci}(V_{ci} + V_r) - 4V_{ci}V_r\left(\frac{V_{ci} + V_r}{2V_r}\right)^3]$$

$$B = \frac{1}{(V_{ci} - V_r)^2}[4(V_{ci} + V_r)\left(\frac{V_{ci} + V_r}{2V_r}\right)^3 - (3V_{ci} + V_r)] \tag{2.7}$$

$$C = \frac{1}{(V_{ci} - V_r)^2}[2 - 4\left(\frac{V_{ci} + V_r}{2V_r}\right)^3]$$

Hourly wind speeds can be converted to power output values by using the WTG power curve. The wind speed model characterized by a discrete probability distribution of wind speeds can therefore be converted to a wind generation model represented by a discrete distribution of wind power states and their corresponding probabilities. This model can be referred to as the COPT of a WTG. Table 2.1 presented the COPT of a WTG unit using 20 years of historical wind speed data of Swift Current and a power curve with the parameters described earlier. The COPT is also graphically illustrated in Fig. 2.6. The capacity on outage is shown as a percent of the rated WTG capacity, and the probability distribution is plotted using an interval width of 5%.

Table 2.1: COPT of a WTG unit using 20 years of historical wind speed data for Swift Current

Capacity Outage (%)	Probability
0	0.0575
2.5	0.0000
7.5	0.0164
12.5	0.0000
17.5	0.0000
22.5	0.0274
27.5	0.0142
32.5	0.0139
37.5	0.0000
42.5	0.0352
47.5	0.0000
52.5	0.0445
57.5	0.0000
62.5	0.0503
67.5	0.0000
72.5	0.0509
77.5	0.0675
82.5	0.0000
87.5	0.1486
92.5	0.0767
97.5	0.0880
100	0.3091

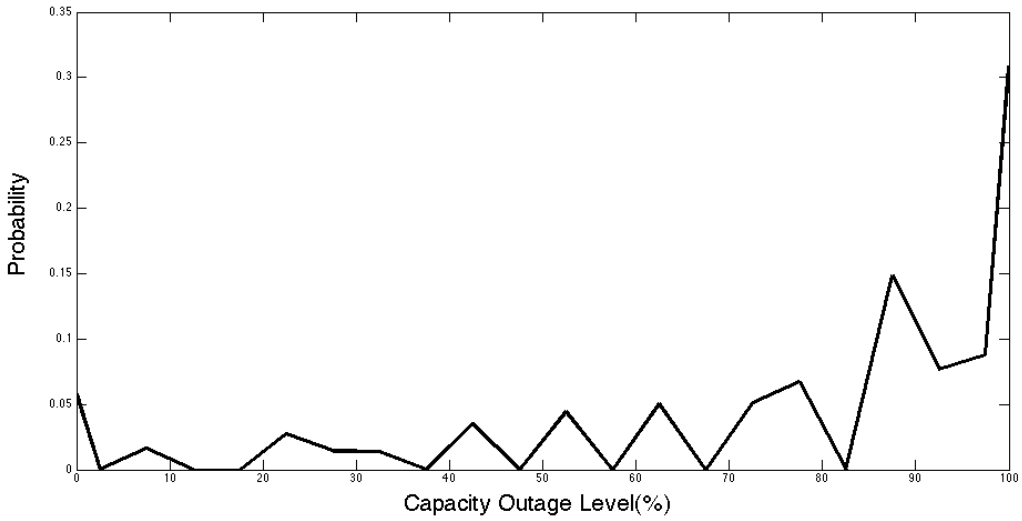

Figure 2.6: Capacity outage level for a WTG unit using historical wind data of 20 years

It can be seen from Table 2.1 and Fig. 2.6 that the COPT of the WTG unit is discontinuous because of insufficient wind speed data. This generation model cannot represent WTG units accurately. Table 2.2 and Fig. 2.7 present COPT of the WTG unit when wind speed data of 2000 simulated years are considered. A large sample of wind data is therefore required to provide a reasonably accurate model for WTG units in reliability evaluation.

Table 2.2: COPT of a WTG unit using 2000 years of simulated wind data

Capacity Outage (%)	Probability
0	0.0552
2.5	0.0068
7.5	0.0076
12.5	0.0087
17.5	0.0098
22.5	0.0112
27.5	0.0127
32.5	0.0145
37.5	0.0164
42.5	0.0188
47.5	0.0215
52.5	0.0246
57.5	0.0282
62.5	0.0322
67.5	0.0372
72.5	0.0430
77.5	0.0498
82.5	0.0579
87.5	0.0680
92.5	0.0809
97.5	0.0989
100	0.2961

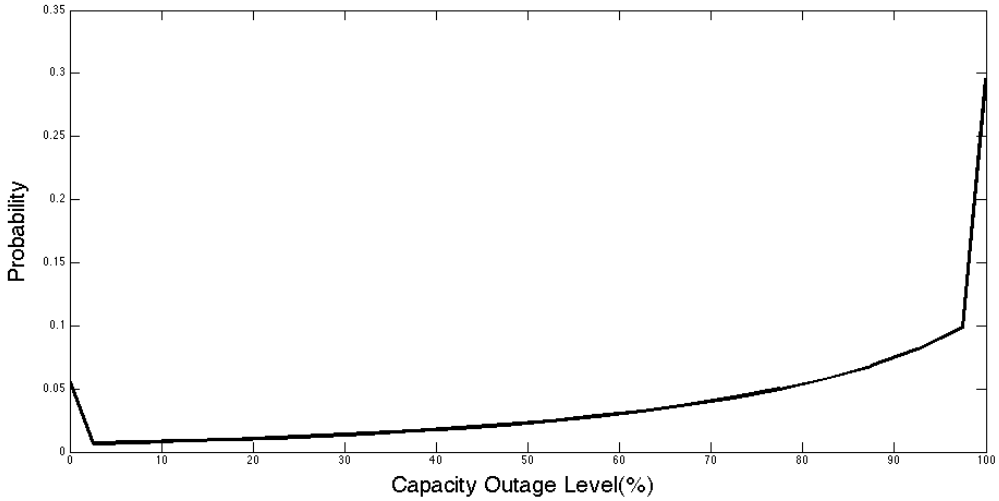

Figure 2.7: Capacity outage level for a WTG unit using simulated wind data of 2000 years

A Wind Energy Conversion System (WECS) is composed by a number of wind turbine generators. A WTG unit can reside in many de-rated states in the course of its operation history [19]. The requirement of a reasonable model is it can be used to simplify the wind model by reducing the number of capacity states [16, 20-21].

Two conclusions from [16] are considered in the studies carried out in this research: (1) The effect of FOR of WTG units can be neglected in WECS reliability evaluation without sacrificing reasonable accuracy, and (2) a 5-state generation model can be used to present a WECS in an acceptable adequacy in practical studies. If the WECS is composed of identical WTG units with zero FOR, it can be represented by the same multi-state model of the WTG unit. Table 2.3 presents the 5-state model of WECS obtained by using an apportioning method. This model is used to modify input file of MECORE software for reliability evaluation in this research.

Table 2.3: 5-state COPT model of the WECS

Capacity Outage (%)	Probability
0	0.07021
25	0.05944
50	0.11688
75	0.24450
100	0.50897

The WECS model presented in this section is used in the studies to access the impact of wind power and PHEV on bulk system reliability, and is presented in Chapter 5. The WECS model is considerably different from generation models of conventional generating units that are dominant in power systems.

2.3.3 Load model and Loss of Load Indices

The generation model of a power system can be convolved with an appropriate load model to produce the system risk indices. There are a number of possible load models that can be used, and therefore there are a number of risk indices that can be produced. The simplest load model and one that is used quite extensively is the daily peak load variation curve (DPLVC) in which each day is represented by its daily peak load and is formed by arranging the individual daily peak loads in descending order. When the individual hourly load values are used and arranged in descending order, the load duration curve (LDC) is created [1].

The hourly chronological load of the IEEE-RTS expressed in per unit of its peak is shown in Fig. 2.8. It can be seen that the annual peak load occurs during the winter season in the test system. The power demand in the winter is high due to the electrical heating load. The LDC of the IEEE-RTS is shown in Fig. 2.9. A LDC is utilized as the system load model in this thesis.

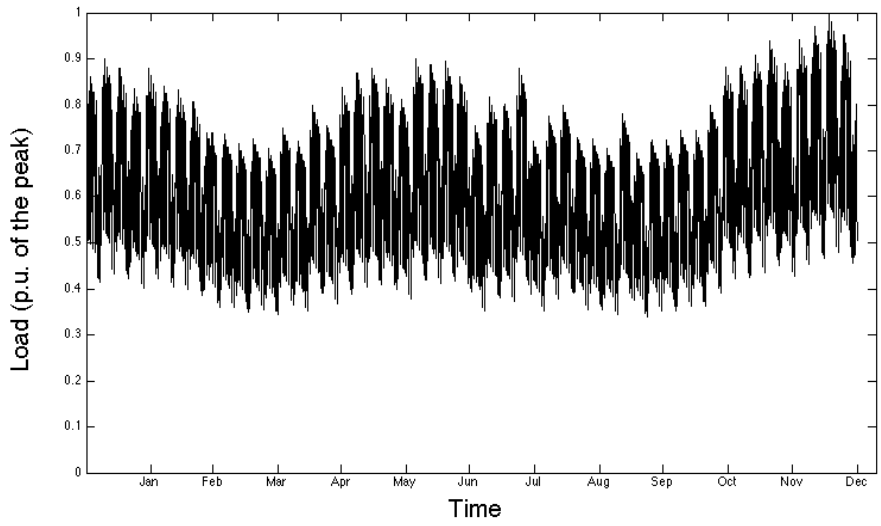

Figure 2.8: The IEEE-RTS chronological hourly loads for one year

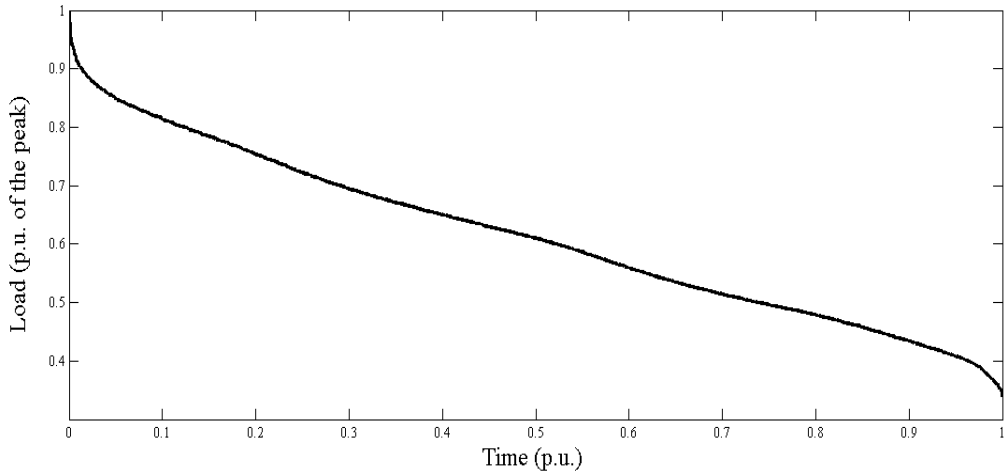

Figure 2.9: LDC of IEEE-RTS load model

The load model of a system is influenced by the amount of energy and charging characteristics of PHEV, when significant number of PHEV depend on the power system. The system load model is therefore modified to incorporate the impact of PHEV, and the details of this methodology are presented in the next chapter. The generation model of a power system is convolved with the system load model in the form of LDC to obtain the system risk indices.

The evaluation is usually done for a period of one year, and the indices are referred to as annual indices. The annual evaluation can be divided into a number of periods to incorporate the impact of seasonality in the risk indices. In the period analysis, the results obtained for each period combined to obtain the annual indices.

Fig. 2.10 shows the 24-hour chronological load for the winter day with the highest annual load and the summer day with the lowest load. The yearly load model of the IEEE-RTS is divided into two seasonal loads in order to assess seasonality effects on the system reliability. It is assumed that summer runs from April to September and contains 4392 hours, winter consists of 4368 hours, from October to March. The two days are respectively from December and September.

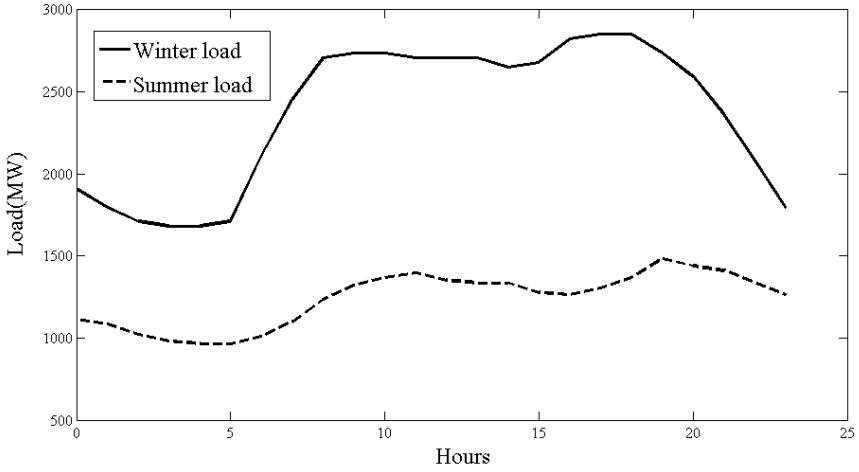

Figure 2.10: The IEEE-RTS daily load curves with the highest and lowest annual loads

The loss of load expectation (LOLE) is the most widely used reliability index in capacity planning which determines the loss of load probability. The loss of energy expectation (LOEE) index quantifies the energy not supplied due to capacity outage, and can be used to assess the cost of unreliability [1]. The product of LOEE and Interrupted Energy Assessment Rate (IEAR) can be used to measure system monetary loss as a function of the energy not supplied. The system LOLE and LOEE can be calculated as expressed in (2.8) and (2.9) respectively.

$$LOLE = \sum_{i=1}^{m} \sum_{k=1}^{n} t_k . p_k \quad hours / year \tag{2.8}$$

$$LOEE = \sum_{i=1}^{m} \sum_{k=1}^{n} E_k . p_k \quad MWh / year \tag{2.9}$$

Where, m is the number of periods in a year considered in the period analysis; n is the number of capacity outage states in the COPT developed for Period i; p_k is the probability of capacity outage in the k^{th} outage state in the COPT; t_k is the number of hours of load curtailment caused by the k^{th} outage state; E_k is the energy curtailment caused by the k^{th} outage state.

Probability of load curtailment (PLC) can be defined in Equation (2.10), where P_i is the probability of system state i and C is the set of all system states associated with load curtailments. The expected duration of load curtailment (EDLC) and expected energy not supplied (EENS) are two commonly used indices in system HL-II analysis. They are defined in Equations (2.11) and (2.12), where C_i is system load curtailment in system state i.

$$PLC = \sum_{i \in C} P_i \tag{2.10}$$

$$EDLC = 8760 \times PLC \quad hours / year \tag{2.11}$$

$$EENS = \sum_{i \in C} 8760 C_i P_i \quad MWh / year \tag{2.12}$$

2.4 Software Used for the HL-I and HL-II Studies

SIPSREL (Small Isolated Power System Reliability) and MECORE are the two reliability analysis tools used in this research, which were both developed at the University of Saskatchewan. The SIPSREL program incorporates analytical techniques for HL-I reliability to evaluate a number of system risk indices, including LOLE and LOEE. The MECORE software is a Monte Carlo based composite generation and transmission system reliability evaluation tool designed to perform reliability and reliability worth assessment of bulk electric power systems. MECORE was initially developed at University of Saskatchewan and subsequently enhanced at BC Hydro [22]. It can be used to assess composite generation and transmission reliability, generation reliability in a composite system, transmission reliability in a composite system, and provides a wide range of reliability indices for the system as well as for the individual load point. It also provides unreliability cost indices, which reflect reliability worth. The indices produced by the program can be used to aid in comparing different planning alternatives from a reliability point of view. MECORE is based on a combination of Monte Carlo simulation (state sampling technique) and enumeration techniques. The state sampling technique is used to simulate system component states and to calculate annualized indices at

the system peak load level. A hybrid method utilizing an enumeration approach for aggregated load states is used to calculate annual indices using an annual load curve. MECORE is designed to handle up to 1000 buses and 2000 branches [22].

2.5 Summary

This chapter describes basic concepts of reliability evaluation on power systems. IEEE-RTS is the test system for reliability analysis in this thesis. The system diagram is firstly introduced. Analytical method is explained by introducing generation model and load model as well as several widely used loss of load indices. Basic theory of developing generation model and load model is introduced. A multi-state wind model is also presented in this chapter. SIPSREL and MECORE as two powerful tools for calculating reliability indices are briefly introduced. They are utilized respectively for HL-I and HL-II analysis. This chapter is composed by basic theory of power system reliability evaluation, which will be carried out in the following chapters when new types of system load and generation are considered.

3 DEVELOPMENT OF PHEV MODEL FOR RELIABILITY ANALYSIS

3.1 Introduction

There is growing environmental concern associated with conventional transport vehicles that burn petroleum fuel and release harmful greenhouse gas emissions. PHEV provides a means of transportation that utilizes sustainable energy since electrical energy stored in PHEV can be generated from renewable energy sources, such as wind and photovoltaic. Many researchers have been involved in the study of various issues associated with PHEV injection in power systems since the first PHEV prototype was built. Existing literatures cover a broad range of PHEV technology research and applications. Reference [23] predicts the potential impacts of PHEV on electricity demand and prices, generation structure, and associated emission levels. The work in [24] emphasizes on power quality and analyzes PHEV impacts on power losses as well as voltage deviations. PHEV impacts on a distribution system are analyzed in [6] using both deterministic and stochastic analytical methods considering PHEV penetration and the charging behaviors. Reference [25] presents PHEV impacts on a distribution system considering fast charging scenario. Reference [26] shows the improvement in power quality by using coordinated charging realized by a smart metering system and also indicates the uncoordinated charging of PHEV decreases the distribution system efficiency. Sustainable energy sources are considered in some literatures related to PHEV. Results of Reference [27] show renewable energy sources can reduce the impacts of charging PHEV on the distribution system in system losses as well as customers' cost. Reference [28] presents a system model with PHEV and renewable energy resources, and analyzes related energy, economic and environmental impacts to power grid. The flexibility in the PHEV characteristics enables them to be charged when needed as long as electric outlet is available. When the number of PHEV connected to a power system is considerable, the resulting change in the energy demand characteristic will adversely affect the overall system reliability. The reliability of a power system will be highly influenced by PHEV characteristics and operation strategies in the near

future since PHEV penetration is expected to significantly increase. There is a definite need for further research in this area.

This chapter is structured as follows. The development of the PHEV reliability model that incorporates the important PHEV characteristics is firstly presented. The individual PHEV model is then combined with other PHEV units to create a model for an entire PHEV fleet that consists of a number of PHEV with different charging and driving behaviors. A sequential Monte Carlo simulation method is used to incorporate the various models while maintaining the chronology of the events and the correlation between the PHEV behavior and load variation. This analytical model considering certain PHEV characteristics and charging scenarios can be used in evaluating the reliability of a power system with PHEV penetration that will be demonstrated in the next chapter.

The commuting data provided by the United States transportation survey indicate that privately owned PHEV account for a large proportion in current market, and a majority of the people choose home to be the charging place at the end of the day. However, vehicles can also be charged in public parking places wherever the power outlet is available. In North America, PHEV models introduced by main automobile companies have two optional charging voltage levels: 120V and 240V, which are also known as the normal charging and fast charging scenarios. The charging duration time at the higher voltage level is much shorter than the time required at the lower voltage level. Different scenarios of charging places and charging voltage levels are considered in this study.

3.2 Introduction of PHEV-30

PHEV is a hybrid electric vehicle in which a gasoline engine and an electric motor are both used for propulsion. The vehicle includes rechargeable battery packs that can be charged as needed through an external electric power source. A fully charged PHEV will initially operate in the “all-electric mode” using the electric energy available in battery packs. The battery state of charge (SOC) is used to indicate the amount of electric energy available in the battery. As the vehicle is operated, battery packs are gradually discharged and the value of battery SOC

declines until it reaches the minimum value about 0.2, which means 20% of the full capacity. When the minimum battery SOC is reached, the vehicle is switched to the "gasoline mode". Then gasoline becomes the main energy source to drive the vehicle, and battery SOC may fluctuate due to regenerative braking. The fuel-switching capability provides further flexibility on the driving range and the charging behavior of PHEV [29].

Lithium-ion batteries are widely used in PHEV and are normally sized to provide enough capacity for short commutes [30]. PHEV-30 is a typical model used by many manufactures. The number 30 refers to 30 miles commute distance capability in the all-electric mode of operation. Several research institutes, such as the Sloan Automotive Laboratory at MIT (U.S.) [31], United States Advanced Battery Consortium and National Renewable Energy Laboratory [32][33] use similar modes. Table 3.1 provides important parameters of PHEV-30, which are extracted from a leading 2014 vehicle manufacture model description [34]. The methodology developed and presented in this chapter is illustrated using the parameters of PHEV-30. Along with the fast development of battery technology and control methodology, PHEV is expected to have longer all-electric range and faster charging options in the near future. The modeling methodology can, however, be similarly applied to other types of PHEV and charging scenarios. The results will obviously depend on the PHEV model parameters.

Table 3.1: Parameters of PHEV-30

Body size	Midsize vehicle
Battery type	Lithium-ion
Battery size (kWh)	8
Full recharge time (120V outlet)	7 hours
Full recharge time (240V outlet)	2.5-3 hours
All-electric range (Miles)	30

3.3 PHEV Charging Scenarios

There are a number of options available to the PHEV owners in deciding the modes and places to recharge the batteries in their vehicles. PHEV charging scenarios can be classified according to different charging places. The phrases, “home charging” and “public/home charging” are used in this thesis to describe the different charging locations. The former scenario refers to the charging behavior when home is the only place for PHEV charging. If the PHEV can also be plugged into the power grid during daytime in public areas, it is termed as “public/home charging”. These choices affect the time of day charging patterns, and therefore impact the charging characteristics that need to be represented in the developed models.

The growing environmental concerns are leading PHEV development towards reducing gasoline and increasing electric energy usage. In order to achieve this goal, vehicle owners will need to utilize battery energy as the primary propulsion source before using gasoline. The PHEV are being primarily designed for gasoline aided electric propulsion energy stored from home charging. The “home charging” characteristics will have a large impact on system reliability as the PHEV load coincides with the evening peak of the daily load profile in residential consumers. This scenario has therefore been primarily considered in the modeling process. In order to consider the impact of daytime charging of PHEV on system adequacy, the “public/home charging” scenario has also been incorporated in the model development. The main contribution to adequacy indices comes from the coincidence of PHEV charging with the daytime peaks, and the effect will be significant in summer peaking systems.

Table 3.1 shows that PHEV-30 can be charged either at 120V or 240V, which are designated as “normal charging” and “fast charging” respectively. It should be noted the charging time is significantly reduced and the charging power is increased when fast charging method is selected. Assumptions are usually made in system modeling based on reasonable practical significance in order to reduce complexity. A reasonable assumption is that “fast charging” is employed during public charging to minimize charging time, and consequently owners will fully charge their vehicles to prolong battery life [26]. Due to these reasons, partial and

multiple public charging is not considered. Normal charging at 120 V is considered for home charging that usually occurs at the end of a day. Because of the relatively short all-electric mileage of PHEV-30, it is highly likely that PHEV subjected to public charging will also need to be recharged at home. The limitation of the model is based on these practical assumptions.

3.4 Important PHEV Characteristics for Model Development

When PHEV are plugged into power system for charging, they act as power system load with specific characteristics when compared with other load forms. The key PHEV characteristics for reliability modeling are described in this section.

3.4.1 Daily Driving Distance

PHEV behavior is determined in general by several factors, such as, transportation habits, charging infrastructure, price incentives and the battery technologies [35]. The daily driving distance of a vehicle is an important parameter that can vary considerably from one day to another, and for different vehicles. Vehicle travel data published in the latest National Household Travel Survey (NHTS) 2009 [36], was analyzed to obtain the probability distribution of the daily driving distance, *D*. A lognormal distribution shown in Fig. 3.1 described by the mathematical equation in (3.1) was obtained using the MATLAB best-fit criterion. A similar lognormal distribution was also obtained in [37] from 2001 NHTS data. The mean value of the daily driving distance data obtained from the survey was calculated to be 54.6 miles. Its lognormal is 4.0, and is the value of the parameter μ_D in (3.1). The standard deviation σ_D parameter of 0.92 was obtained from MATLAB best-fit analysis of the distribution of the survey data.

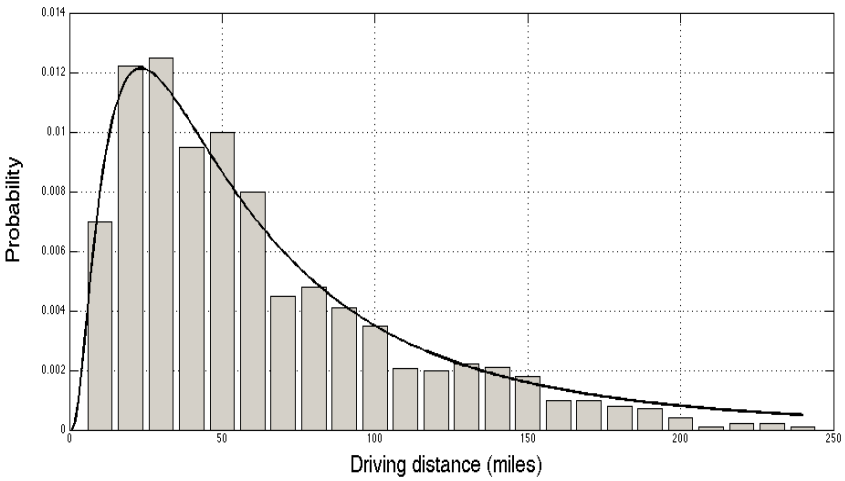

Figure 3.1: Probability distribution of daily driving distance

$$f_D(x) = \frac{1}{x\sigma_D\sqrt{2\pi}} e^{[-(\ln x - \mu_D)^2/2\sigma_D^2]} \tag{3.1}$$

3.4.2 Battery Performance during Driving

For a fully charged PHEV, the battery performance during discharging process can be divided into two distinct periods: the initial "all-electric" driving period, and the "gasoline" driving period. The SOC is another parameter of a PHEV that indicates the amount of electric energy available in the battery at any instant in time. A toolbox called ADVISOR operated in MATLAB/Simulink environment has been used to assess the battery performance during the driving period of a day. Fig. 3.2 shows the battery SOC as a function of the driving distance.

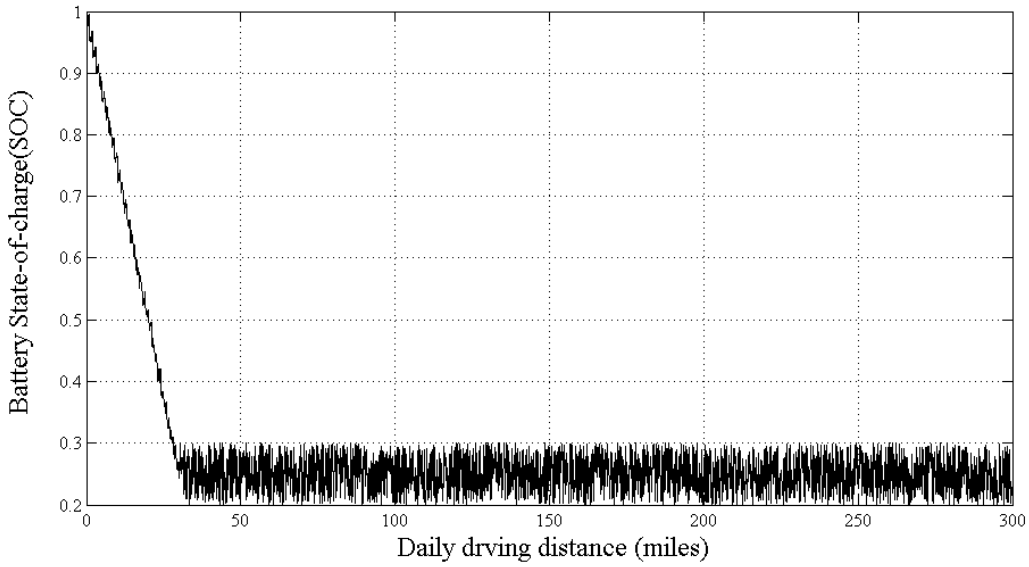

Figure 3.2: Battery SOC as a function of driving distance

Equation (3.2) gives the battery *SOC* during vehicle driving period. The first condition of (3.2) gives the SOC for the "all-electric period", which is battery dependent, and the battery SOC declines almost linearly with the driving distance, *D*. The minimum battery SOC is 0.2, i.e. 20% of the rated capacity. In the case of PHEV-30, the first stage will approximately last for 30 miles. The second condition of (3.2) is for the "gasoline" mode, where the battery SOC fluctuates as it frequently and randomly charges and discharges. The battery charges for short durations due to regenerative braking, which allows restoring energy whenever a PHEV slows down. The battery is discharged to provide energy as the vehicle speeds up again. A uniformly distributed random number *Y* between 0.2 and 0.3 is used to obtain the *SOC* value in the second stage of the driving period.

$$SOC = \begin{cases} \max\{0.2, 1 - 0.0333D\}, D \le X \\ Y, D > X \end{cases} \tag{3.2}$$

3.4.3 Battery Performance during Charging

In order to utilize battery energy as the primary propulsion source to reduce environmental impact of gasoline combustion, the PHEV owners must exploit the opportunity to recharge

their PHEV before the next commute. It has therefore been assumed that the electric power is the primary driving source and the owners will recharge their vehicle battery to full when the battery SOC falls below 0.8 in order to reduce the reliance on gasoline. Due to these concerns and the development trend of PHEV, similar assumptions have also been used by other researchers, such as in [38]. For typical lithium-ion battery, the battery *SOC* increases almost linearly with the charging time as shown in Fig. 3.3.

The PHEV during its charging mode becomes an electric load to the power system that supplies the electric energy. The load profile of a PHEV is characterized by the charging power and duration. Fig. 3.4 shows the power supplied to the battery during the charging process in per unit of the rated charging power. The duration of the PHEV load is the time taken to fully charge the battery, and can be calculated using Fig.3.3 with the knowledge of the initial battery *SOC*. The power demand of PHEV load as a function of the charging time can be calculated using Fig.3.4.

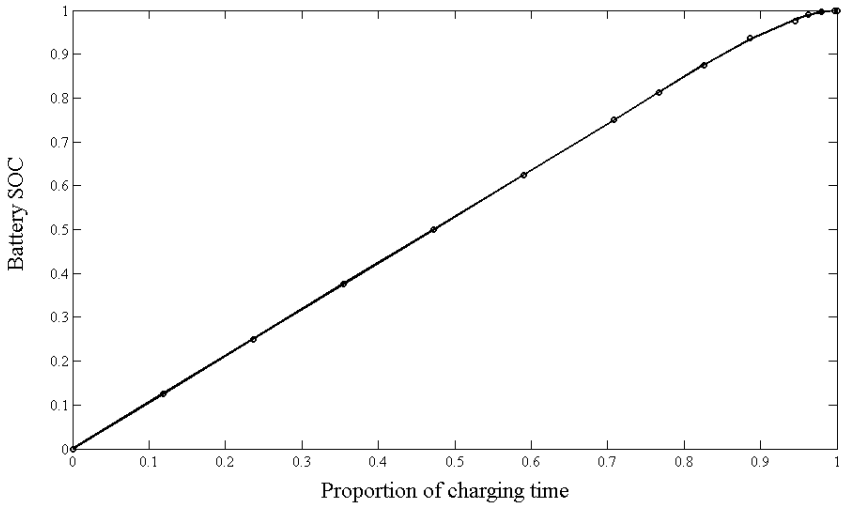

Figure 3.3: Battery SOC during the charging process

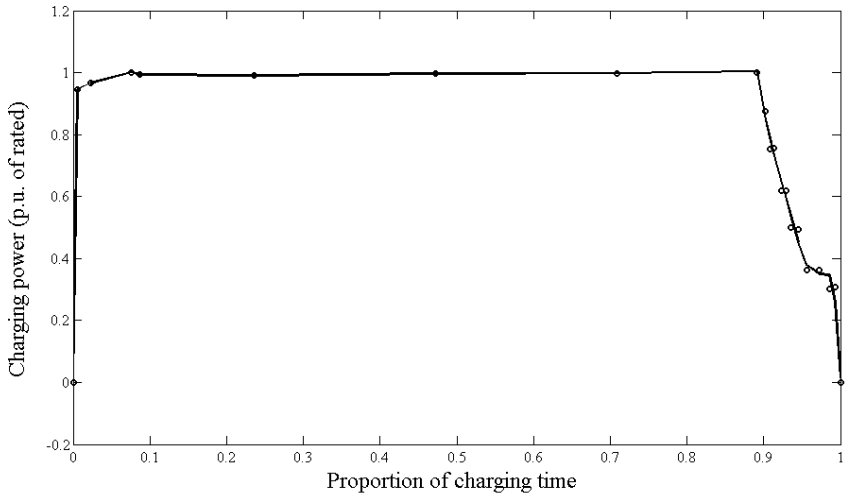

Figure 3.4: Power demand of a PHEV during the charging process

As we can see from the above figures, the x-axis is proportion of the charging time (or the full recharging time), and in Fig. 3.4 the vertical coordinate is proportion of rated charging power. For different charging scenarios the fully charging time and charging power are different. Figures 3.3 and 3.4 can be applied for both normal and fast charging scenarios to obtain the PHEV load profile when relevant rated value is applied.

Fig. 3.5 compares the power demand of a PHEV under the two scenarios: normal charging and fast charging. Fast charging scenario is used for "public charging" and full recharge time is 3 hours. It can be seen that the fast charging method requires less than half the charging time and about three times higher charging power when compared to the normal charging method.

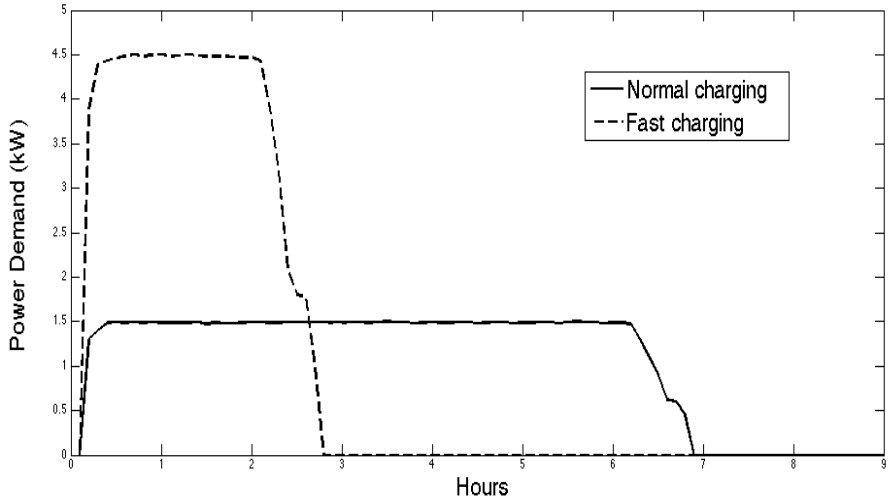

Figure 3.5: Comparison of the power demand and charging time of the normal and fast charging methods

As earlier indicated, the load profile of a PHEV is characterized by the charging power and duration. The duration on the PHEV load is the time taken to fully charge the battery, and can be calculated using Fig. 3.3 with the knowledge of the initial battery SOC prior to the charging process. The power demand of the PHEV load as a function of the charging time under different charging scenarios can be calculated using Fig. 3.5.

3.4.4 Charging Start Time

The charging start time is another important parameter in PHEV load modeling. It will determine the start point of PHEV load profile relative to the entire system load model in time chronology. In a normal situation, a PHEV charging would commence as soon as the vehicle arrives home. In this case, the "last trip ending time" is also the start time of the home charging scenario. Daily travel data collected and reported in NHTS 2009 can be used to obtain the "last trip ending time" for a PHEV for each day. The probability distribution of the "last trip ending time" data is shown in Fig. 3.6. The travel data of "last trip ending time" T_h obtained from the NHTS 2009 survey [39] was analyzed to obtain a mean value μ_{Th} of 17.4 hours, or 5:24 PM, and standard deviation σ_{Th} of 3.3 hours. Using the MATLAB best-fit analysis tool, the data was

described by two normal distributions for ending times before and after (μ_{Th} – 12) hours expressed mathematically by Equation (3.3).

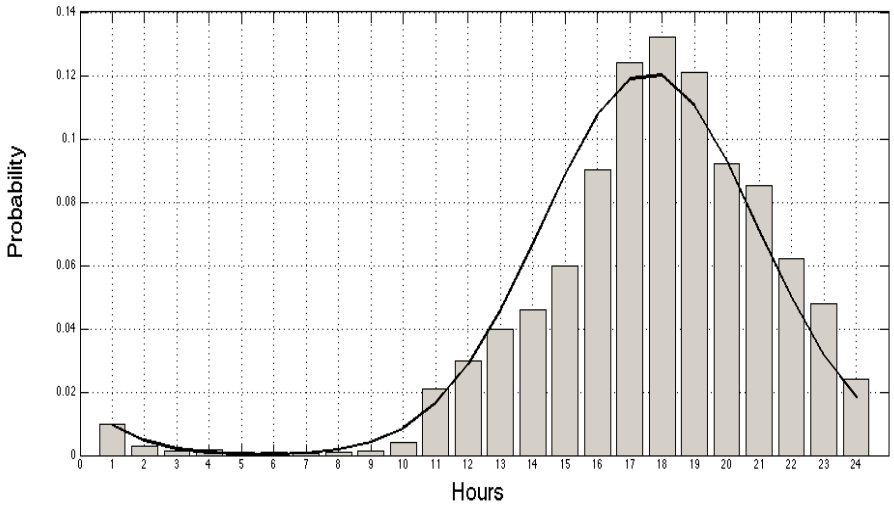

Figure 3.6: Probability distribution of charging start time for home charging

$$f_{T_h}(x) = \begin{cases} \frac{1}{\sigma_{T_h}\sqrt{2\pi}} e^{[-(x-\mu_{T_h})^2/2\sigma_{T_h}^2]}, (\mu_{T_h} - 12) < x \le 24 \\ \frac{1}{\sigma_{T_h}\sqrt{2\pi}} e^{[-(x+24-\mu_{T_h})^2/2\sigma_{T_h}^2]}, 0 < x \le (\mu_{T_h} - 12) \end{cases} \quad (3.3)$$

It is assumed that the public charging of the PHEV will begin as soon as the vehicle reaches the workplace. The load profile of PHEV under the "public/home charging" scenario is separated into two parts: daytime charging and nighttime charging. During the daytime, it is assumed the fast charging facility is utilized for public charging and it will commence as soon as PHEV arrive the workplaces. Similar to previous statement, the travel data of "arriving workplace time" reported in NHTS 2009 can be used to obtain the "public charging start time". Using best-fit criterion, the mathematical expression is shown in Equation (3.4). The travel data of "arriving workplace time" T_p obtained from the NHTS 2009 survey [39] was analyzed using MATLAB best-fit analysis tool to obtain a normal distribution described by the mathematical equation (3.4). In this equation, the mean value μ_{Tp} is 8.5 hours, or 8:30 AM, and standard deviation σ_{Tp} is 2.4 hours.

$$f_{Tp}(x) = \frac{1}{\sigma_{Tp}\sqrt{2\pi}} e^{[-(x-\mu_{Tp})^2/2\sigma_{Tp}^2]} \tag{3.4}$$

The charging power and fully charging time of fast charging scenario showed in Fig. 3.5 are used to build the public charging load profile. The second part of "public/home charging" scenario is the "home charging" process that occurs after the PHEV arrive home at the end of the day. The vehicles needing recharge will start their normal charging scenario as discussed earlier.

3.5 Individual PHEV Modeling

The important PHEV parameters and their characteristics described in the preceding sub-sections are analyzed to develop an appropriate load model for a PHEV in one charging cycle, which refers to the period from the beginning of a discharging process after a full charging behavior to the end of next full charging behavior. The number of charging cycles within a day depends on the frequency of the PHEV charging processes available in a day. If charging at home is the only option that occurs at the end of the day, only be one charging cycle assumed in a day. If a PHEV is charged both in public and at home throughout the day, there are two charging cycles that are considered. Fig. 3.7 presents an algorithm that can be used to obtain the load model of an individual PHEV for one charging cycle.

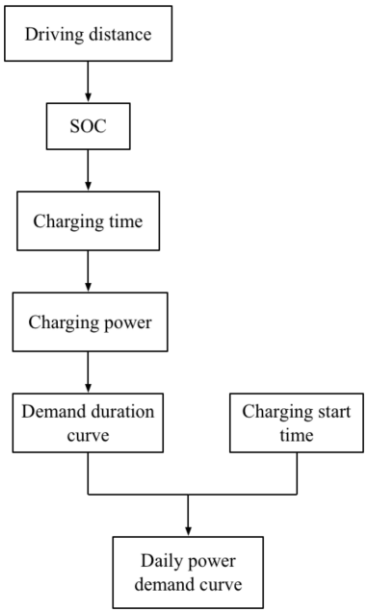

Figure 3.7: Individual PHEV load model development for one charging cycle

Each block in Fig. 3.7 represents a model development for a specific PHEV parameter. As indicated before, it is assumed that a PHEV will be plugged in for charging if the battery SOC is lower than 0.8. The battery SOC can be calculated from the knowledge of the driving distance using the relation in Fig. 3.2 and Equation (3.2). For "home charging" scenario, the daily driving distance is used to estimate battery SOC. But for "public/home charging", the driving distance prior to public charging is assumed to be half of the daily driving distance. The fully charged PHEV at the workplace will then be discharged on the way home. The driving distance prior to home charging is also assumed to be half of the daily driving distance. If the calculated SOC is less than 0.8, the PHEV will be plugged in for charging. It is important to record the charging start time. Charging duration or the time taken to fully recharge the PHEV battery is then calculated depending on the charging scenario. The amount of power supplied to the battery for the charging duration is then determined, which provides the load or demand profile of an individual charging cycle in time chronology. If there is more than one charging cycle within a day for the PHEV, the load profiles are similarly created for each charging cycle, and a time sequential load profile is obtained for the entire day.

3.6 PHEV Fleet Modeling

A PHEV fleet consists of a number of PHEV with different charging and driving behaviors. These parameters are stochastic and interrelated with each other. The models developed for individual PHEV within a fleet need to be aggregated using an appropriate technique to obtain the characteristic model for the overall fleet, which is then be used for reliability evaluation.

A MCS method is used to build the overall model for a PHEV fleet by combining individual PHEV models. Fig. 3.7 shows how the important parameters of an individual PHEV are sequentially modeled to obtain the daily load profile of the PHEV. The sequential modeling is repeated for all the PHEV that exist in the fleet by using the MCS technique to obtain the overall daily load profile for the fleet.

In the beginning of the simulation, a random number Z_i is generated to obtain the daily driving distance D_i of the i^{th} PHEV. The random number Z_i is used to calculate a lognormal value M_i of the driving distance, using Equation (3.5) where the parameters μ_D and σ_D are given in Equation (3.1).

$$M_i = \mu_D + \sigma_D * Z_i \tag{3.5}$$

The calculated value of M_i is then used in Equation (3.6) to obtain the daily driving distance D_i of the i^{th} PHEV.

$$D_i = e^{M_i} \tag{3.6}$$

For "home charging" scenario the value of D_i obtained from Equation (3.6) is then used in Equation (3.2) to calculate the SOC_i of the i^{th} PHEV. The SOC value is then fitted in Fig. 3.3 to determine the time required to fully charge, or the charging time CT_i of the i^{th} PHEV by using full charging time of normal charging scenario.

For "public/home charging" scenario, the driving distance prior to public charging as well as home charging is $0.5*D_i$. Then SOC value can be calculated through Equation (3.2). Time

required of fully home charging is obtained by using the same method as "home charging" scenario. Fully public charging time can be obtained by using 3 hours as rated full recharge time instead of 7 hours in Fig. 3.3.

In order to simulate the home charging start time T_i for the i^{th} PHEV, a uniformly distributed random number U_i between 0 and 1 is first generated. The random number U_i is transformed to a normally distributed variable Y_i using Equation (3.7) to (3.10). The home charging start time T_{hi} is then calculated using Equation (3.11) where μ_{Th} and σ_{Th} are obtained from Equation (3.3). Similarly, public charging start time T_{pi} can be calculated by Equation (3.12), in which μ_{Tp} and σ_{Tp} are from Equation (3.4).

$$Q_i = \begin{cases} 1 - U_i, 0.5 < U_i \le 1.0 \\ U_i, 0 \le U_i \le 0.5 \end{cases} \tag{3.7}$$

$$Y_i = \begin{cases} a_i, 0.5 < U_i < 1.0 \\ 0, U_i = 0.5 \\ -a_i, 0 \le U_i < 0.5 \end{cases} \tag{3.8}$$

Where,

$$b_i = \sqrt{-2\ln Q_i} \tag{3.9}$$

And

$$a_i = b_i - \frac{2.515517 + 0.802853 b_i + 0.010328 b_i^2}{1 + 1.432788 b_i + 0.189269 b_i^2 + 0.001308 b_i^3} \tag{3.10}$$

$$T_{hi} = \mu_{Th} + \sigma_{Th} Y_i \tag{3.11}$$

$$T_{pi} = \mu_{Tp} + \sigma_{Tp} Y_i \tag{3.12}$$

To effectively specify this sequential modeling process, a "home charging" scenario cycle is illustrated as an example. The calculated SOC_i and charging time CT_i is used in Fig. 3.4 to

obtain a time sequential power demand of the i^{th} PHEV for the charging time duration. This creates the sequential load profile for which the start time is T_{hi} and duration is CT_i. This provides the load model for the i^{th} PHEV for a charging cycle. The sequential process in this charging cycle is shown in Figure 3.8.

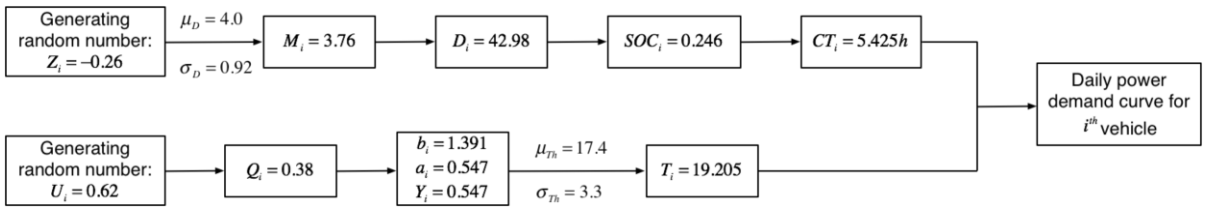

Figure 3.8: A sample run of the PHEV charging cycle methodology

Similarly, daily power demand curve of "public/home charging" scenario can be obtained. The sequential modeling process is carried out for all the *n* PHEV in the fleet as shown in Fig. 3.9.

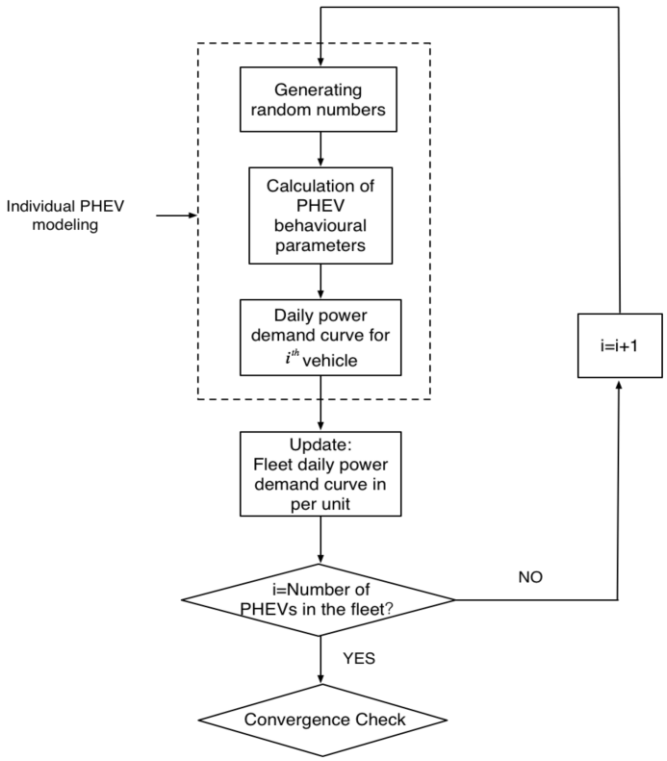

Figure 3.9: PHEV fleet modeling procedure

The daily sequential loads obtained as discussed above are recursively aggregated for all the *n* vehicles as shown in Equation (3.13) to obtain the sequential load model for the entire fleet.

$$L_h = \sum_{i=1}^{n} L_{PHEV_{i,h}} \quad (3.13)$$

Where,

h | 24 is the hour of the day;

L_h is the fleet load at Hour h;

$L_{PHEVi,h}$ is the load of the i^{th} PHEV at Hour h.

The simulation process for all the vehicles in fleet are repeated until convergence criteria are met, i.e. when the fleet load model is not changed with further simulation runs. Fig. 3.10 shows the daily sequential load model considering the "home charging" scenario for a fleet of 100 PHEV. The individual updated load models in per unit of the respective peak loads are also shown.

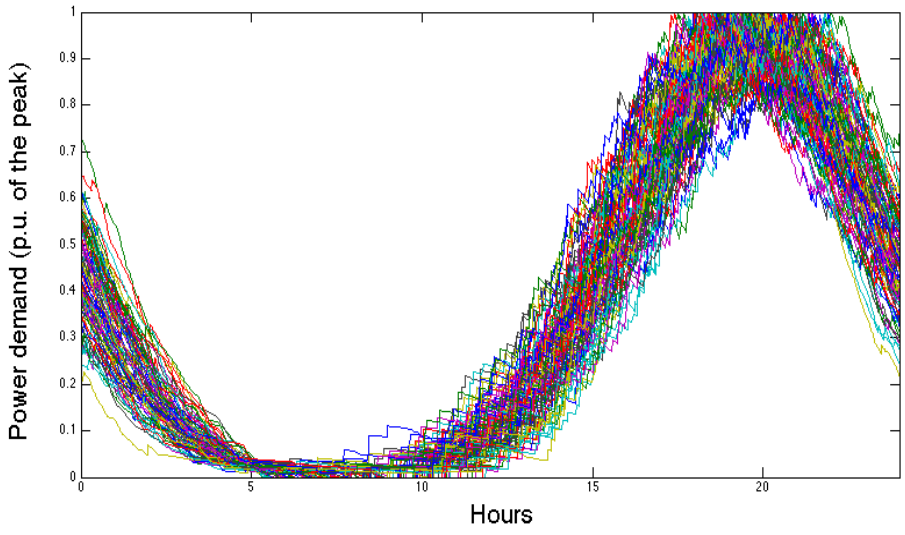

Figure 3.10: "Home charging" scenario daily load model of individual PHEV and of the entire fleet

Fig. 3.11 shows the daily sequential load model for a fleet with 100 PHEV under "public/home charging" scenario and the individual updated load models in per unit of the respective peak loads. The daily load model shown in Fig. 3.11 can be compared with Fig. 3.10 obtained for the "home charging" scenario. It can be observed from Fig. 3.11 that there is a new peak during

daytime introduced due to public charging, and the peak value during the daytime is higher than the evening "home charging" peak because of the higher charging power needed for public charging as shown in Fig. 3.5.

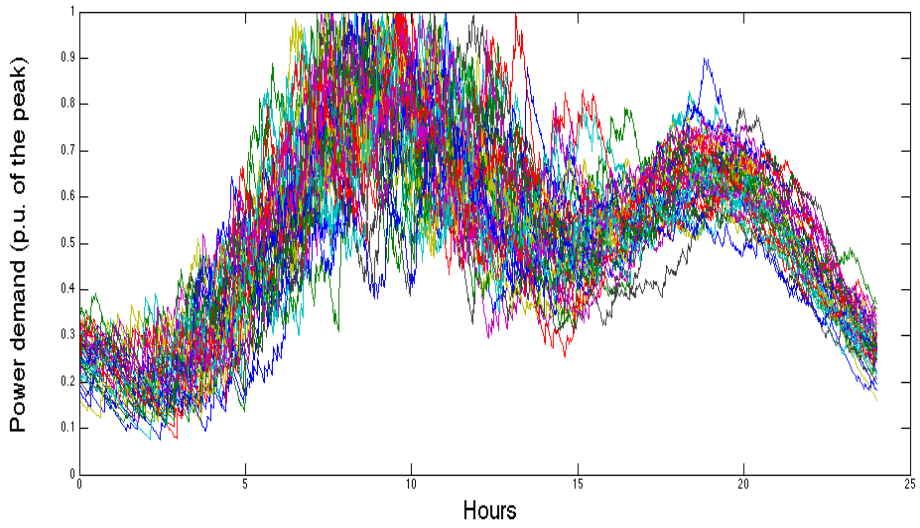

Figure 3.11: "Public/home charging" scenario daily load model of individual PHEV and of the entire fleet

3.7 System Load Model Modification Incorporating PHEV Load

When PHEV are connected to power system for charging, they form a new type of load with specific characteristics. The system load model of the IEEE-RTS is used to illustrate the modification of the system load due to PHEV penetration in the system. PHEV "penetration" is defined to be the ratio of the maximum PHEV power demand and the system peak load in this thesis. For example, a 10% PHEV penetration means a maximum PHEV demand of 285 MW, which is 10% of IEEE-RTS peak load of 2850 MW. The total system load model is then obtained by aggregating the original load with the PHEV fleet model.

Fig. 2.10 shows the daily load curves of two days with the highest and lowest load in the annual model. These two load curves are used to illustrate how the system load model is modified by incorporating PHEV model. Fig. 3.12 and Fig. 3.13 present the modified summer and winter daily load models obtained by aggregating the original system load with the PHEV load

considering 25% PHEV penetration. The two charging scenarios, "home charging" and "public/home charging" are shown in these figures. For the "public/home charging" scenario, it is assumed that all the PHEV can be charged at home and only 40% of the PHEV can also be charged in public through fast charging facilities. The original load is also shown for comparison. The horizontal line indicates the annual peak load of the IEEE-RTS.

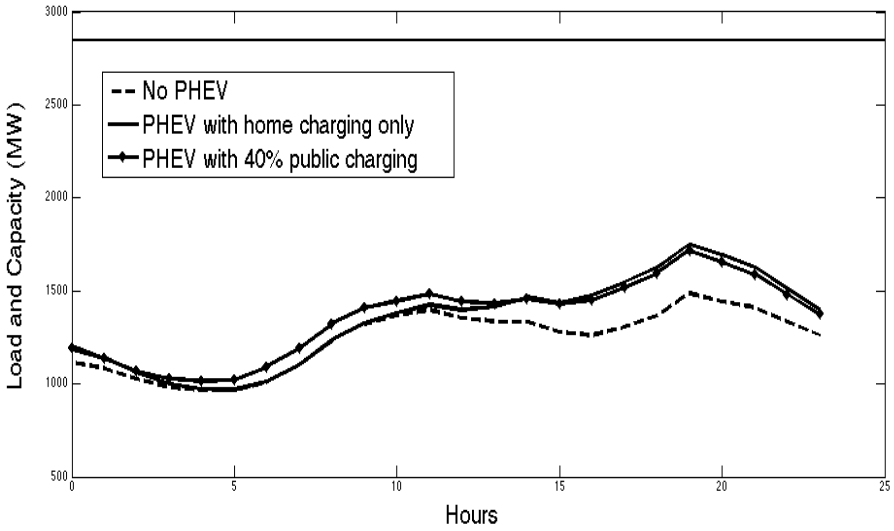

Figure 3.12: Summer daily load models with and without PHEV

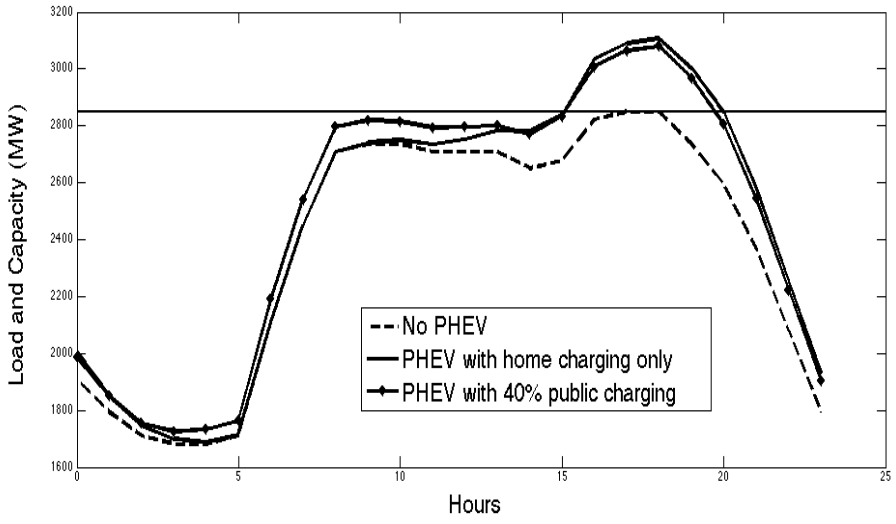

Figure 3.13: Winter daily load models with and without PHEV

It can be observed from Fig. 3.12 and 3.13 that the overall power demand is significantly increased due to PHEV charging during the peak hours (approximately from 16:00 to 21:00) on both the daily load profiles. The peak load value substantially exceeds the original annual peak load of 2850 MW during the winter season, which indicates the overlap of PHEV fleet charging demand and system original demand.

A comparison of the two charging scenarios in Fig. 3.12 and Fig. 3.13 shows that the "home charging" scenario has a greater impact on increasing the annual peak load. The annual peak load is also increased significantly in the "public/home charging" scenario. This scenario, however, utilizes additional power throughout the day including the "valley" period in the morning.

The above method is used to modify the load model using the PHEV model under different charging scenarios for each day. A modified chronological hourly load model can then be obtained for a year, which can be transformed to an appropriate load model for reliability analysis at the HL-I and HL-II levels. The load models will be further modified to be compatible to the data input requirements of the software used in the analysis.

3.8 Summary

The development of an analytical PHEV model for reliability evaluation is presented in this chapter. PHEV-30 is introduced to provide the basic behavioral parameters of a PHEV. The PHEV creates a new kind of load with unique characteristics compared to conventional power system load. Based on the research of popular PHEV models in the recent market, "fast charging" and "normal charging" modes, and "home charging" and "home/public charging" scenarios are considered in the model development process. The daily driving distance, battery performance during driving, battery performance during charging and charging start time are recognized as important PHEV characteristics for reliability modeling. Transportation data from NHTS 2009 are used to create the mathematical models of these parameters.

A MCS method was applied to combine individual PHEV models and build the overall model for a PHEV fleet. Aggregated PHEV fleet models for different charging scenarios are presented. Then the modification of system load model is presented by aggregating fleet model with the original load model considering PHEV penetration levels and charging scenarios. The development of appropriate annual load models that incorporate PHEV are discussed with respect to their application in HL-I and HL-II reliability studies.

4 GENERATION SYSTEM RELIABILITY EVALUATION INCORPORATING PHEV

4.1 Introduction

This chapter presents reliability analysis of a power system at the HL-I level incorporating PHEV as a part of the system load. The chapter presents a methodology to create a modified system load model for overall system reliability evaluation by combing the PHEV model presented in Chapter 3 and the system load model. Studies considering a wide range of PHEV penetration levels, varying from 5% to 50% are considered in the presented studies to analyze the impact of PHEV growth on power system reliability. The impacts of key influencing factors are examined through selected studies considering one factor at a time.

The software SIPSREL is used for the HL-I reliability analyses. A period analysis is carried out to incorporate the effect of seasonality by dividing a year into summer and winter periods. System capacity models in the form of COPT and system load models in the form of LDC are created for each period. The capacity models and the load models are convolved in each period and aggregated to obtain the annual system reliability indices. The results from the presented studies are analyzed to assess the impacts of various factors on power system reliability. Based on that, some reliability enhancement measures are presented, which are believed to be valuable for planning and operating of future power systems that are expected to accommodate an increasing penetration of PHEV.

4.2 Development of the Overall Load Model Incorporating PHEV

Fig. 2.10 shows the daily load curves of the IEEE-RTS for the summer day with the minimum system load and the winter day with the peak load for a year. It can be observed that there is significant difference in power demand between the summer and winter seasons. Therefore it is worthwhile to divide the yearly load model into two seasonal loads in order to assess seasonality effects on system reliability. The time sequential PHEV fleet model obtained using

the MCS method as described in Chapter 3 is superimposed on the chronological system load and added to obtain a sequential modified system load. Fig. 4.1 and 4.2 show the modified sequential system loads obtained from the two sequential load curves presented in Fig. 2.10 by incorporating PHEV at various penetration levels under the "home charging" scenario. The horizontal line represents the system annual peak load of 2850 MW without PHEV, and the dashed horizontal line indicates the total system installed capacity of 3405 MW.

It can be observed from Fig. 4.1 and 4.2 that the overall system demand is significantly increased because the PHEV charging demand overlaps with system original household demand during the peak hours (approximately from 16:00 to 21:00). As a result, the system peak load increases as the penetration of PHEV is increased in a power system. It is noted that the peak load value substantially exceeds the original annual peak load of 2850 MW in the winter season.

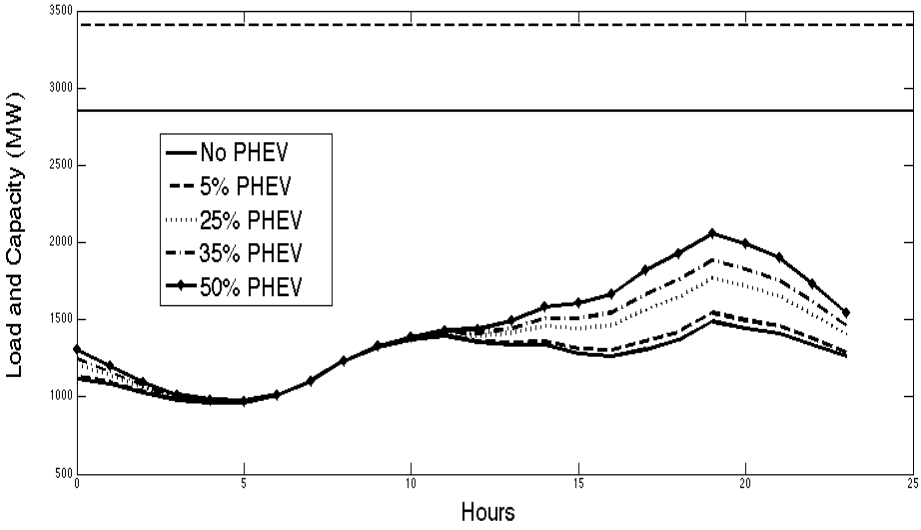

Figure 4.1: The impact of PHEV penetration on the summer daily load models

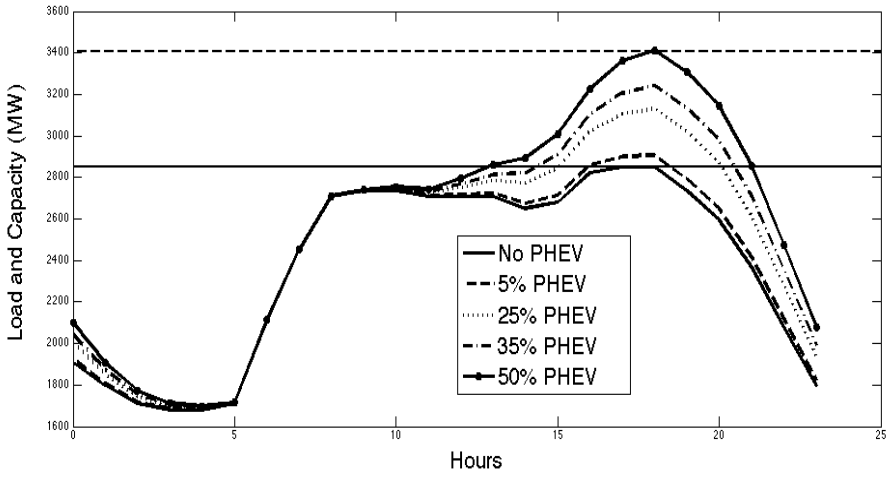

Figure 4.2: The impact of PHEV penetration on the winter daily load models

The 24-hour modified chronological load model that incorporates the PHEV model is obtained sequentially for the summer and winter seasons. An LDC is created for each season by aggregating the hourly loads, sorting them in a decreasing order and plotting the load profile against time. Fig. 4.3 shows the winter LDC that incorporates PHEV at different penetration levels. The LDC is plotted in per unit of the original system peak load of 2850 MW in the y-axis, and in per unit of the total winter time period of 4368 hours in the x-axis. It can be seen that there is approximate 20% increase in the annual peak load when PHEV penetration is 50%. Fig. 4.4 similarly shows the summer LDC under various PHEV penetration levels considering 4392 summer hours. It can be seen that the peak load situation is not very severe even at 50% penetration level during summer season. These two figures show the seasonality effects of PHEV penetration on the load model.

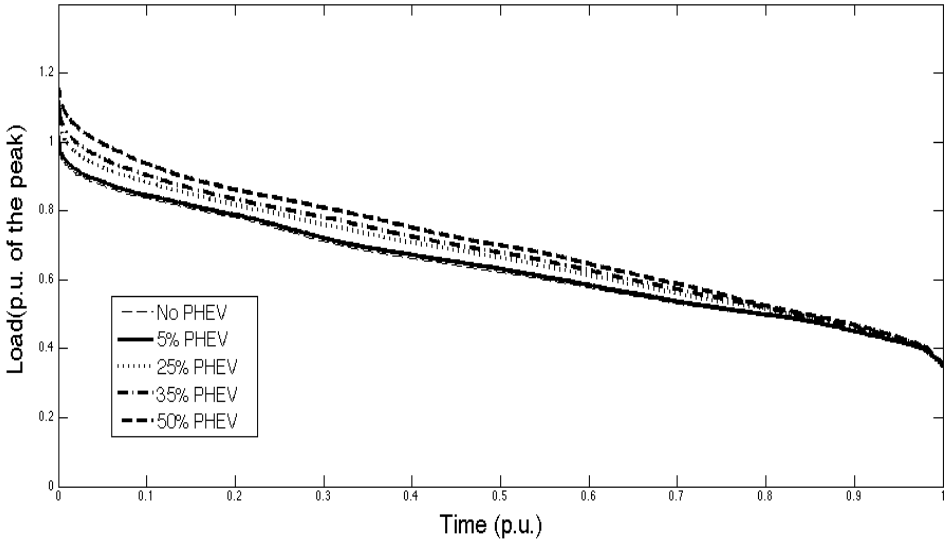

Figure 4.3: Winter LDC with varying PHEV penetration levels

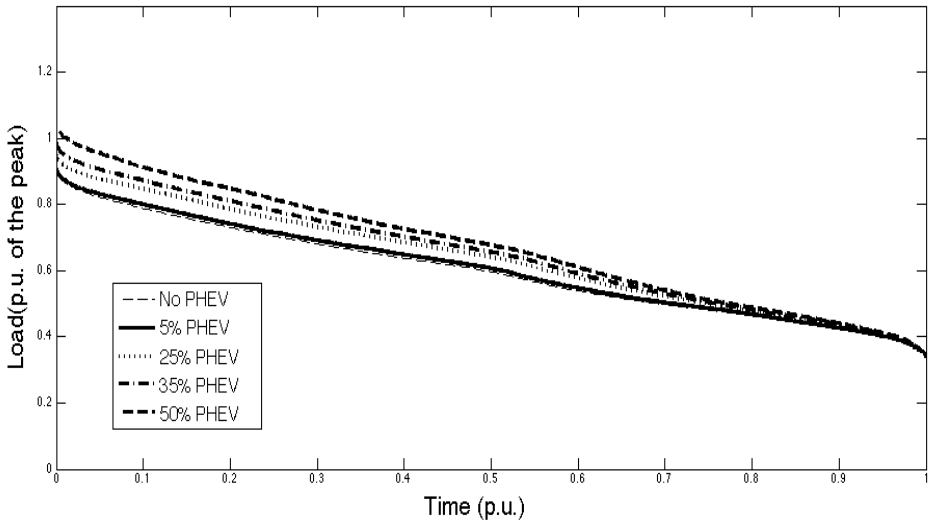

Figure 4.4: Summer LDC with varying PHEV penetration levels

Fig. 4.5 shows the annual LDC obtained by aggregating the hourly loads of the whole year and then sorting in a decreasing order. This model requires less computation time than the seasonal models in reliability evaluations, and can be used to analyze the impacts of various system factors, even though this model does not recognize the seasonality effects.

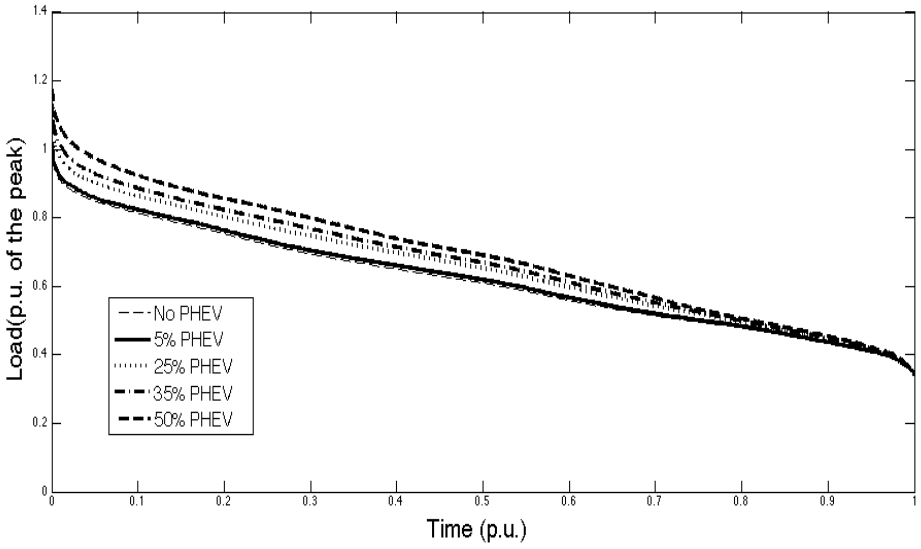

Figure 4.5: System annual LDC with varying PHEV penetration levels

The peak load of the IEEE-RTS load model is 2850 MW when PHEV is not considered and is equivalent to 1.0 per unit. The effective system peak load will increase to a value larger than 1.0 per unit as shown in Fig. 4.5 when PHEV is incorporated in the system load model. Table 4.1 shows the first and last twenty states of the LDC.

Table 4.1: Sample states of the IEEE-RTS LDC Incorporating 25% PHEV penetration (2850 MW is 1.0 per unit)

First twenty states		Last twenty states	
Load Level (p.u.)	Probability	Load Level (p.u.)	Probability
1.09741	0	0.35502	0.99760
1.08214	0.00011	0.35496	0.99783
1.07741	0.00023	0.35486	0.99795
1.06741	0.00034	0.35454	0.99806
1.06214	0.00046	0.35436	0.99817
1.05779	0.00057	0.35398	0.99829
1.05741	0.00068	0.35350	0.99840
1.05692	0.00080	0.35309	0.99852
1.05214	0.00091	0.35297	0.99863
1.04941	0.00103	0.35161	0.99874
1.04801	0.00114	0.35090	0.99886
1.04214	0.00126	0.35066	0.99897
1.03941	0.00137	0.35057	0.99909
1.03859	0.00148	0.34986	0.99920
1.03741	0.00171	0.34674	0.99932
1.03712	0.00183	0.34625	0.99943
1.03414	0.00194	0.34570	0.99954
1.03274	0.00205	0.34521	0.99966
1.03037	0.00217	0.34186	0.99977
1.02899	0.00228	0.34082	1.0

As SIPSREL does not take a load level greater than 1.0 per unit, the load levels of LDC are normalized by the new peak load obtained after incorporating the PHEV. In the above example, the new peak load increases from 2850 MW to 3128 MW when 25% PHEV is incorporated in the load model. Table 4.2 shows the first and last twenty states when the modified peak load of 3128 MW is considered as 1.0 per unit.

Table 4.2: Sample states of LDC under 25% PHEV penetration (3128 MW is equivalent to 1.0 per unit)

First twenty states		Last twenty states	
Load Level (p.u.)	Probability	Load Level (p.u.)	Probability
1.0	0	0.32351	0.99760
0.98608	0.00011	0.32345	0.99783
0.98178	0.00023	0.32336	0.99795
0.97266	0.00034	0.32307	0.99806
0.96786	0.00046	0.32290	0.99817
0.96390	0.00057	0.32255	0.99829
0.96355	0.00068	0.32212	0.99840
0.96310	0.00080	0.32174	0.99852
0.95874	0.00091	0.32164	0.99863
0.95626	0.00103	0.32040	0.99874
0.95498	0.00114	0.31975	0.99886
0.94963	0.00126	0.31953	0.99897
0.94715	0.00137	0.31945	0.99909
0.94640	0.00148	0.31880	0.99920
0.94533	0.00171	0.31596	0.99932
0.94506	0.00183	0.31552	0.99943
0.94234	0.00194	0.31501	0.99954
0.94107	0.00205	0.31456	0.99966
0.93891	0.00217	0.31152	0.99977
0.93765	0.00228	0.31056	1.0

The LOLE and LOEE are two reliability indices that are widely used in capacity planning. The LOLE determines the loss of load probability and the LOEE quantifies the energy not supplied due to loss of load. These two reliability indices are used in this work to assess the impact of PHEV on system HL-I reliability. Table 4.3 shows the reliability indices obtained from SIPSREL when PHEV penetration is increased from 0 to 50%.

Table 4.3: System LOLE and LOEE with increasing PHEV penetration in the home charging scenario

PHEV Penetration Levels	LOLE (hrs/yr)	LOEE (MWh/yr)
0%	9.418	1.174
5%	11.191	1.425
25%	25.462	3.593
35%	40.077	5.949
50%	76.858	12.694

It can be seen from the results shown in Table 4.3 that the system LOLE and LOEE increase substantially as PHEV penetration level is increased. The reliability level shown by the indices in Table 4.3 would be unacceptable in most power systems with rise in PHEV penetration level. It can therefore be concluded that the system reliability will quickly deteriorate as PHEV sales increase in response to environmental support unless reliability enhancement measures are taken.

The results shown in this section are obtained when "home charging" is considered to be the only charging option for PHEV. In the following sections of this thesis, other options of PHEV charging will be incorporated in system reliability evaluation, and an analysis of the corresponding impacts will be presented.

4.3 Impacts of PHEV Charging Scenarios on System Reliability

The flexibility of PHEV usage can also be illustrated through charging time and locations. Various scenarios are available for PHEV charging. Accessibility to "public charging" is receiving increasing attention in response to the increasing environmental concerns leading to growth of charging facilities in public areas. Considering the relatively limited charging time during "public charging", it is practical to assume that "fast charging" mode is utilized for "public charging" scenario. This section presents the development of the system load model incorporating PHEV under "public/home charging" scenario. The main difference in

methodology with the "home charging" scenario presented previously is the requirement for multiple charging cycles in a day.

As indicated previously, it is assumed in the studies of this thesis that "fast charging" mode is utilized during public charging, and "normal charging" mode is used for home charging that usually occurs at the end of a day. It can be seen from the results shown in earlier part of this chapter, the reliability impacts on power system greatly depend on PHEV penetration levels. Therefore, PHEV penetration level is also considered in the studies presented in this section when different charging scenarios are taken into account.

In practical utilization of PHEV, a certain percentage of PHEV will have the access to public charging in a power system due to driving behavior and the limitation in public charging stations. The system load model obtained incorporating PHEV will also depend on the percentage of vehicles having access to public charging. Fig. 4.6 shows the PHEV load profile for a fleet of 10,000 vehicles. It can be seen that the load profiles change significantly when considering the percentage of vehicles having access to public charging varies from 20% to 80%. The load profile for "home charging" scenario is also shown in this figure for comparison. It is important to note that for "public/home charging" scenario the vehicle may also be charged at home depending on the battery SOC when the PHEV arrives home.

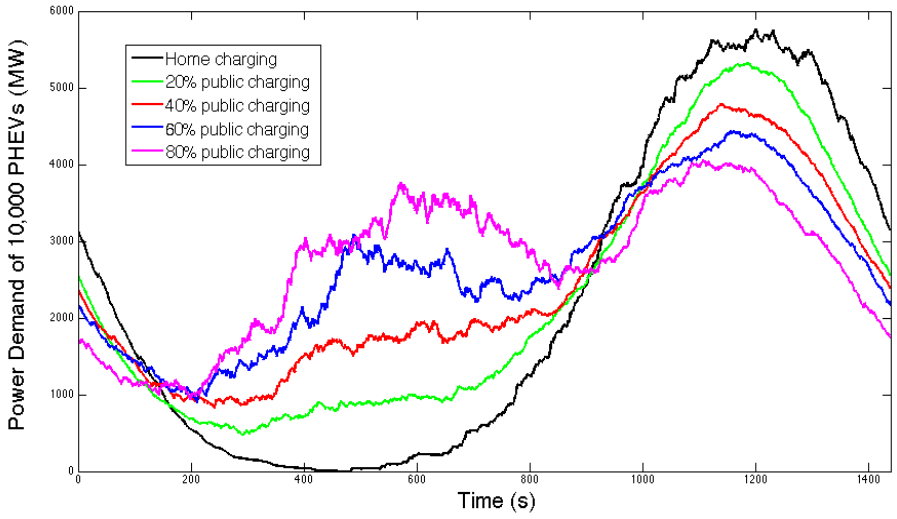

Figure 4.6: Load model of 10,000 PHEV in "public/home charging" scenario when different public charging percentage is applied

It can be observed from Fig. 4.6 that power demand of this fleet increases during the daytime and decreases during the nighttime as the public charging percentage increases. When 80% of PHEV have access to public charging, two peaks of power demand appear in the PHEV load profile, which can be compared with the single evening peak that occurs in the "home charging" scenario.

The system load model can be modified by time sequential superimposition of the PHEV load model with the hourly chronological system load model as introduced in Chapter 3. Seasonality studies are carried out for various charging scenarios to investigate their impacts on different seasons of the year. Fig. 2.10 shows the summer and winter daily load curves for the IEEE-RTS without considering PHEV load. Fig. 4.7 and 4.8 show the 24-hour summer and winter load models obtained by aggregating the original load model with the PHEV load considering PHEV public charging percentage of 20% under different PHEV penetration levels. Similarly, Figures from 4.9 to 4.14 provide the summer and winter 24-hour load curve when public charging percentage increases from 40 to 80%.

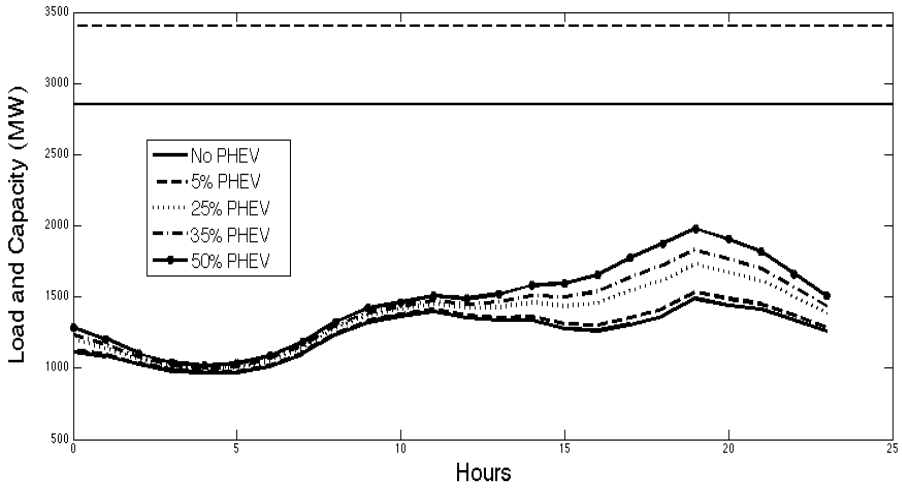

Figure 4.7: 24-hour summer load curve with 20% PHEV public charging percentage in different penetration levels

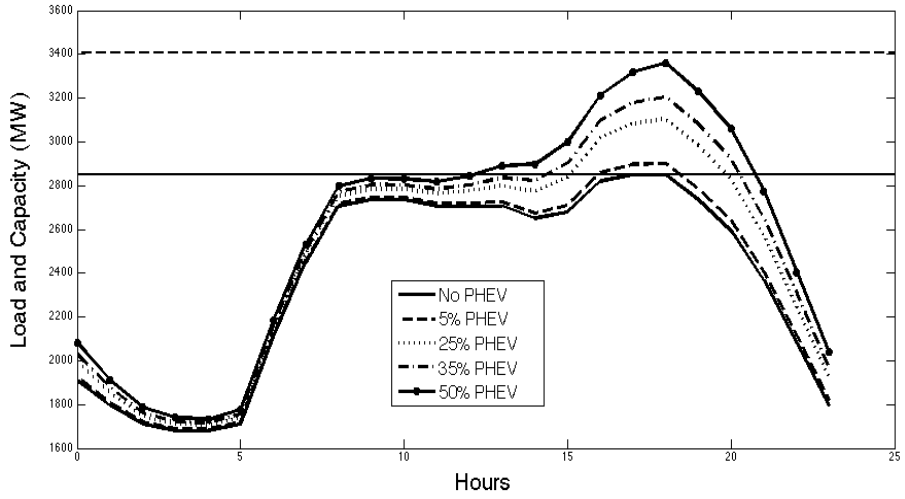

Figure 4.8: 24-hour winter load curve with 20% PHEV public charging percentage in different penetration levels

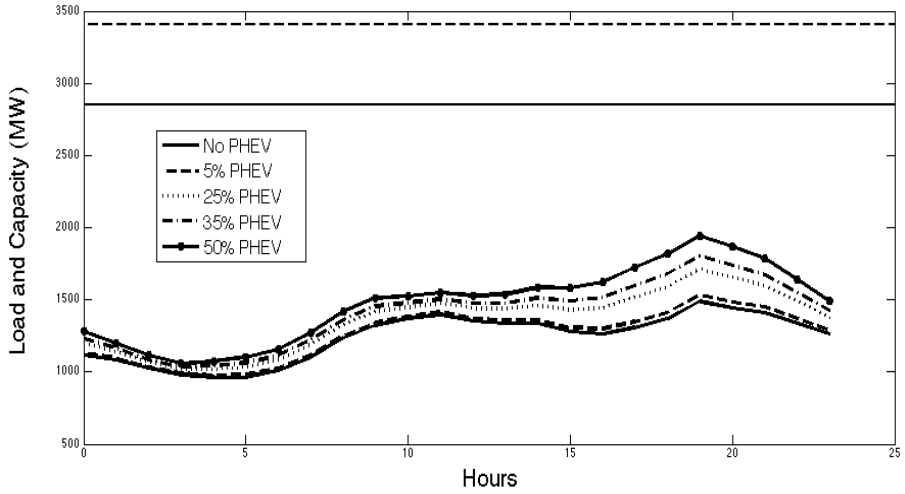

Figure 4.9: 24-hour summer load curve with 40% PHEV public charging percentage in different penetration levels

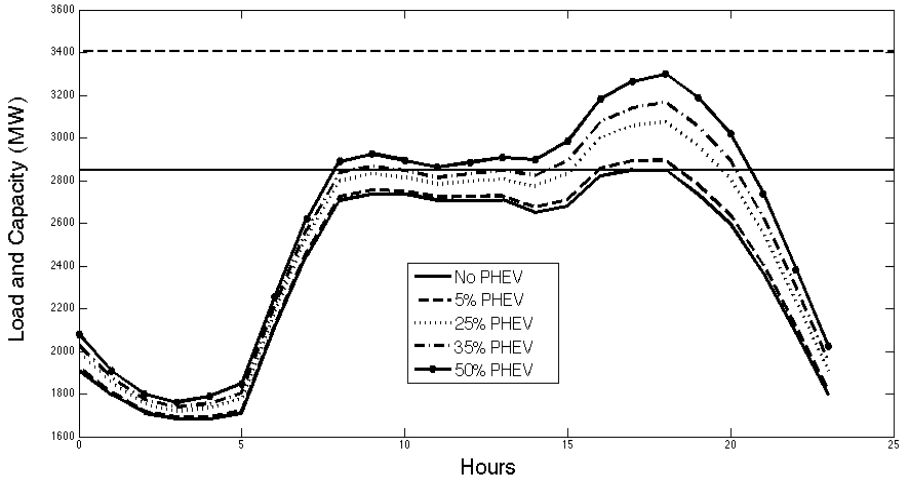

Figure 4.10: 24-hour winter load curve with 40% PHEV public charging percentage in different penetration levels

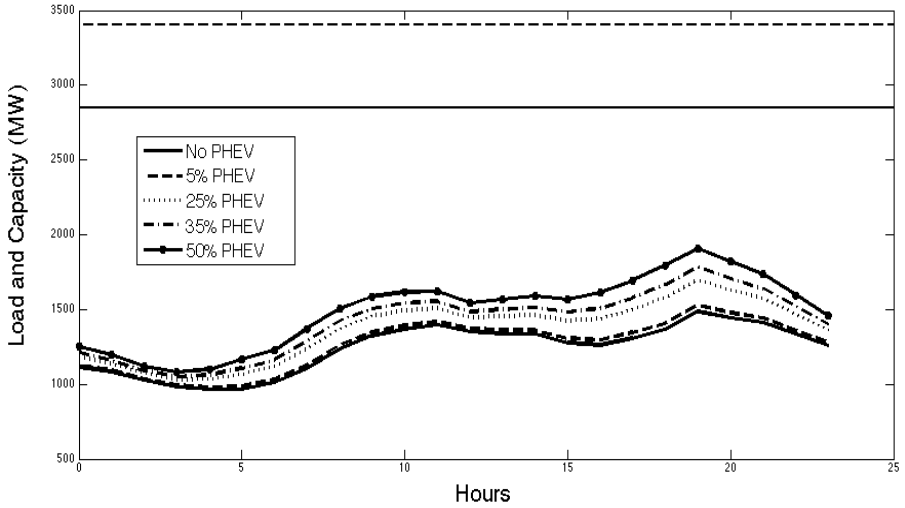

Figure 4.11: 24-hour summer load curve with 60% PHEV public charging percentage in different penetration levels

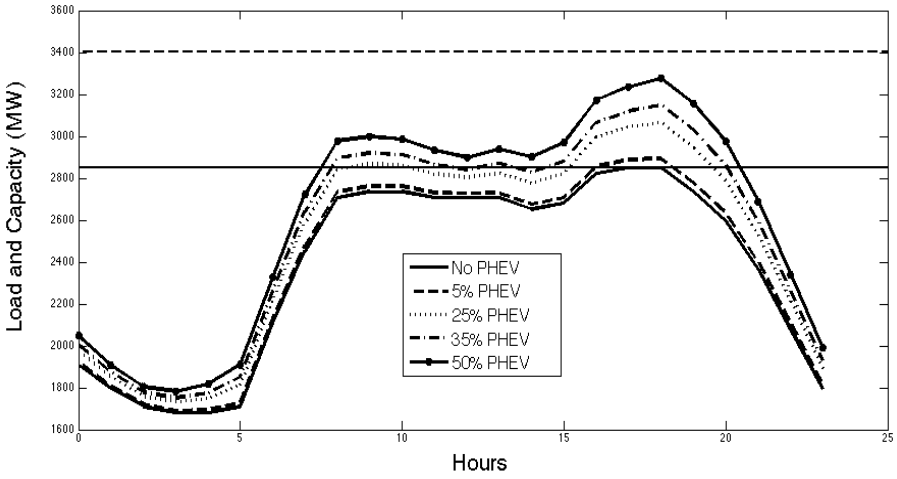

Figure 4.12: 24-hour winter load curve with 60% PHEV public charging percentage in different penetration levels

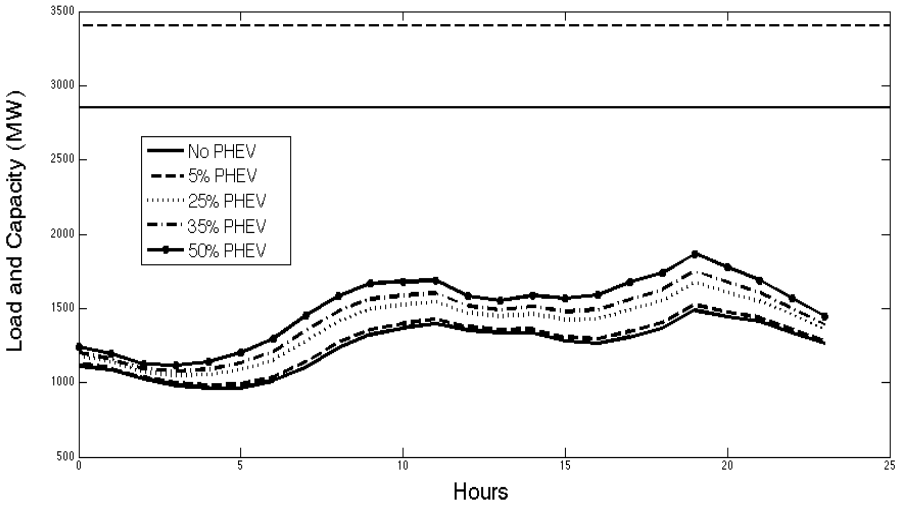

Figure 4.13: 24-hour summer load curve with 80% PHEV public charging percentage in different penetration levels

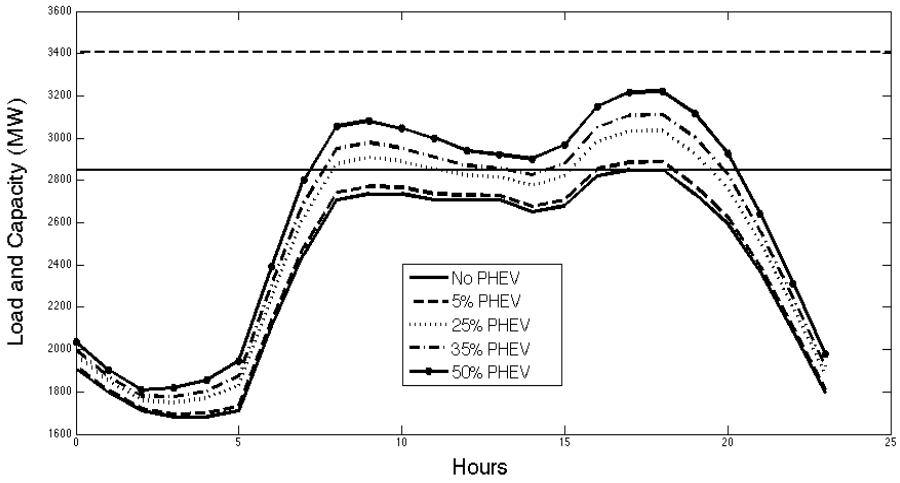

Figure 4.14: 24-hour winter load curve with 80% PHEV public charging percentage in different penetration levels

It can be observed from the above figures that public charging of PHEV greatly changes the system load profile. Power demand in the hours before noon in the sequential summer load curve becomes close to the value of power demand in the nighttime as public charging percentage is increased. A new peak is formed around 10 A.M. as shown in Fig. 4.13 when public charging percentage is increased to 80%. A comparison between Fig. 4.13 and Fig. 4.1 clearly shows that the system power demand is decreased during the nighttime as the public charging percentage is increased. During the winter season, as we can see from Fig. 4.2 "home charging" scenario results in a significant evening peak. When "public charging" is considered, there is a second peak in system power demand at around 10 A.M. The morning peak increases and the evening peak decreases as public charging percentage is increased from 20% to 80%. From the above figures it can see that the peak load value of 24-hour summer load curve is much lower than system original peak value, even under 50% PHEV penetration level and 80% public charging percentage as shown in Fig. 4.13. However, during the winter day under the same penetration level and public charging percentage system peak load value is greater than 2850 MW in 24-hour load curve as shown in Fig. 4.14.

Fig. 4.15, 4.16, 4.17 and 4.18 respectively show annual LDC for a range of PHEV penetration to the IEEE-RTS when 20%, 40%, 60% and 80% of the vehicles have access to public charging.

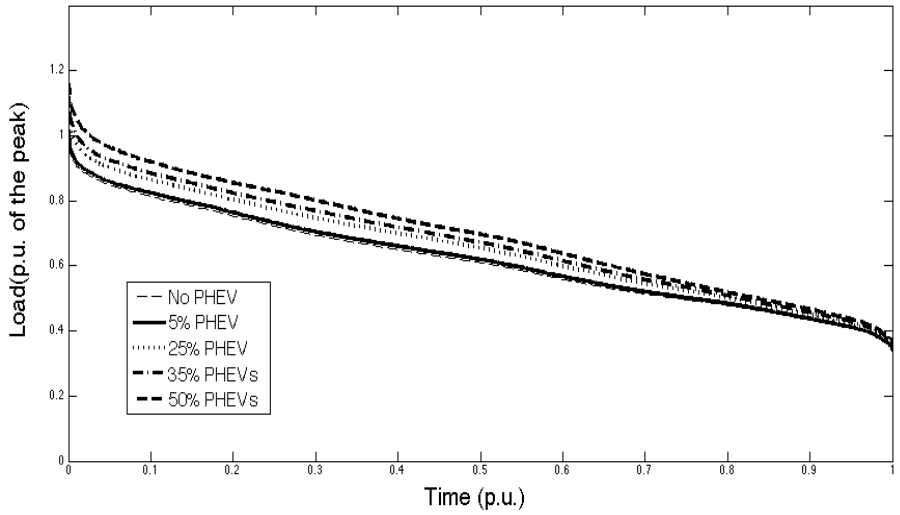

Figure 4.15: System annual LDC with 20% PHEV public charging percentage in different penetration levels

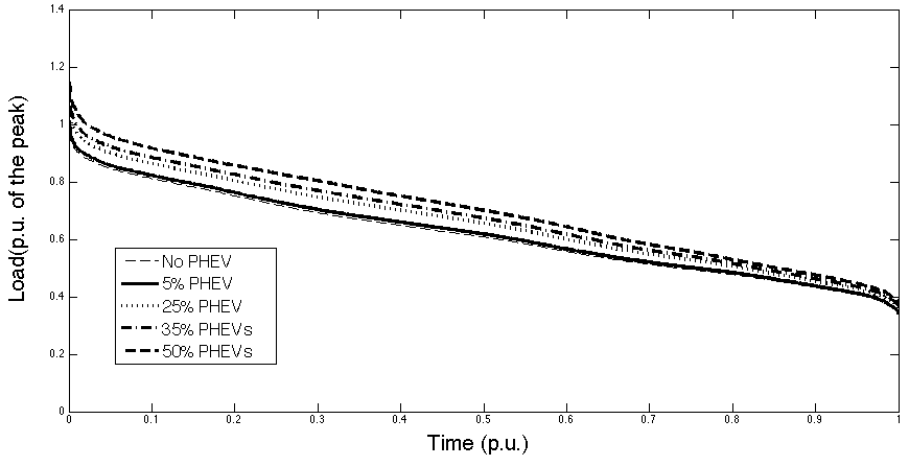

Figure 4.16: System annual LDC with 40% PHEV public charging percentage in different penetration levels

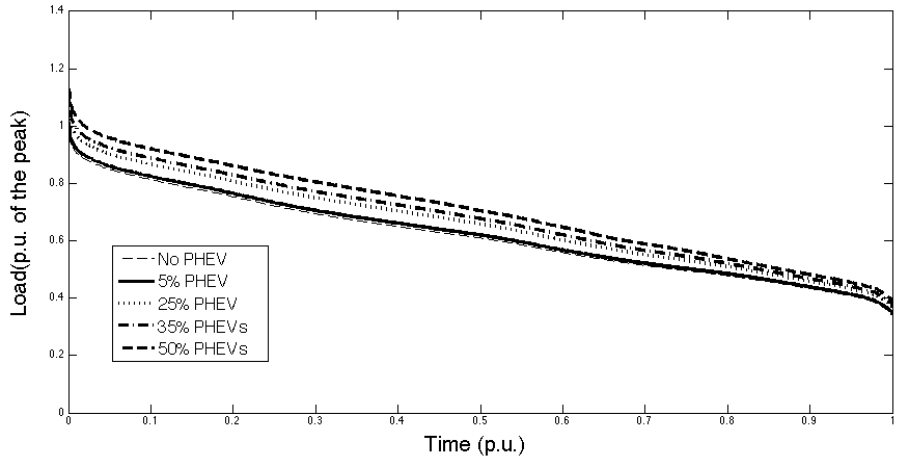

Figure 4.17: System annual LDC with 60% PHEV public charging percentage in different penetration levels

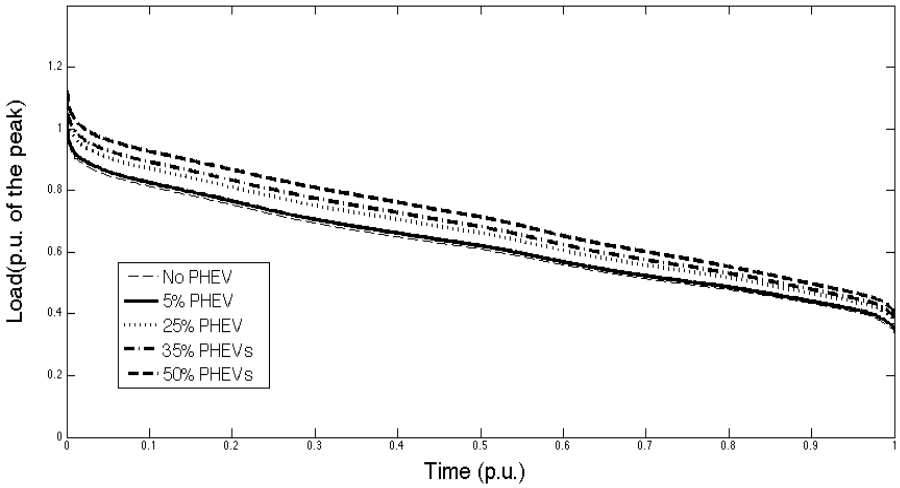

Figure 4.18: System annual LDC with 80% PHEV public charging percentage in different penetration levels

Table 4.4 shows the system LOLE and LOEE when the annual load models shown in Fig. 4.15 to 4.18 are respectively convolved with the generation model of the IEEE-RTS.

Table 4.4: System reliability indices for "public/home charging" scenario considering variable public charging percentages and PHEV penetration levels

Public charging percentage	PHEV penetration levels	LOLE (hrs/yr)	LOEE (MWh/yr)
	0%	9.418	1.174
20%	5%	11.426	1.451
	25%	26.237	3.665
	35%	40.460	5.950
	50%	74.943	12.122
40%	5%	11.566	1.470
	25%	26.985	3.749
	35%	41.027	5.979
	50%	74.457	11.817
60%	5%	11.633	1.481
	25%	26.762	3.695
	35%	39.936	5.742
	50%	70.215	10.859
80%	5%	11.729	1.488
	25%	27.271	3.751
	35%	40.678	5.822
	50%	71.957	10.950

The results show that the system LOLE and LOEE increases or the system reliability degrades as the PHEV penetration is increased in the system. It can also be seen that the system reliability degrades further as more vehicles also have access to public charging in addition to home charging. This is because the PHEV-30 is designed for relatively short commute distance, and a fully charged PHEV in public will then be discharged on the way home. And it is likely that it will be plugged in for charging after it arrives home. The power demand of "home charging" will then coincide with system household peak, which affects system reliability adversely. As public charging percentage increases, power demand is increased dramatically because of high charging power of required for "fast charging" mode. The effect shown in this section becomes more profound as PHEV penetration increases and more vehicles have access to public charging. It can be concluded that the system reliability will quickly deteriorate as PHEV sales increase in response to environmental support unless

reliability enhancement measures are taken. Therefore, some control measures associated with PHEV charging are presented in the next section.

4.4 Reliability Analysis Considering Controlled PHEV Charging

The studies presented in the previous sections assume that PHEV are plugged into the power grid for home charging right after they arrive home. This is a valid assumption when there is no intentional control on PHEV charging behavior. The results of the reliability studies presented in Table 4.3 clearly show that in this case PHEV cause rapid degradation of system reliability as PHEV penetration increases. This section presents system reliability assessments considering different control measures associated with PHEV charging in order to keep system reliability within an acceptable range.

4.4.1 Controlling Charging Start Time

Under "home charging" scenario, power demand of PHEV charging in the nighttime overlaps with system household demand. As a result, the overall system peak load increases as the penetration level of PHEV increases. If peak load of PHEV charging can be shifted and it does not coincide with the household peak load, the overall system reliability could be improved theoretically. Therefore, the impacts of controlling PHEV home "charging start time" on system reliability are investigated in this section.

A specific "charging start time" is selected in the study to shift the PHEV load away from the household peak load. PHEV may arrive home before or after the selected "charging start time". "Home arrival time" of each PHEV can be obtained within a PHEV fleet by using Equation (3.3). Then PHEV can be divided into two groups depending on whether their "home arrival time" is before or after the specified time. It is assumed that the vehicles that arrive home before the specified "charging start time" will wait until the specified time to start charging, whereas, the vehicles that arrive after the specified time will begin charging immediately upon home arrival.

A sensitivity study was carried out by selecting four different charging start times: 19:00, 22:00, 23:00 and 00:00 hours. It should be noted that all the results shown below are obtained when 40% public charging percentage is considered. Fig. 4.19 shows the 24-hour sequential load for a fleet of 10,000 PHEV when the charging start time is set to 19:00, 22:00, 23:00 and 00:00 hours respectively. These load profiles can be compared to the load profile of 10,000 PHEV shown in Fig. 4.6 with no control on the charging time. It can be seen from Fig. 4.19 that there is a demand peak at the specified "charging start time", and as the time goes by the power demand decreases until the vehicles complete the charging process. The four power demand curves shown in this Fig. 4.19 have similar shapes, except that they are shifted in time depending on the starting times. If charging behavior starts at midnight, most PHEV can complete the charging at around 05:30, which should be acceptable for most people driving their vehicles to work.

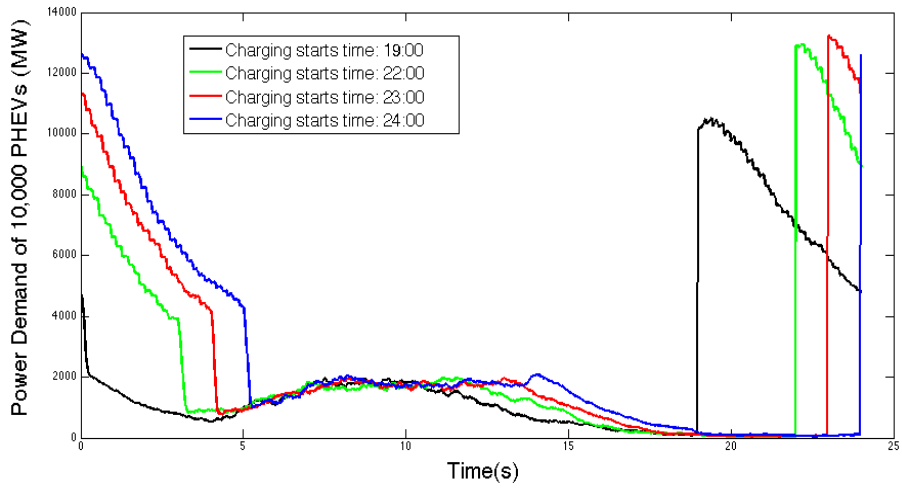

Figure 4.19: Load model of 10,000 PHEV in "public/home charging" scenario with different "charging start time"

The system load models of the two representative days of summer and winter are modified under the given charging start time and are presented from Fig. 4.20 to 4.27 to show the specific impacts of charging start time on the system load profile.

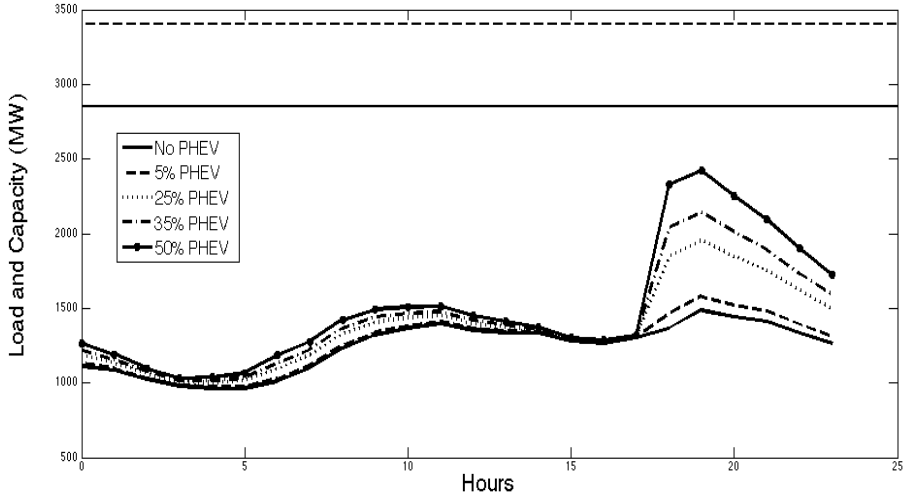

Figure 4.20: 24-hour summer load curve when home charging starts at 19:00 with 40% PHEV public charging percentage in different penetration levels

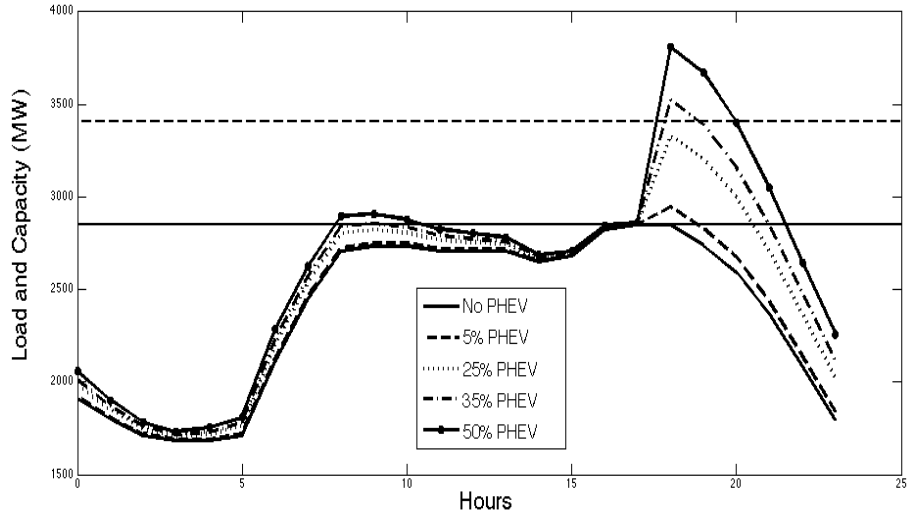

Figure 4.21: 24-hour winter load curve when home charging starts at 19:00 with 40% PHEV public charging percentage in different penetration levels

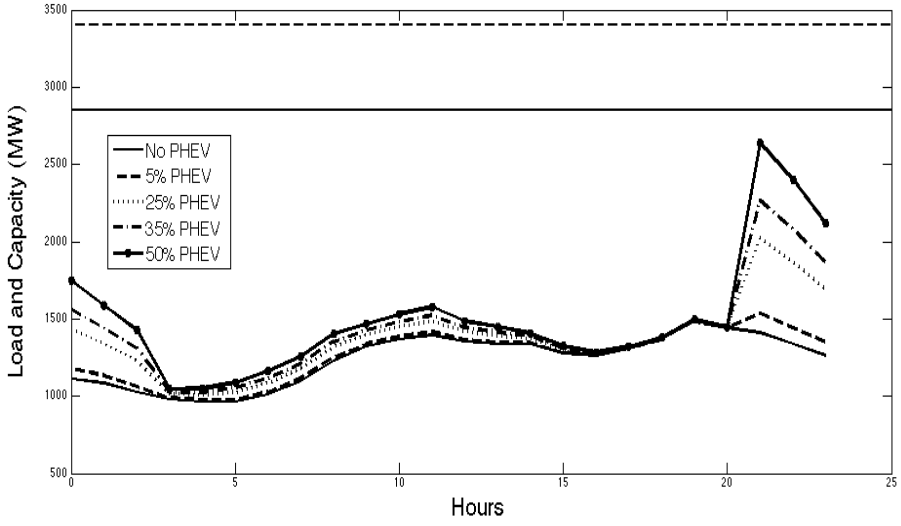

Figure 4.22: 24-hour summer load curve when home charging starts at 22:00 with 40% PHEV public charging percentage in different penetration levels

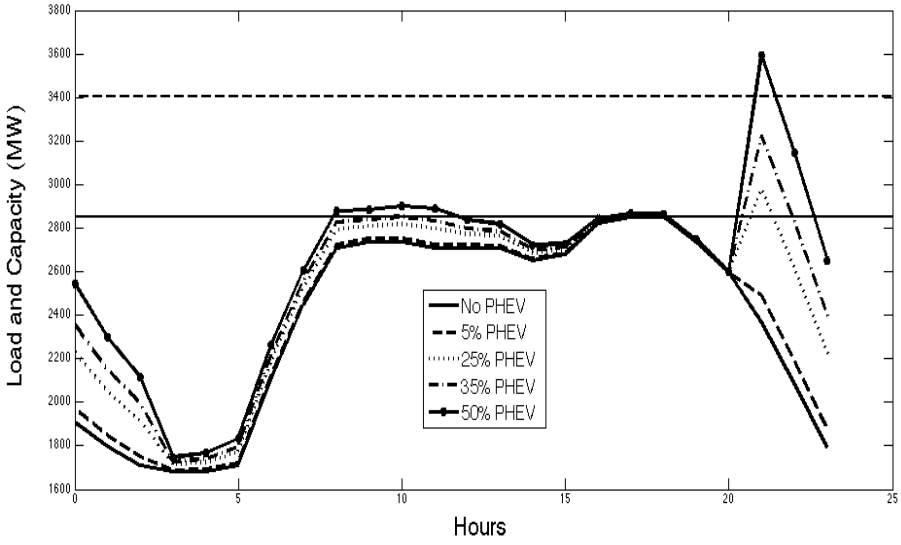

Figure 4.23: 24-hour winter load curve when home charging starts at 22:00 with 40% PHEV public charging percentage in different penetration levels

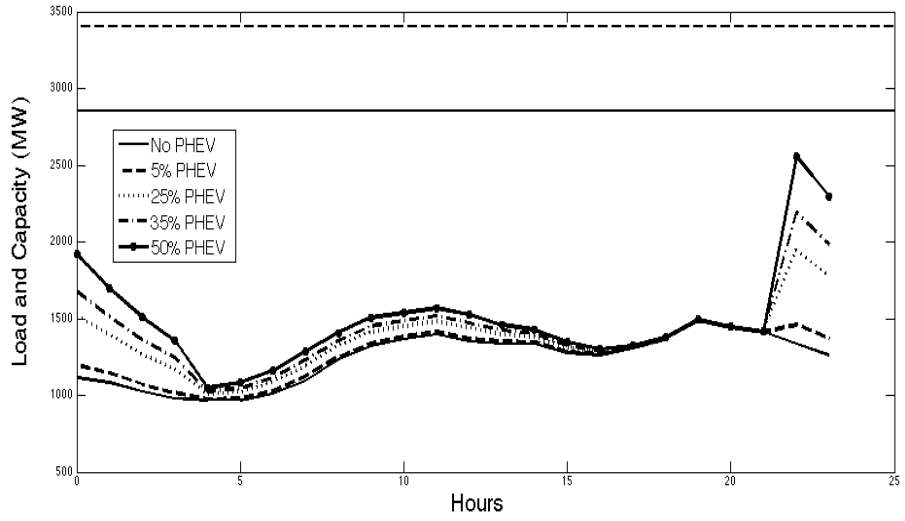

Figure 4.24: 24-hour summer load curve when home charging starts at 23:00 with 40% PHEV public charging percentage in different penetration levels

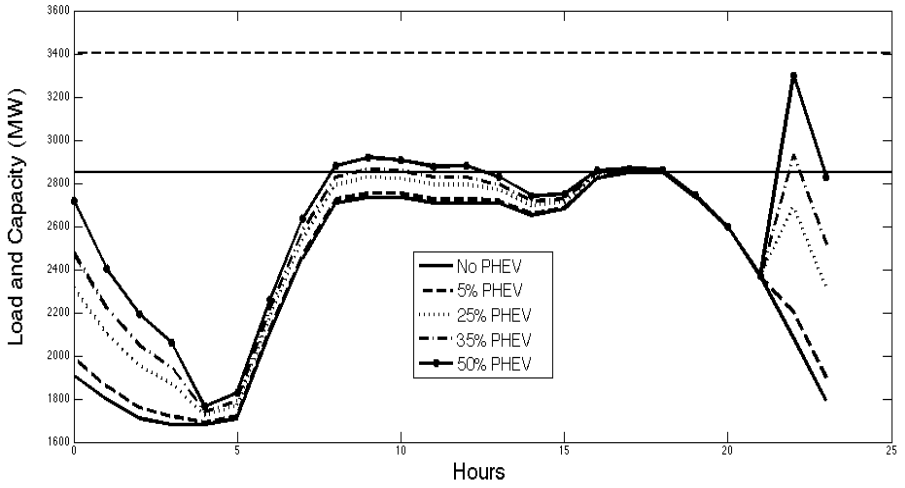

Figure 4.25: 24-hour winter load curve when home charging starts at 23:00 with 40% PHEV public charging percentage in different penetration levels

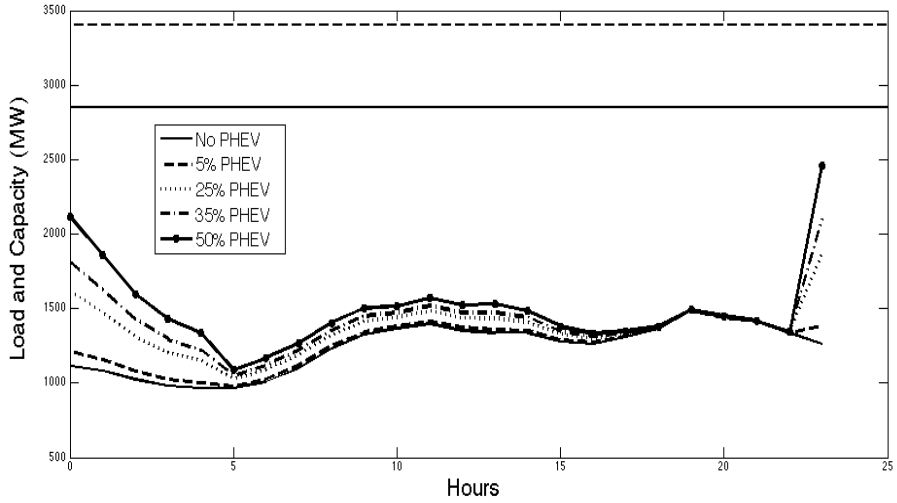

Figure 4.26: 24-hour summer load curve when home charging starts at 00:00 with 40% PHEV public charging percentage in different penetration levels

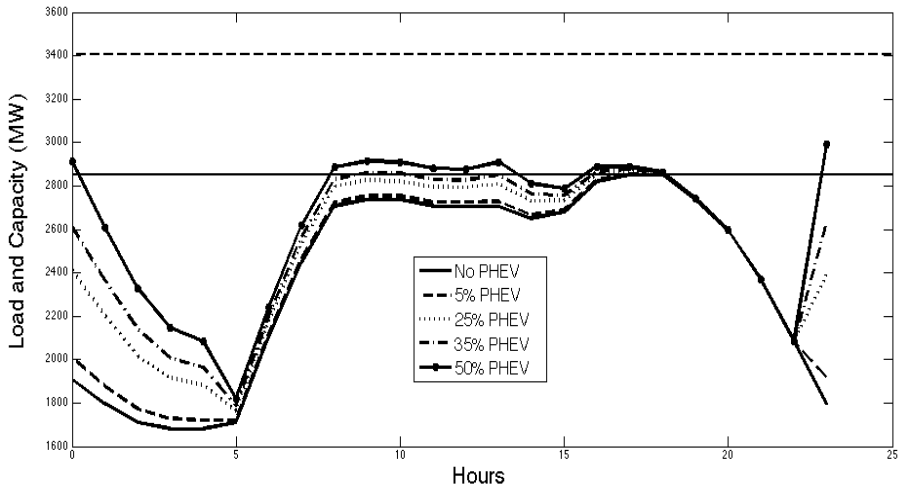

Figure 4.27: 24-hour winter load curve when home charging starts at 00:00 with 40% PHEV public charging percentage in different penetration levels

From the above figures, it can be observed that when home charging is put off to a later time the peak load value of both summer and winter day is decreased. It can be noted in Fig. 4.26 and 4.27, when home charging starts at the midnight the peak load in winter day is only slightly greater than 2850 MW even under the 50% penetration level. Figures 4.28 to 4.31 show annual LDC under different "charging start time" with PHEV penetration levels ranging from 0% to 50%.

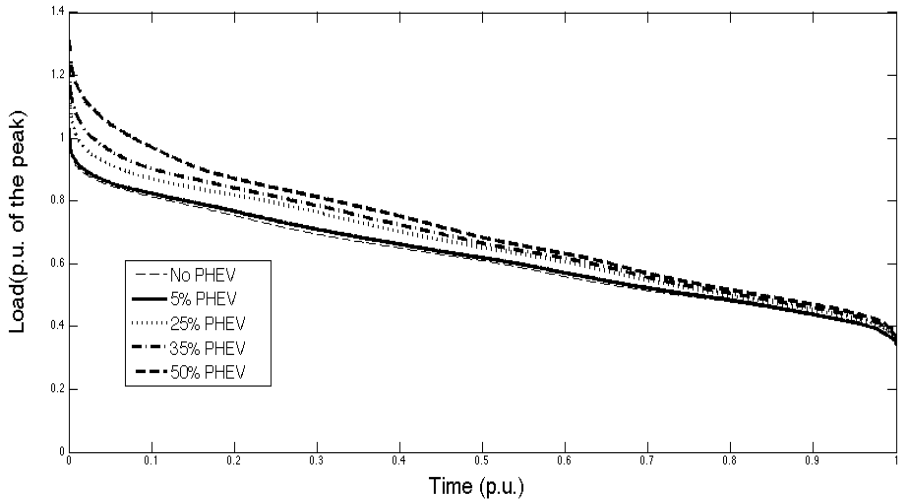

Figure 4.28: System annual LDC when home charging starts at 19:00 with 40% PHEV public charging percentage in different penetration levels

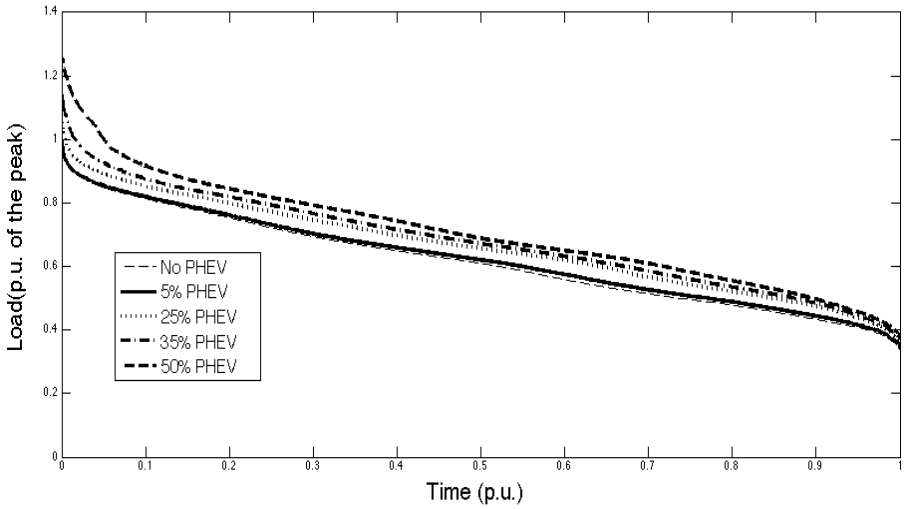

Figure 4.29: System annual LDC when home charging starts at 22:00 with 40% PHEV public charging percentage in different penetration levels

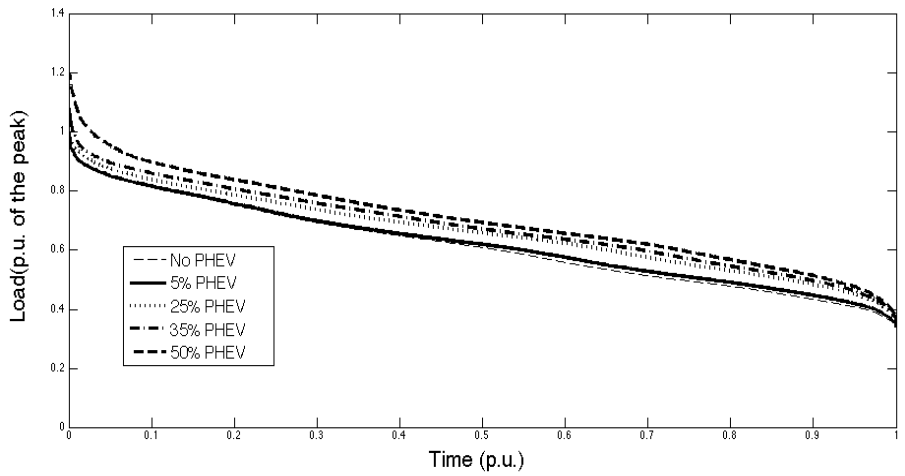

Figure 4.30: System annual LDC when home charging starts at 23:00 with 40% PHEV public charging percentage in different penetration levels

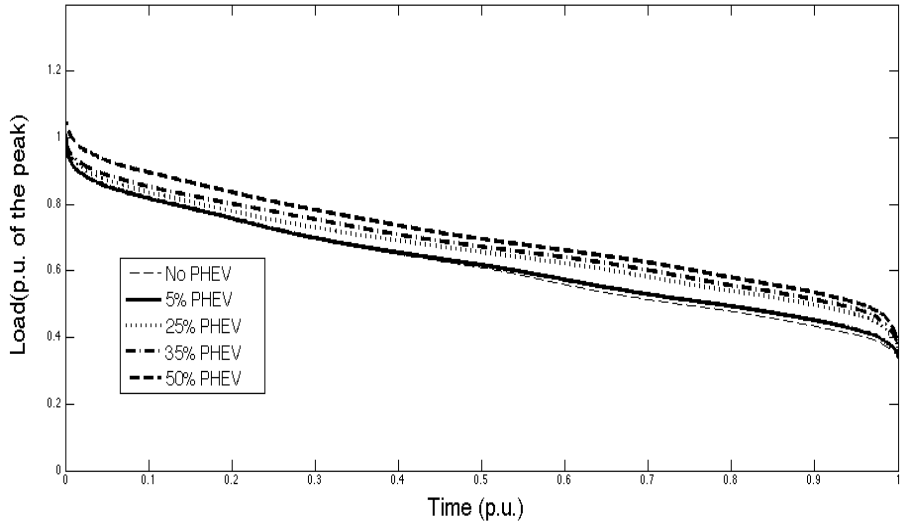

Figure 4.31: System annual LDC when home charging starts at 00:00 with 40% PHEV public charging percentage in different penetration levels

PHEV model under each "charging start time" is developed and combined with system load model, then convolved with the system generation model to obtain the system reliability indices. Table 4.5 presents system LOLE and LOEE under each charging condition.

Table 4.5: System reliability indices with different home charging start time

Home charging start time	PHEV penetration levels	LOLE (hrs/yr)	LOEE (MWh/yr)
	0%	9.418	1.174
19:00	5%	11.349	1.434
	25%	35.878	5.370
	35%	70.577	11.964
	50%	185.476	37.655
22:00	5%	10.103	1.255
	25%	14.965	1.892
	35%	47.915	6.936
	50%	95.997	16.054
23:00	5%	10.103	1.255
	25%	14.764	1.866
	35%	20.794	2.737
	50%	49.596	7.443
00:00	5%	10.030	1.230
	25%	12.331	1.320
	35%	16.126	1.686
	50%	18.988	2.058

The results of system LOLE and LOEE as shown in Table 4.5 are regrouped according to PHEV penetration level and shown in Fig. 4.32 and 4.33. It can been observed in these figures that controlling "charging start time" has little impact on system reliability at 5% PHEV penetration level. But the impact on system reliability increases with the increasing of PHEV penetration. It can be seen that the system LOLE and LOEE are the highest when the "charging start time" is specified to 19:00 hours. This is because the diurnal peak household load occurs between 19:00 and 20:00 hours. As the "charging start time" is moved to later at night, system reliability is improved. It can be seen that even at 50% PHEV penetration the adverse impact on reliability is greatly reduced when the vehicles start to charge at 00:00 hours. Using normal charging scenario, these vehicles can be fully charged at 07:00 in the morning theoretically according to Table 3.1, and is acceptable to most people who need to drive the vehicle to work. If a charging time later than midnight is taken, system reliability can be improved effectively. But it is not a practical proposal from the owners' point of view because they expect their vehicles are fully charged before they head to work. Therefore, in this study 00:00 is the

suggested "charging start time" to improve system reliability without sacrificing normal utilization of PHEV.

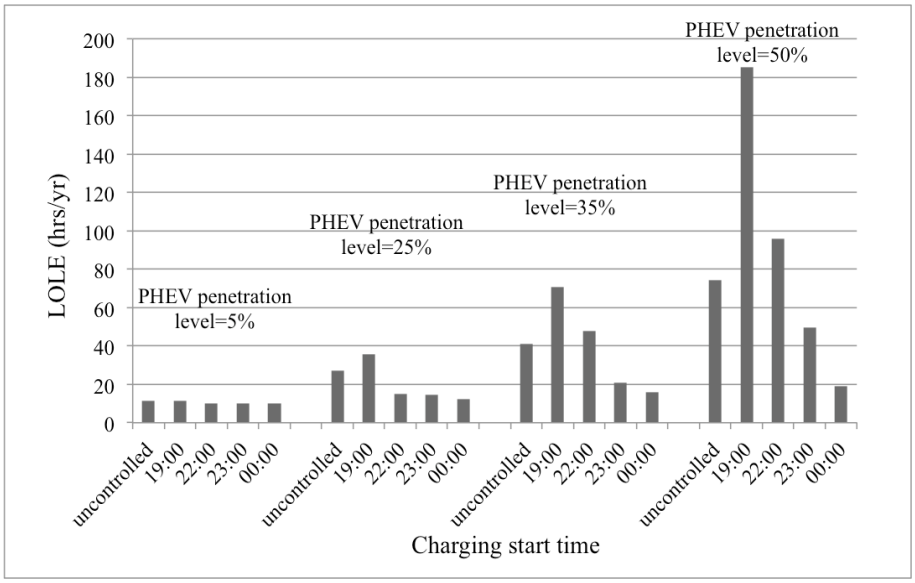

Figure 4.32: System LOLE of different charging start time in different PHEV penetration levels

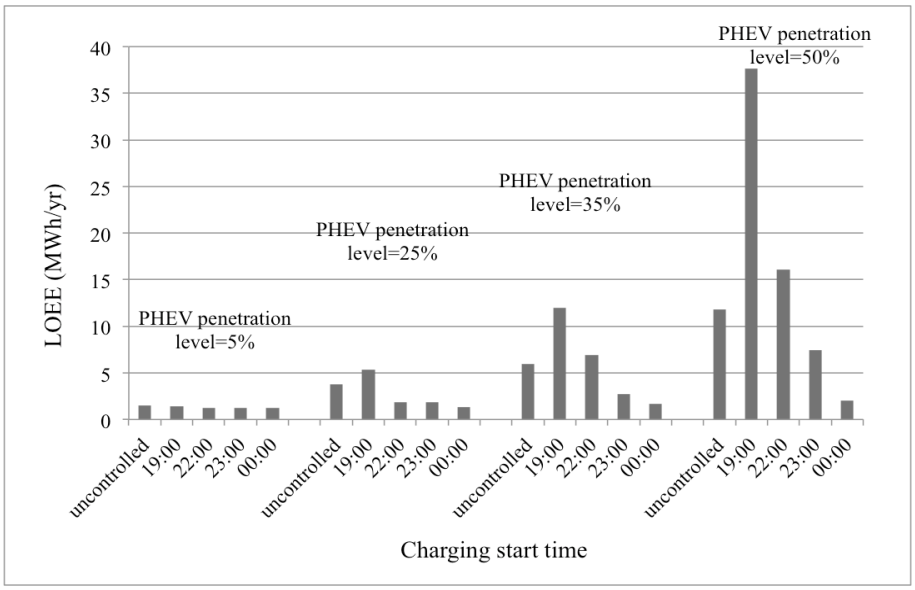

Figure 4.33: System LOEE of different charging start time in different PHEV penetration levels

Capacity Reserve Margin (CRM) is another index that can be used to describe system reliability. It is defined as Equation (4.1). In this section, the system reliability is evaluated by calculating CRM when the charging control methods proposed above are utilized.

$$CRM = \frac{InstalledCapacity - PeakLoad}{InstalledCapacity} * 100\% \quad (4.1)$$

For different "charging start time", peak load value in Equation (4.1) can be obtained through the developed PHEV modeling programs. From the previous studies we can see the PHEV impacts on IEEE-RTS vary significantly between the summer and winter. In this section, the period analysis is carried out to incorporate the seasonality effect on the system reliability. Fig. 4.34 and Fig. 4.35 show the system CRM when PHEV penetration level is 50% and public charging percentage is 40%.

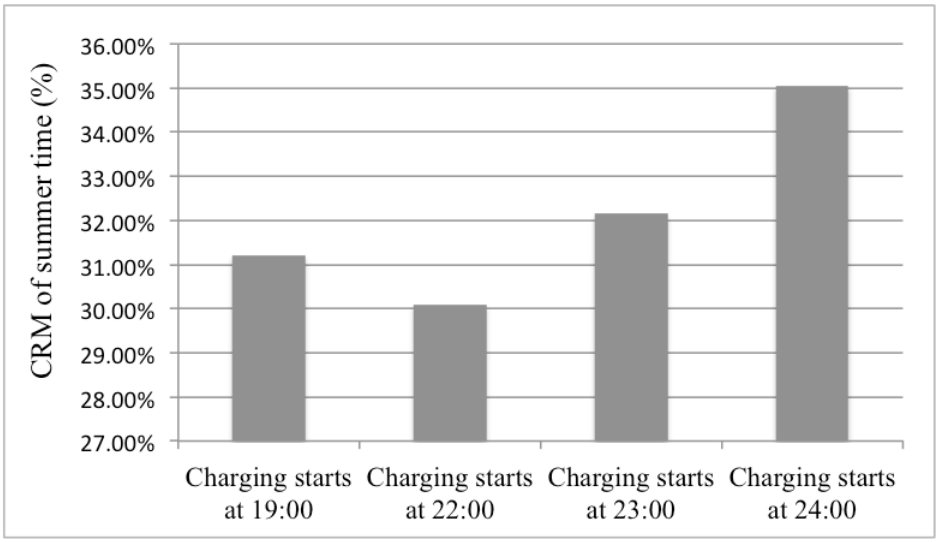

Figure 4.34: CRM of summer period for different charging start time

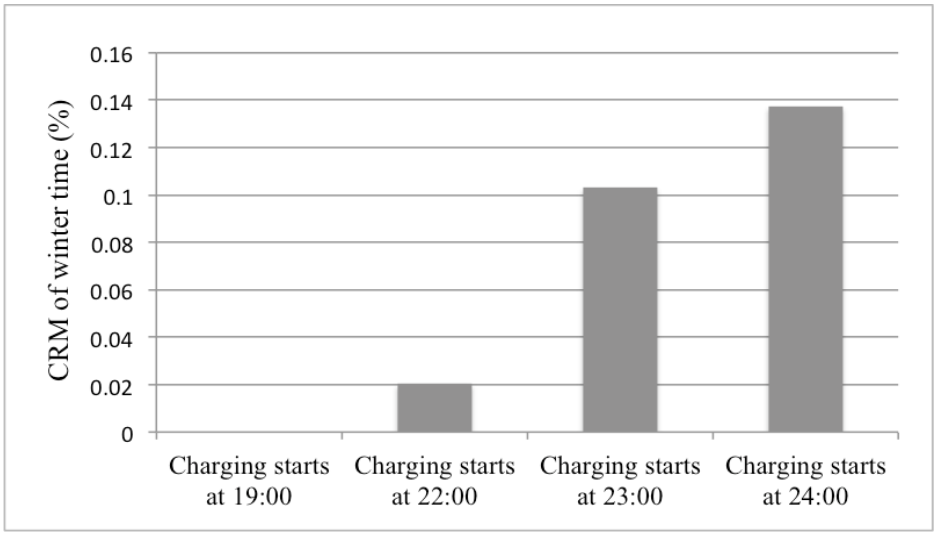

Figure 4.35: CRM of winter period for different charging start time

Fig. 4.34 indicates that system CRM is abundent for all cases in summer time because of the light household load in summer that lead to a consistant conclusion with previous studies when LOLE and LOEE are considered. System CRM is subjected to a significant change when winter months are considered. From Fig. 4.35 we can see if there is no rational management applied in PHEV charging, system reliability would be in a critical condition after numerous PHEV are injected in winter time. Especially when 19:00 is chosen to be the charging start time, system peak load value is even higher than installed capacity.

4.4.2 Determining Public Charging Percentage for Optimal Reliability Benefit

It was assumed in the study of last section that 40% of PHEV could be charged through public charging. However, it is possible to have more or less PHEV charged in public. And it is also possible to improve system reliability through combining control of charging start time and management of public charging percentage. Therefore, the impact of public charging percentage on system reliability when PHEV nighttime charging starts at 00:00 is discussed in this section.

As shown in previous studies, the percentage of PHEV that have access to public charging is varied from 0% to 80% in increments of 20%. 0% public charging means all PHEV are subjected to home charging only. PHEV models were developed considering controlled home

charging start time of 00:00 and public charging scenario considering two charging cycles in a day. The public charging start time can be obtained using Equation (3.4), and the PHEV load model for this charging cycle is repeatedly simulated considering the specified percentage of PHEV that have access to public charging facility. PHEV load model obtained from the two charging cycles can be combined with the original load model, and convolved with the system generation model to obtain the system reliability indices. The system LOLE and LOEE are shown in Fig. 4.36 and 4.37.

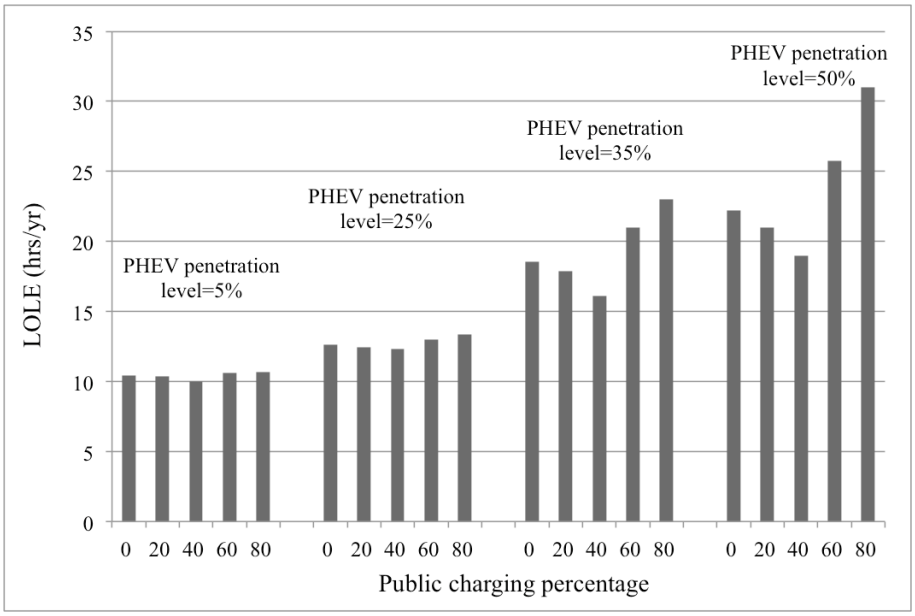

Figure 4.36: System LOLE when different public charging percentages applied to different PHEV penetration levels

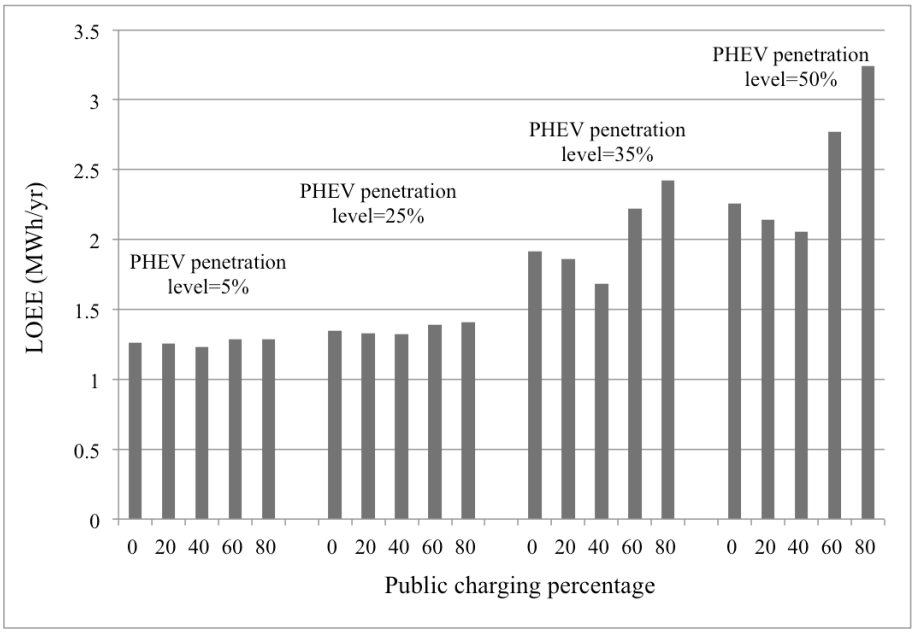

Figure 4.37: System LOEE when different public charging percentages applied to different PHEV penetration levels

Under a specific PHEV penetration level, as the public charging percentage increases from 0% to 40%, both the LOLE and the LOEE indices decrease. The reduction in LOLE and LOEE or the improvement in system reliability is due to some of the evening load being shifted to the daytime and causing the overall system load to decrease. On the other hand, it can be seen from these two figures that when public charging percentage is further increased greater than 40%, the LOLE and LOEE indices begin to increase. This is because the daytime load exceeds the evening load and causes the overall system reliability to degrade. The daytime load can quickly rise with further increase in public charging since "fast charging" method is assumed for this scenario to supply the required energy at high power and less time. When public charging percentage is under 40%, system reliability mainly depends on power demand during the evening influenced by home charging. As public charging is increased above 40%, there are two demand peaks in a day of comparable magnitudes, and they adversely affect the system reliability. Therefore, it is recommended to introduce a policy to provided public charging access to 40% of the PHEV that are primarily charged at home. Further increase or decrease from this ratio results in a degradation of system reliability.

4.5 Summary

The chapter presents system reliability analysis on HL-I considering PHEV charging behavior. PHEV characteristics, such as driving distance, charging times and charging locations are incorporated in reliability analysis by carrying out various charging scenarios. A specific PHEV load model under each charging scenario is combined analytically with the system load and generation models to obtain system reliability indices. The results show that the system reliability degrades very sharply to unacceptable levels with increase in PHEV penetration if no control measures are established for PHEV charging. The study results show that the system reliability is highly dependent on the time that users start to charge their vehicles after they arrive home in the evening. The system reliability can be improved by implementing a mechanism to encourage the users to postpone PHEV charging until later in the evening. The best results are achieved when PHEV start charging at midnight. The impact of introducing a policy to control the percentage of PHEV access to public charging is also investigated. A variation in this percentage resulted in significant changes to the overall system reliability. Based on the results shown in this chapter, it is recommended that some policy should be promoted to limit PHEV public charging percentage to 40%. Further increase or decrease from this ratio results in a degradation of system reliability. The developed PHEV reliability models, and the presented methodology for power system reliability evaluation incorporating PHEV penetration is useful to power system planners, policy makers and PHEV manufacturers as well. The results presented in this chapter will make valuable contribution in providing relevant inputs in decision making for future power systems that are expected to support an increasing penetration of PHEV.

5 BULK SYSTEM RELIABILITY EVALUATION INCORPORATION PHEV LOAD

5.1 Introduction

System reliability analysis can be carried out at different hierarchical levels by combining the three functional zones of generation, transmission and distribution as described in Chapter 1. Chapter 4 presents HL-I evaluation of the IEEE-RTS. This chapter focuses on HL-II analysis, which includes both the generation and transmission facilities, in order to evaluate the influence of PHEV on bulk system reliability.

5.2 Reliability Studies on HL-II of PHEV in the IEEE-RTS

The IEEE-RTS contains 24 buses, which include 10 generating buses, 10 load buses, and 4 connection buses, connected by 33 lines and 5 autotransformers at two voltage levels: 138 kV and 230 kV. A single line diagram of the IEEE-RTS is shown in Fig. 5.1 highlighting the six buses selected for connecting PHEV to conduct HL-II studies.

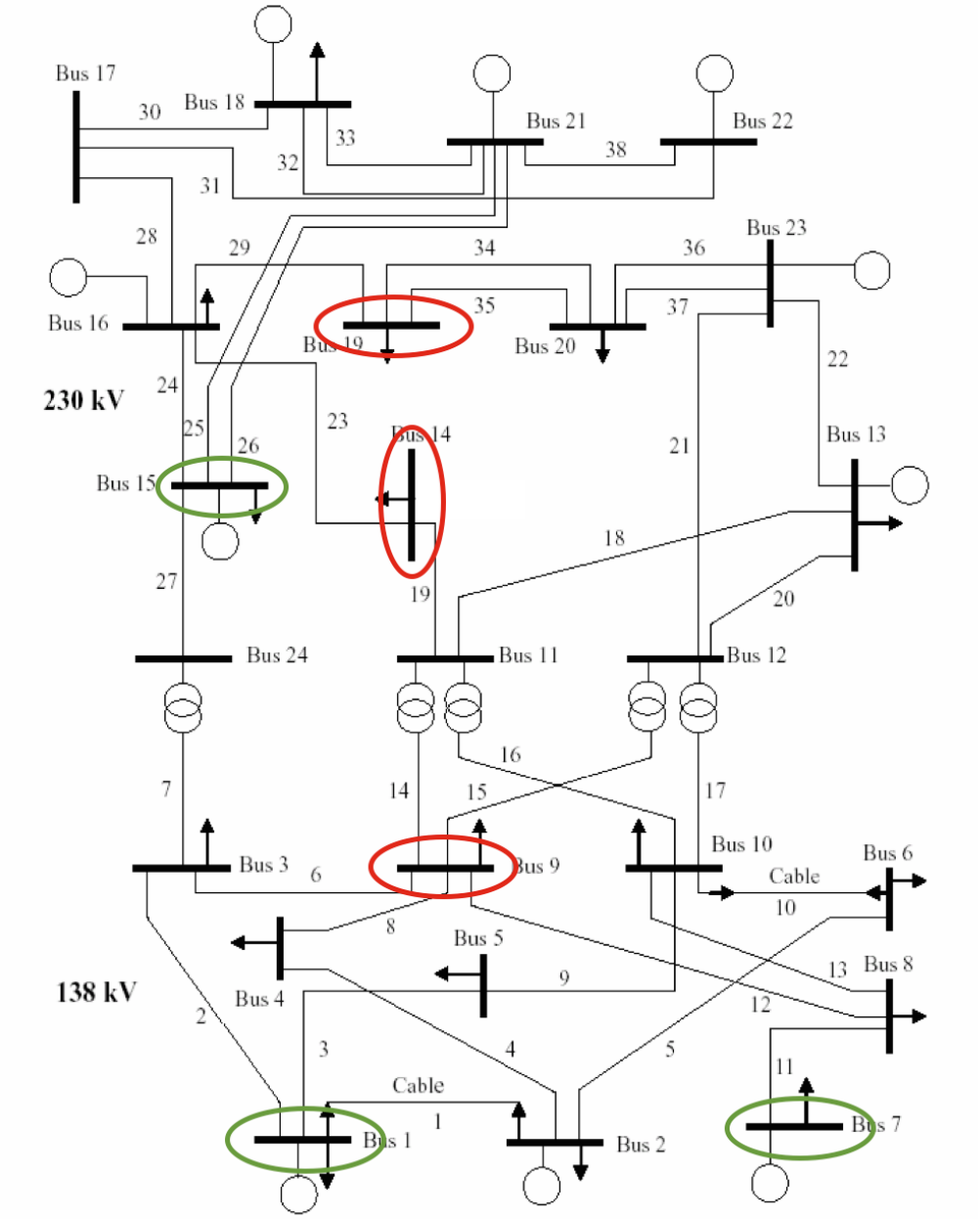

Figure 5.1: Single line diagram of the IEEE-RTS highlighting selected buses for HL-II studies

The six buses can be classified into two groups depending on whether generators are connected to a particular bus. Bus 9, 14 and 15 are non-generator buses. The generating capacity and load connected to the six buses are shown in Table 5.1. It can be seen from the table and from Fig. 5.1 that there are three buses chosen at each voltage level.

Table 5.1: Data of six buses in IEEE-RTS

Bus No.	Bus Voltage (kV)	Generating Units Capacity (MW)	Load Level (MW)
1	138 kV	192	108
7	138 kV	300	125
9	138 kV	None	175
14	230 kV	None	194
15	230 kV	215	317
19	230 kV	None	181

The MECORE software is used for HL-II reliability analysis in the studies. The original program was modified to incorporate renewable generators by making changes to the input file, and can also accept customized load model. Reliability indices for individual load points and for the overall system can be obtained. The program has the capability to perform load shedding during an outage condition based on the priority order of the load buses. There are different methods to assign priority order of each load bus, but a common approach is to rank the buses based on the customer costs associated with power interruptions. In the IEEE-RTS, the priority order of each bus is determined by the Interrupted Energy Assessment Rate (IEAR), which is an index commonly used to measures the customer monetary loss as a function of the energy not supplied [1]. The higher the IEAR, the greater the outage costs at the load point, and therefore, is assigned a higher priority. The IEAR values for each load bus in the IEEE-RTS and the corresponding priority order are shown in Table 5.2. The six buses mentioned above are highlighted in grey.

Table 5.2: Bus IEAR values and priority order in the IEEE-RTS

Bus No.	IEAR ($/kWh)	Priority Order
1	6.20	1
2	4.89	9
3	5.30	8
4	5.62	3
5	6.11	2
6	5.50	4
7	5.41	5
8	5.40	6
9	2.30	16
10	4.14	10
13	5.39	7
14	3.41	14
15	3.01	15
16	3.54	13
18	3.75	11
19	2.29	17
20	3.64	12

The MECORE software was originally designed to consider the same load profile for all the load buses. But when PHEV is integrated in a power system, its penetration can vary significantly at different buses, and also be subjected to different charging models. Public charging will likely occur in parking lots in business area, influencing the commercial load profile, whereas, home charging will affect the residential load profile. The resulting modified load profiles at the different load buses will therefore be substantially different. The original load profile will not be affected in the buses without PHEV. It is therefore required to consider different load profiles at different load buses when reliability evaluation is done considering PHEV fleets. MECORE has an option to consider different fixed loads at the different buses, but this option cannot incorporate the entire load profiles in the assessment. A bridge program in Visual Basic was developed in this work to run MECORE repeatedly in a loop to create different load profiles at different buses using a conditional probability method. The simulation is carried out with different fixed load levels at the different buses during each loop and the

multiply risk indices obtained during each loop are multiplied by the corresponding probabilities of each load level to obtain the expected load point and system indices. This program is able to expand MECORE's function to incorporate different types of load profiles at different buses of a power system. In this work, both the system load and the PHEV load are represented by a 20-state load model. The load profile of PHEV fleet depends on the charging scenarios.

A study was carried out by considering PHEV load ranging from 30 MW to 300 MW added to the six buses of the IEEE-RTS. The corresponding PHEV penetration range is from 1% to 10% of the system original peak load. Similar to HL-I analysis, three charging scenarios are considered in HL-II studies, which are "home charging", "public/home charging" and delayed "public/home charging". They are designated as charging scenario "H", "HP" and "HPD", respectively in this thesis. For home charging behavior in "H" and "HP" scenario, it is assumed that PHEV starts charging as soon as it arrives home at the end of a day if battery SOC falls below 0.8. In the "HP" scenario, PHEV with full battery is discharged in the morning as the vehicle is driven to work, and public charging behavior starts as soon as PHEV arrives public location with fast charging facilities. PHEV would be discharged again on the way home. The charging start time of "home charging" is delayed to 00:00 in the "HPD" scenario. It is assumed in all cases that 40% of the PHEV have access for "public charging".

The PHEV load is first added to the three generating buses, Bus 1, 7 and 15. A range of penetration levels and three charging scenarios are considered in the study. The EDLC and EENS are the system reliability indices evaluated in the HL-II analysis. Fig. 5.2 presents the system EDLC when PHEV fleet is connected to Bus 1.

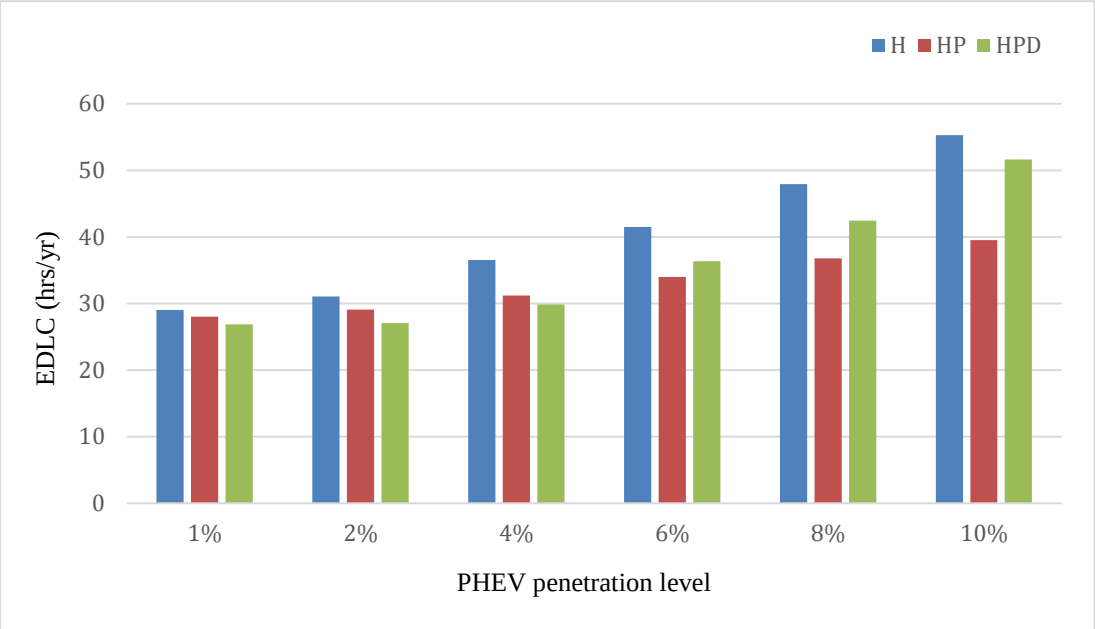

Figure 5.2: System EDLC when PHEV fleet is connected to Bus 1

It can be seen from Fig. 5.2 that the system EDLC increases as the PHEV penetration level increases from 1% to 10% for all the three charging scenarios. This means the system reliability deteriorates as PHEV penetration is increases in a power system. At a relatively low PHEV penetration level (i.e. between 1% to 4%), the EDLC is the highest under the "H" scenario and the "HPD" is the most beneficial charging scenario for system reliability. This is because the delay in home charging avoids the overlap between the PHEV demand and the system evening peak demand. With further increases in PHEV penetration level, the system EDLC increases sharply for the "HPD" scenarios. The reason for this phenomenon is that a new peak load will be created at 00:00 hours when a large number of PHEV start charging at this time simultaneously and cause congestion in transmission lines. When PHEV penetration level is higher than 6%, the "HP" scenario is the best choice for PHEV charging. "Public charging" during the daytime can release some pressure of "home charging". Fig. 5.3 shows that the system EENS shows similar characteristics as that of the EDLC indices.

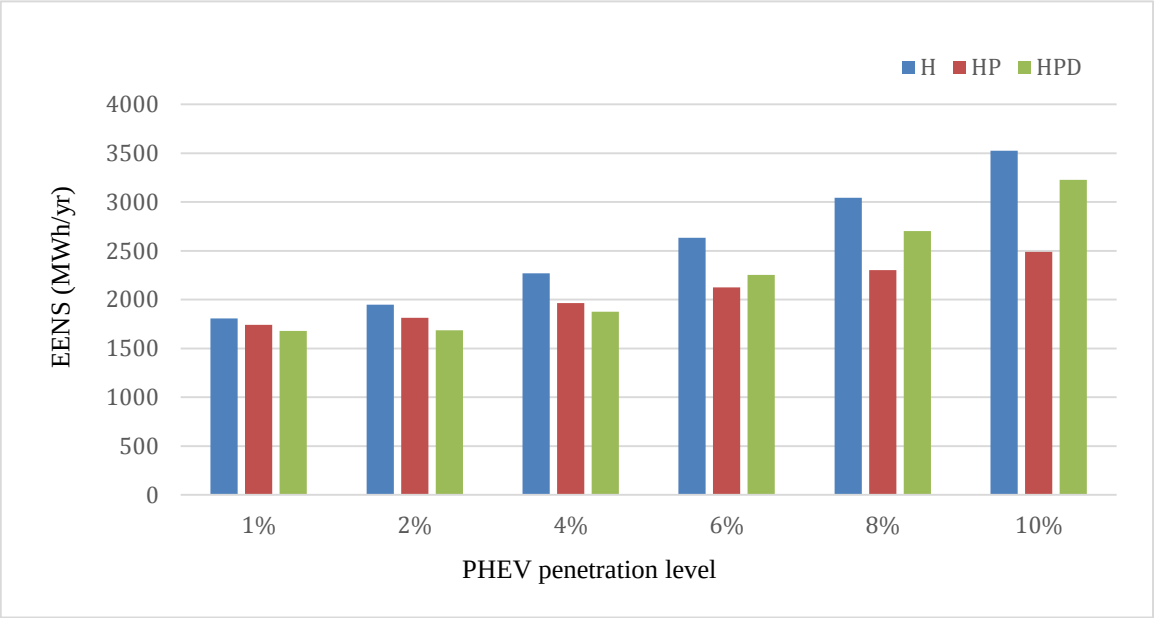

Figure 5.3: System EENS when PHEV fleet is connected to Bus 1

A similar study was carried out by adding the PHEV to Bus 7, and it can be seen in Fig. 5.4 and 5.5 that the two indices EDLC and EENS show a similar characteristic with increase in PHEV penetration as in the previous case when the PHEV were added to Bus 1.

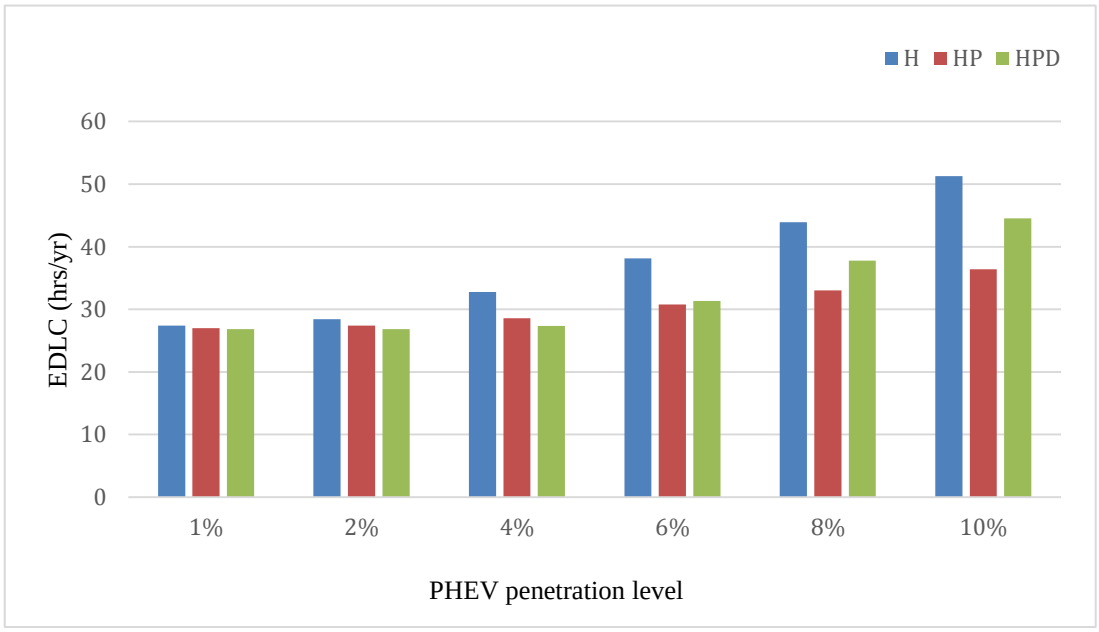

Figure 5.4: System EDLC when PHEV fleet is connected to Bus 7

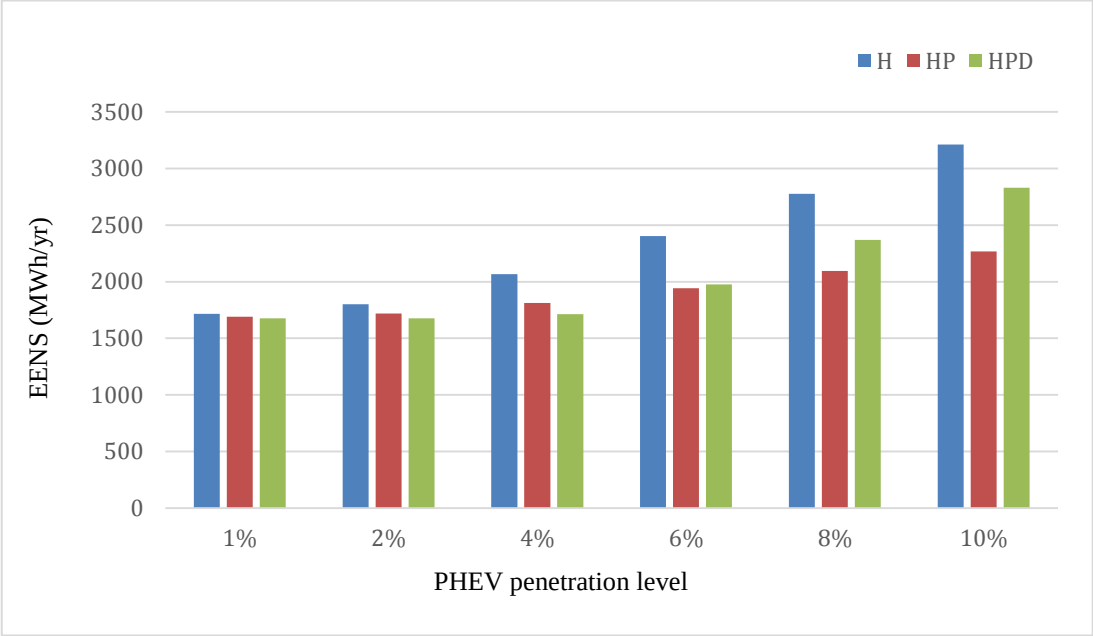

Figure 5.5: System EENS when PHEV fleet is connected to Bus 7

Fig. 5.4 shows that the system EDLC for the Bus 7 study is lower than that of the Bus 1 study for a given charging scenario and PHEV penetration level. It can be noted from Fig. 5.1 that there are three transmission lines connected to Bus 1 and only one connected to Bus 7, which indicates that adjacent buses could share load on Bus 1 more effectively than Bus 7. According to Table 5.1, there is generating capacity of 300 MW with load level of 125 MW on Bus7, whereas, Bus 1 has 192 MW generating capacity with 108 MW of load. The margin between generating capacity and the bus load is wider for Bus 7 in comparing to Bus 1, which indicates Bus 7 can satisfy additional PHEV load without causing congestion in the transmission line. When PHEV load is increased at Bus 1, there is inadequate local generating capacity, and therefore, other buses will provide power through transmission lines making the system less reliable due to increased transmission congestion.

Fig. 5.6 and 5.7 shows the system EDLC and EENS when PHEV load is added to Bus 15.

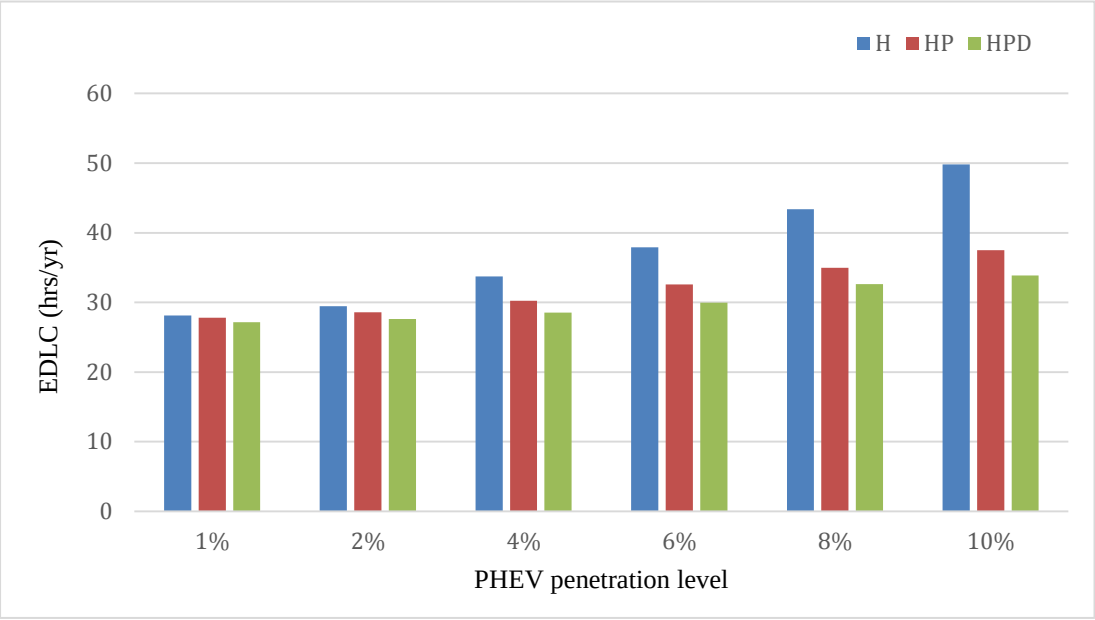

Figure 5.6: System EDLC when PHEV fleet is connected to Bus 15

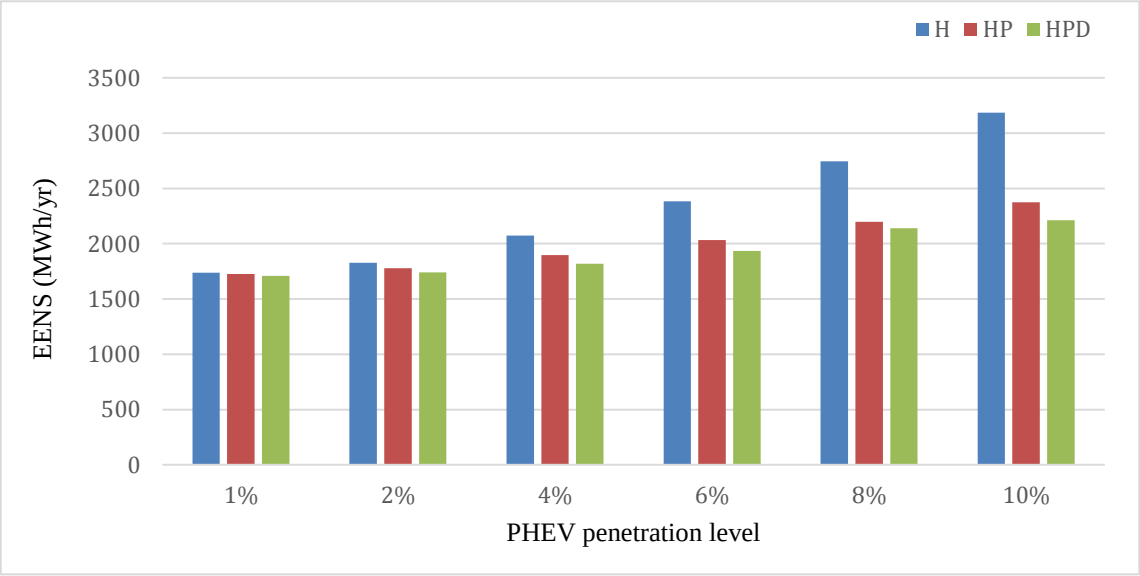

Figure 5.7: System EENS when PHEV fleet is connected to Bus 15

The system EDLC and EENS increases as PHEV penetration increases for each charging scenario, which are similar results to the cases when PHEV are added to Bus 1 and Bus 7. Contrary to the results for Bus 1 and Bus 7 studies, the "HPD" scenario provides the highest level of system reliability when PHEV is added to Bus 15. It can be observed from Fig. 5.1 that there are four transmission lines connected to Bus 15. The generating capacity is 317 MW at Bus 15 and the load level is 215 MW. For the same PHEV penetration and charging scenario,

the system reliability indices are lowest when Bus 15 is the PHEV charging location among the three generating buses shown previously. The results for the Bus 15 study are similar to the results obtained in the HL-I analysis. It can therefore be concluded that when PHEV is added to a bus that is connected to multiple transmission lines with large transfer capacity, the results obtained are close to HL-I results, as the effect of transmission is insignificant in such cases.

Fig. 5.2 to 5.7 show system reliability indices when PHEV load is added to a generating bus. The second group of buses chosen in the IEEE-RTS is the group of non-generating buses. Studies were carried out to assess the impact on system reliability of adding PHEV to non-generating buses. Fig. 5.8 and Fig. 5.9 present system EDLC and EENS considering Bus 9 as the PHEV charging location.

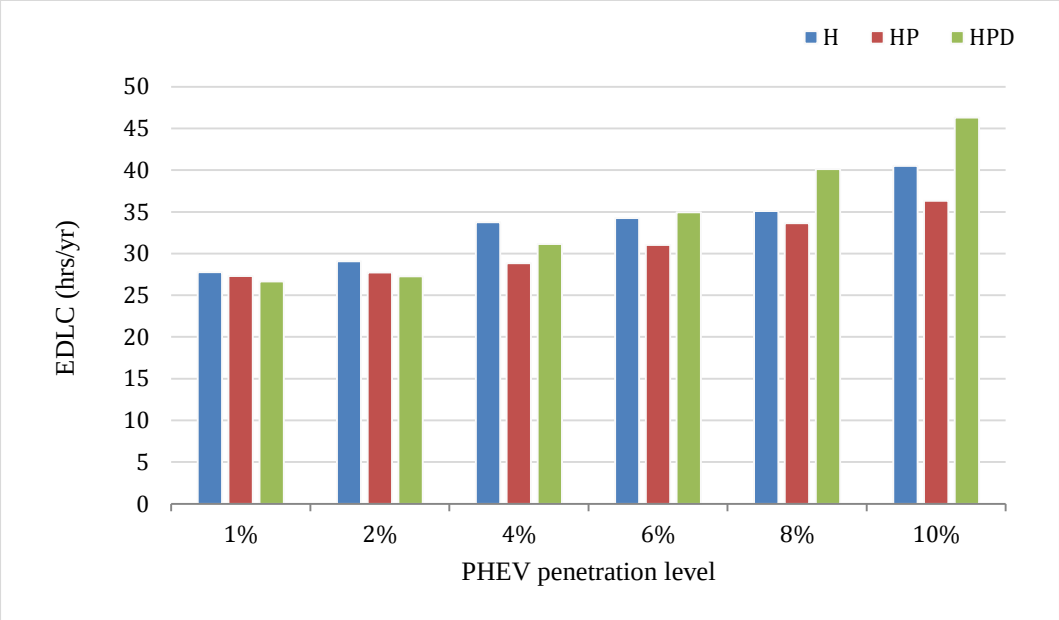

Figure 5.8: System EDLC when PHEV fleet is connected to Bus 9

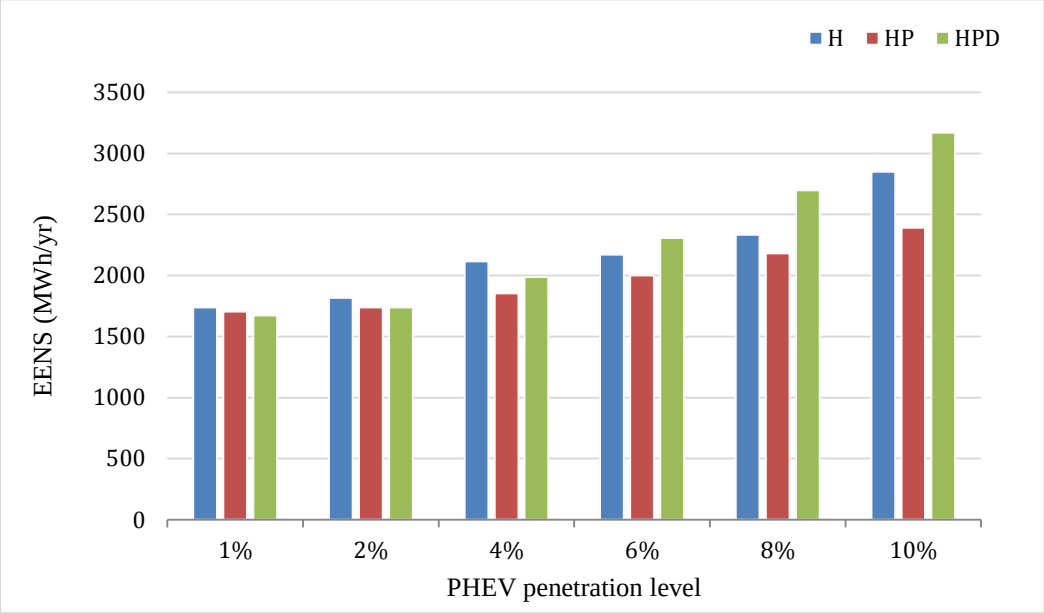

Figure 5.9: System EENS when PHEV fleet is connected to Bus 9

It can be seen from the above figures that the system EENS and EDLC under the "HPD" scenario is the lowest among the three scenarios when PHEV penetration level is lower than 4%. At 4% PHEV penetration level, both the indices under the "HPD" scenario increase significantly and become larger than those for the "HP" scenario. When the PHEV penetration is more than 6%, the "HPD" scenario becomes the worst option among three charging scenarios, and the "HP" becomes the best scenario for system reliability. It can be seen from Fig. 5.1 that there are five transmission lines connected to Bus 9, therefore other buses can supply power to meet the additional PHEV load. However, since there is no generating source at Bus 9, the system reliability will be deteriorated when PHEV charging creates load peak, which occurs for the "H" and "HPD" scenarios at 4% penetration. If Fig. 5.8 is compared with Fig. 5.2, it can be observed that system EDLC is higher when PHEV are charged on Bus 1 than Bus 9, which is because of different connections on these two buses. Bus 1 has three transmissions lines connected, 192 MW generating capacity and 108 MW load level. Bus 9 is without generating unit but has five transmission lines connected. Therefore, when relatively large amount of PHEV are connected for charging, Bus 9 is more beneficial for system reliability comparing to Bus 1.

Studies were also carried out to evaluate the impact of PHEV penetration at 230 kV buses by considering PHEV additions to Bus 14 and 19. The results of the system EDLC and EENS are shown in Figures 5.10 to 5.13.

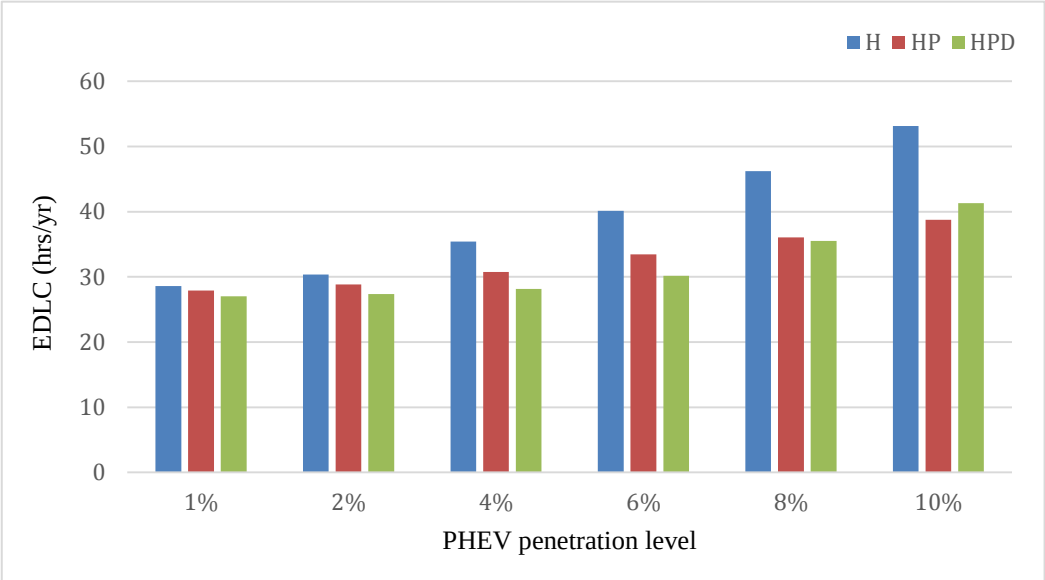

Figure 5.10: System EDLC when PHEV fleet is connected to Bus 14

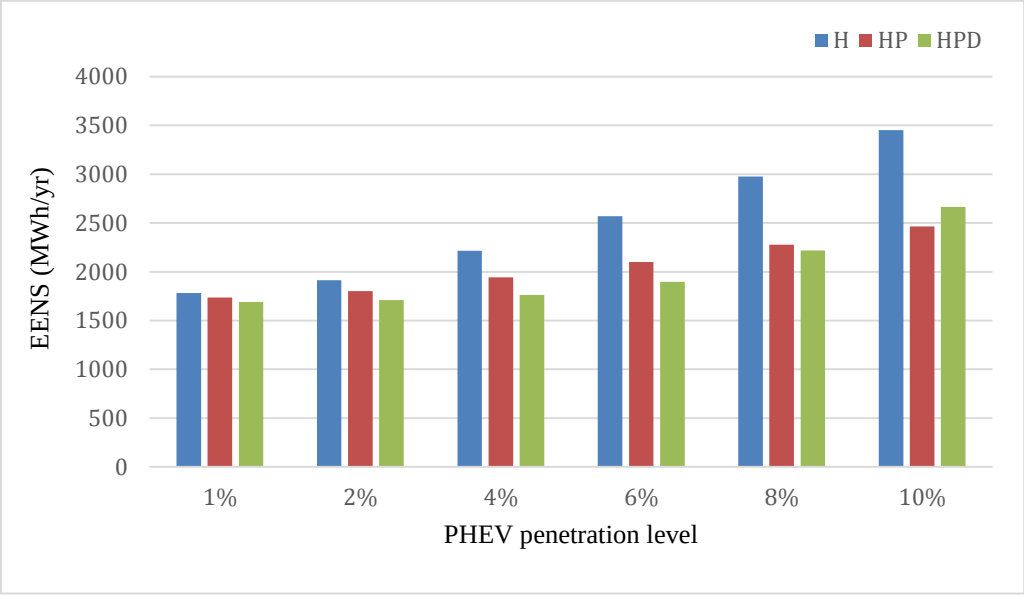

Figure 5.11: System EENS when PHEV fleet is connected to Bus 14

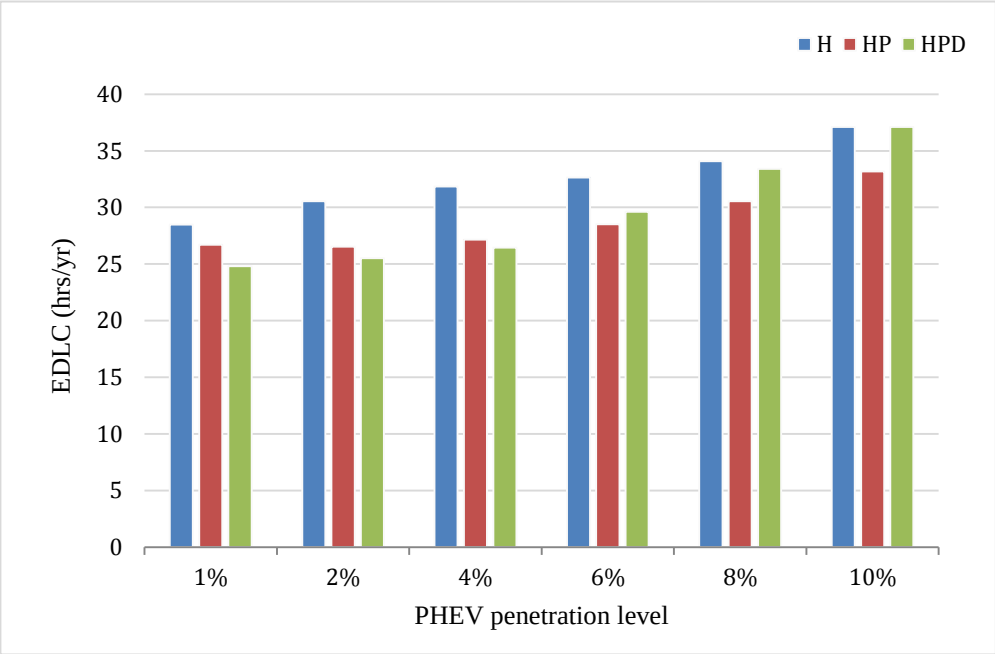

Figure 5.12: System EDLC when PHEV fleet is connected to Bus 19

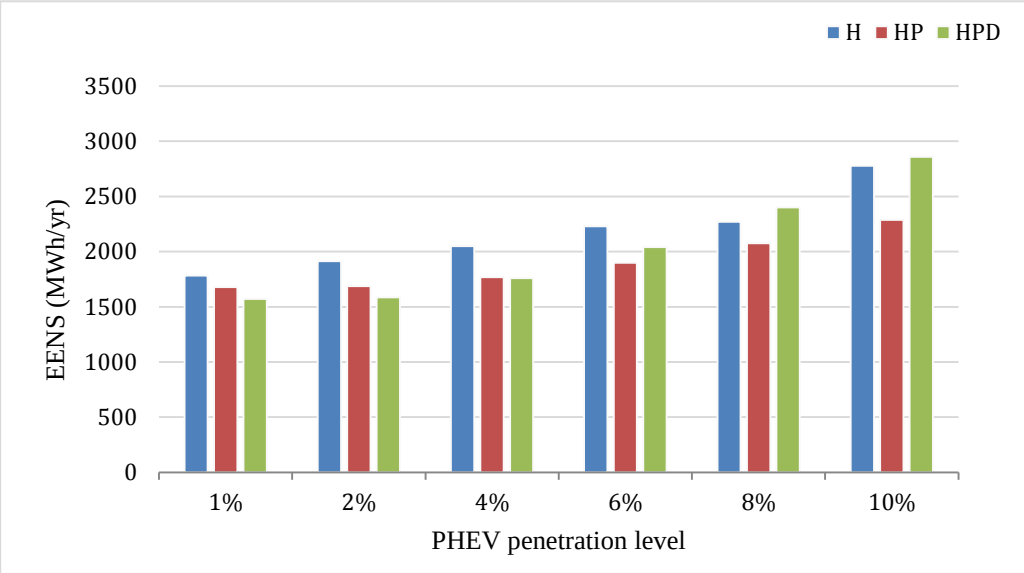

Figure 5.13: System EENS when PHEV fleet is connected to Bus 19

A comparison of the system EDLC in Fig. 5.10 and 5.12 shows that the system EDLC with PHEV connected to Bus 14 is higher than the case of Bus 19 under the same PHEV penetration and charging scenarios, which can be explained by fewer transmission lines and higher load at Bus 14 and at Bus 9. Bus 14 is connected to two transmission lines and Bus 19 to three transmission lines. The load level of Bus 14 and Bus 19 is 194 MW and 181 MW respectively. From the results and discussion presented above, it can be concluded that bulk system

reliability is determined by generation capacity and load level at the different buses, as well as the capability and the number of transmission lines available to transfer the capacity to the load points.

Fig. 5.14 shows the system EDLC when different amounts of PHEV are located at Buses 1, 7 and 15 respectively considering the "HPD" charging scenario. These three buses also have generating units connected to them. Similarly, Fig. 5.15 shows the system EDLC when PHEV are located at non-generating buses, Bus 9, 14 and 19. EENS remains similar shape to EDLC, therefore it is not shown here.

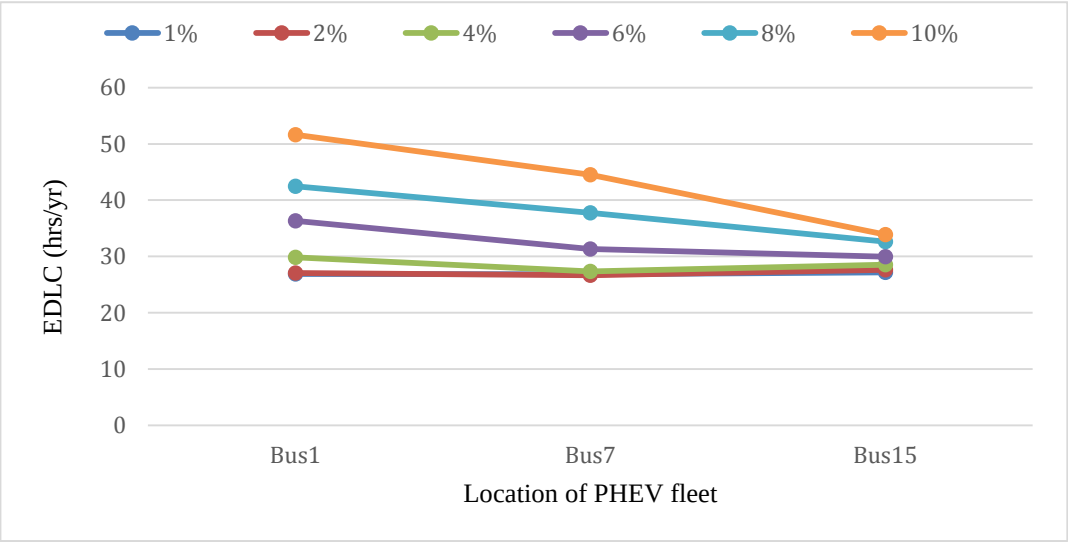

Figure 5.14: System EDLC when PHEV fleet is added to a particular generator bus

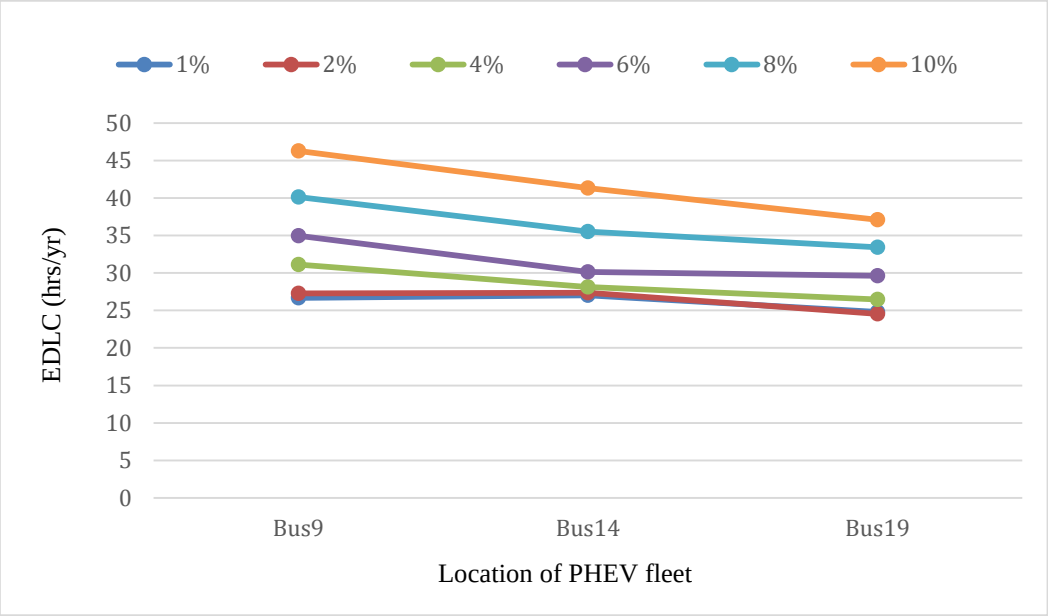

Figure 5.15: System EDLC when PHEV fleet is added to a particular non-generator bus

The impacts of the "HPD" scenario on different buses can be observed clearly from the above figures. Among the six buses chosen in the studies, the impact of PHEV penetration on the system EDLC is the lowest on Bus 15, and it is therefore the least sensitive bus to PHEV load increases. This is because Bus 15 has three transmission lines connected to other generator buses and therefore, the additional power can effectively be delivered to the increased PHEV load. On the contrary, Bus 1 and Bus 9 are very sensitive to PHEV penetration. Bus 1 has three transmission lines connected, but only one of them connects to a generator bus. Bus 9 has no connection to a generator bus. We can also see from Fig. 5.14 and 5.15 that the "HPD" scenario can be beneficial to system reliability when PHEV penetration level is under 4%. When the PHEV penetration level is higher than 4%, the system reliability will deteriorate fast.

The results shown above are the system indices. The MECORE software also provides load point indices, which are helpful for comprehensive reliability analysis. Fig. 5.16, 5.17 and 5.18 present the system EENS as well as the EENS at each bus when Bus 9 is PHEV charging location. The system and load point EDLC follow similar trend with EENS and therefore are not shown here.

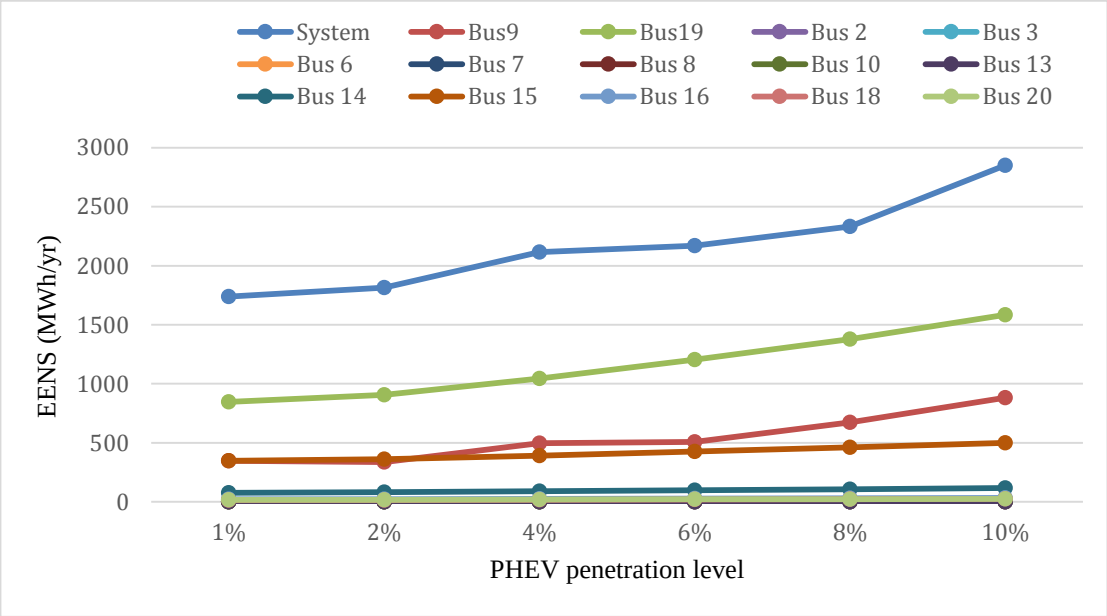

Figure 5.16: System and Bus EENS when PHEV fleet is connected to Bus 9 under the "H" scenario

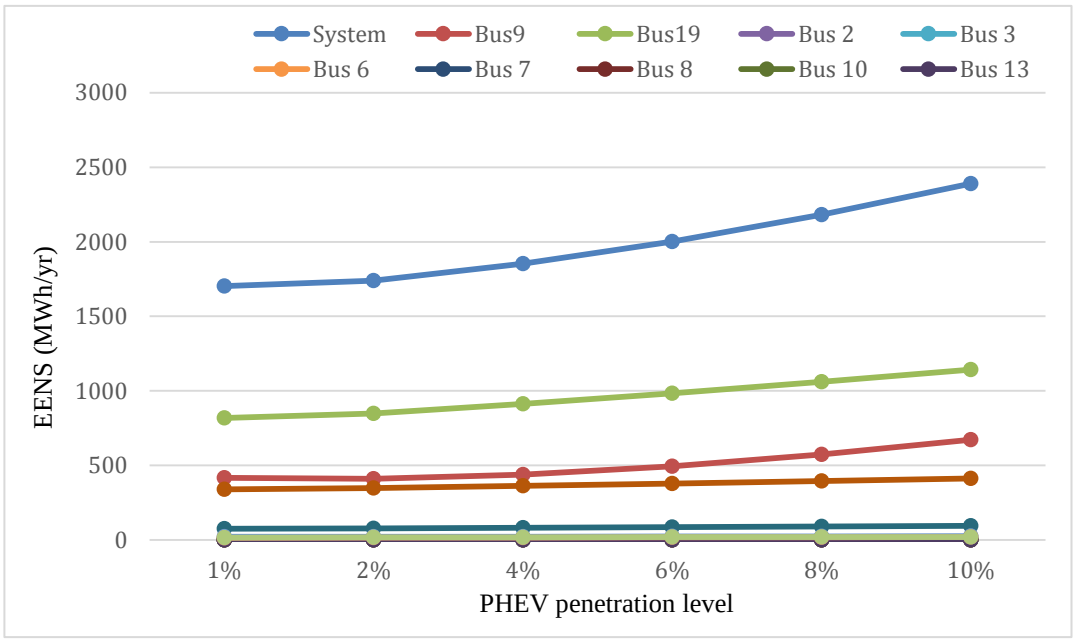

Figure 5.17: System and Bus EENS when PHEV fleet is connected to Bus 9 under the "HP" scenario

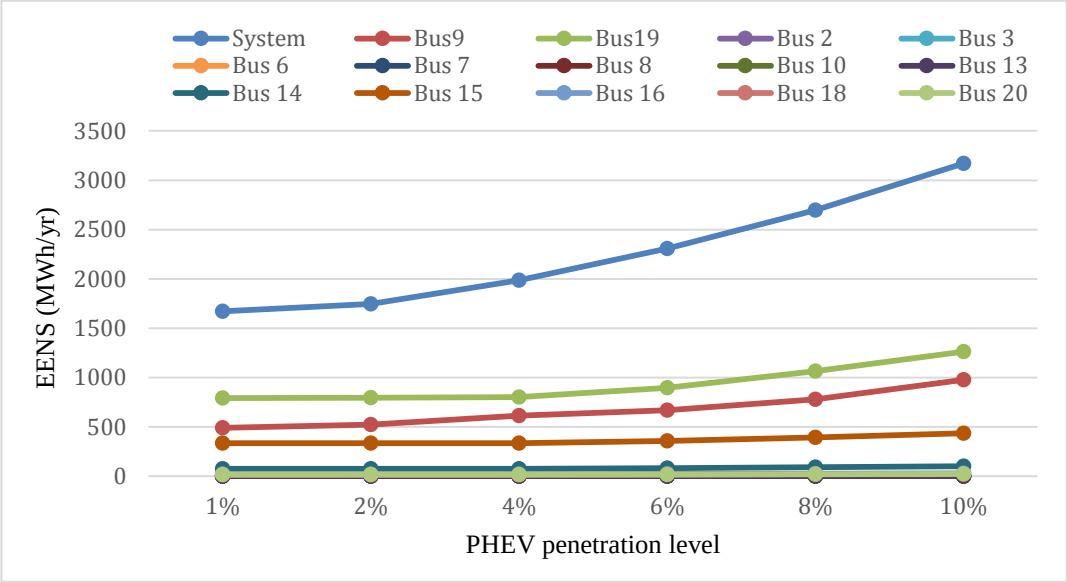

Figure 5.18: System and Bus EENS when PHEV fleet is connected to Bus 9 under the "HPD" scenario

It can be observed from above figures that under the three charging scenarios the system EENS increases when more PHEV are connected to the power system. However, the increment as PHEV penetration level increases is different. Bus 19 and Bus 9 are the two buses with highest and second highest load-point EENS. Fig. 5.16 shows when PHEV penetration level increases from 2% to 4%, there is a significant increase of EENS under the "H" scenario, which is caused by load congestion on Bus 9. As PHEV penetration level increases further, system reliability deteriorates fast under both "H" and "HPD" scenarios. However, the increment of the "HP" scenario is not as significant as the other two scenarios. Therefore, when there are 10% PHEV added to the power system, "HP" scenario is the best PHEV charging scenario. From the results shown above, it is can be observed that "home charging" of PHEV negatively impacts system reliability because of the overlap of charging power demand and system original peak load. The "HPD" scenario can also bring negative effects on system reliability due to the high power demand at the charging start time when large amount of PHEV are connected to the power system. The overload problem causes congestion in transmission lines and deteriorates system reliability, which is the reason why HL-II results are different from HL-I. It can also be seen from the figures that when there are small amount of PHEV injected to the power system, the "HPD" scenario is still the best from system reliability point of view. The number of

transmission lines, generation capacity, and original load level as well as priority order of different buses determine the system reliability when PHEV are connected to different buses for charging.

5.3 Reliability Studies of PHEV and WECS in the IEEE-RTS

In the last few decades the development and utilization of renewable energy sources to satisfy electrical demand has been given considerable attention due to expressed concerns regarding dwindling fossil fuel sources and enhanced public awareness of the potential adverse effects of conventional energy systems on the environment. In various kinds of renewable energy sources, wind is widely considered to be a free, non-depletable and environment friendly energy option. Huge investments are being made in this sector, which have led to considerable advancement in wind power technology. Many wind farms have been successfully operated throughout the world, which illustrates that wind energy is a promising source of alternative energy. In recent years, some scholars are exploring the interplay of electric vehicles and renewable energy. A number of valuable results have been published. Ref. [40] [41] reveal that popularization of PHEV can accommodate renewable generation to a greater extent. Exploring the interaction of wind energy and PHEV load from a system reliability point of view is an interesting perspective that needs to be understood by power system planners to accommodate variable generation sources and new load types in the near future.

A comprehensive model of WECS for the purpose of reliability analysis has been presented in Chapter 2. The WECS model shown in Table 2.3 is incorporated in the HL-II evaluation using the MECORE software. A study is carried out to investigate the impacts of wind generation and PHEV on a power system by considering a 100 MW WECS and PHEV added to the same bus in the IEEE-RTS. Bus 15 and Bus 19 are selected as representatives of generating and non-generating buses. A bulk system reliability evaluation was carried out considering different amounts of PHEV at the wind power integrated bus.

Figures 5.19 shows the system EDLC for the three PHEV charging scenarios when the PHEV and WECS are connected to Bus 15. Fig. 5.20 shows similar results when the PHEV and WECS are at the non-generating bus, Bus 19.

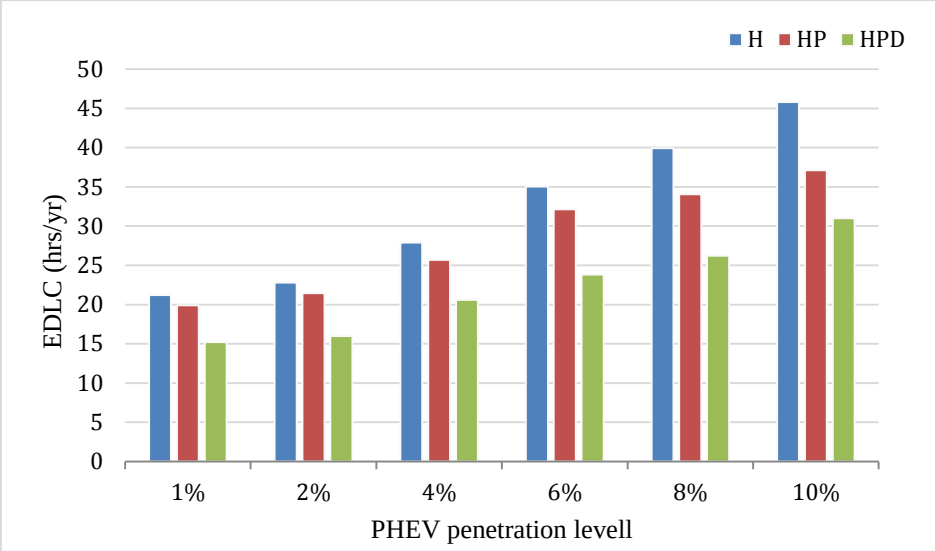

Figure 5.19: System EDLC when PHEV fleet and WECS is connected to Bus 15

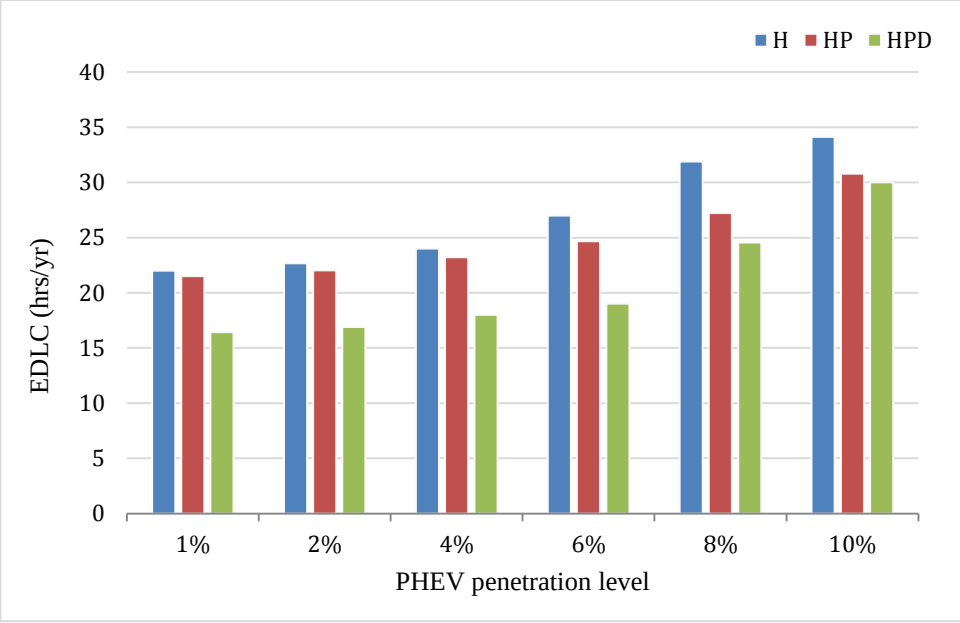

Figure 5.20: System EDLC when PHEV fleet and WECS is connected to Bus 19

The results in Fig. 5.19 and 5.20 can be compared to Fig. 5. 6 and 5.12 where similar studies were carried out without considering wind power. The system EDLC is decreased when 100

MW WECS is added to the system. When PHEV penetration level is lower than 4%, the system EDLC increases slowly in the three charging scenarios as the number of PHEV increases. As PHEV penetration level increases further, system EDLC increases significantly especially under the “H” and “HPD” scenarios. It is because WECS is not able to satisfy the additional load. When Bus 19 is the PHEV charging location, the “HPD” is the most beneficial scenario for system reliability which is not the case when WECS is not added. The benefits of including WECS in the system can be observed as WECS contributes to relieving transmission congestion to some extent, and system reliability can be further improved effectively by delaying home charging start time.

5.4 Summary

This chapter presents HL-II reliability analysis on the IEEE-RTS considering PHEV load injection at different types and locations of network buses. Contrary to the results from the HL-I analysis, bulk system reliability is greatly influenced by transmission line capacity and configurations. Six buses in the IEEE-RTS are selected for the presented studies and divided into two groups of generating and non-generating buses. PHEV penetration level from 1% to 10% is taken into account and PHEV are connected to one bus at a time. The system EDLC and EENS are obtained using the MECORE software. Three different charging scenarios are considered at the different PHEV penetration levels. The results show that the bulk system reliability is influenced by multiple factors, such as, connection structure, generation capacity and original load level of the bus where the PHEV are connected. Generating buses connected to multiple transmission lines can integrate more PHEV load without causing severe reliability problems. However, at relatively high PHEV penetration, the system reliability will deteriorate, and delaying home charging start time cannot improve system reliability. Load congestion caused by starting the PHEV charging at the same time adversely affects system reliability as PHEV penetration is significantly increased. Wind energy is also considered in this chapter as it is a highly attractive generation type which has different characteristics from conventional generators. Studies are presented with WECS added to the PHEV charging bus.

The results show that additional generation facilities will be helpful for alleviating reliability degradation caused by PHEV charging.

6 SUMMARY AND CONCLUSIONS

Environmental concerns in recent years has triggered rapid development in electric vehicles that provide a means of transportation that utilizes electric energy instead of petroleum fuel. The application of electric vehicles provides opportunity for utilization of renewable energy and offsets harmful emissions from traditional vehicles.

PHEV can either utilize electric energy stored in battery packs to drive the vehicle, or use gasoline. The fuel-switching capability of PHEV provides an option to utilize gasoline and electric energy in a more efficient way and makes it possible to customize energy-consuming mode depending on customer's preference. Therefore, PHEV has received increasing attention in recent years around the world. Along with the fast development of battery technology and control methodology, PHEV is expected to have less emissions and petroleum fuel dependency in the near future. The charging behavior of PHEV tends to be more flexible in charging locations and duration. Therefore, PHEV is chosen to be the representative of electric vehicles in this research work to evaluate the impacts of their charging behavior on power system reliability.

PHEV as a new type system load with specific characteristics can change the load profile of existing power systems and potentially impact system planning and operating. The fast development of PHEV and their immense potential for future use dictates the need to consider their possible impacts on power system reliability. It becomes increasingly important to develop suitable reliability models to incorporate and analyze the important characteristics of PHEV that would influence the overall system performance. Behavioral parameters of PHEV-30 are utilized in the PHEV modeling procedure in this thesis. A MCS method is utilized to develop the overall PHEV fleet model. The developed fleet model incorporates multiple charging scenarios and consider different PHEV penetration levels. The developed PHEV model is utilized in reliability analysis of the IEEE-RTS at both the HL-I and HL-II domain. The proposed PHEV model in this thesis has high flexibility for further modification and can be utilized for PHEV with different behavior parameters and battery sizes. The

technique presented can also be used to model other types of electric vehicles along with their development in the near future.

Chapter 1 presents an introduction of this thesis and provides some relevant basic reliability concepts of power system reliability. Electric vehicle and wind energy that is widely incorporated in modern power system are introduced. Research problems are stated and an outline of this thesis is presented.

Chapter 2 describes basic concepts of reliability evaluation in power systems. The IEEE-RTS is introduced as the test system for reliability analysis in this thesis. Analytical reliability evaluation method is explained by introducing generation model and load model. Development of a multi-state wind model is presented as an example of generation model. Frequently used power system reliability indices at the HL-I and HL-II levels are introduced. SIPSREL and MECORE are two software tools for calculating reliability indices, and they are used in the HL-I and HL-II analysis respectively in this thesis.

Chapter 3 proposes an analytical PHEV model for reliability evaluation. Parameters of PHEV-30 obtained from PHEV manufacture are provided and they are utilized as basic behavioral parameters in PHEV modeling. Unique characteristics of PHEV compared to conventional power system load are analyzed and included into the model development procedure. The “fast charging” and “normal charging” modes, and “home charging” and “public/home charging” scenarios are considered in the model development process. Different charging modes and charging scenarios of PHEV have different influence on system reliability. A MCS method was applied to combine individual PHEV models and build the overall model for a PHEV fleet. The modification of system load model is presented by aggregating fleet model with the original load model considering PHEV penetration levels and charging scenarios. The development of appropriate annual load models that incorporate PHEV are discussed and they are used in the HL-I and HL-II reliability studies.

Chapter 4 presents HL-I or generating system reliability analysis considering PHEV charging behavior. Specific PHEV load models under different charging scenarios are combined

analytically with the system load and generation models to obtain system reliability indices. PHEV penetration level is used to present the number of PHEV that are connected to the power system.

Bulk system reliability analysis or HL-II evaluation is carried out using PHEV fleet model in Chapter 5. Six buses are chosen as PHEV charging locations and the results obtained from the MECORE software show that the system reliability is greatly influenced by transmission line connection and generation capacity at the power system network bus where the PHEV is located. PHEV penetration level from 1% to 10% and three charging scenarios are considered in the reliability evaluation.

The results from the studies described in this thesis show that the system reliability degrades sharply to unacceptable levels with increase in PHEV penetration from 5% to 50% and system reliability is highly dependent on the start time of the normal home charging scenario. It is proposed to implement a policy to encourage PHEV users to postpone vehicle charging until midnight for best reliability results. The methodology introduced in this thesis can be widely used for PHEV application and different conclusions may be obtained depending on PHEV behavioral parameters. By comparison of bulk system reliability indices of the different case studies, it can be concluded that system reliability is influenced by bus connection structure, generation capacity and original load level. Generating buses connected to multiple transmission lines with large transfer capacity are less sensitive to PHEV load increases, and potentially can carry more PHEV load without causing severe reliability problem. The results from HL-II studies considering wind energy and PHEV show that additional generation facilities will be helpful for alleviating reliability degradation caused by PHEV charging.

This research provides methodologies and case studies relevant to real world scenarios that may be encountered in the near future, and presents results of reliability evaluation of a power system including PHEV fleet. The developed PHEV load model can be easily modified for other PHEV models to include various charging and driving characteristics. The results shown in generating system and bulk system analysis provide useful information on the reliability

impacts of PHEV application in electric power systems. System reliability can be improved by determining a suitable percentage of PHEV to have access to public charging. It is recommended to limit PHEV public charging percentage to 40% for PHEV-30. System reliability in bulk power systems is determined by multiple factors which need to be analyzed when determining the best charging location and scenario for PHEV extensive application. Wind energy is helpful to improve system reliability and reduce negative effects caused by PHEV charging.

The methodologies of PHEV modeling and evaluation methods for their impacts on power system reliability developed in this research work can be applied to conduct a wide range of reliability analysis of power systems including PHEV. The concepts presented and the examples illustrated in this thesis could help system planners to decide on appropriate application PHEV in existing power systems. Conclusions reached in this thesis will be useful to policy makers and PHEV manufacturers as well. The combination of renewable energy and electric vehicles covered in this thesis is an important and promising trend in power systems of near future. The results presented will make valuable contribution and solid foundation for future research on reliability analysis of future power systems that are expected to support an increasing penetration of PHEV.

7 REFERENCES

[1] R. Billinton and R. Allan, Reliability Evaluation of Power Systems, 2nd Edition, Plenum Press, New York, 1996.

[2] R. Billinton and R. Allan, "Power System Reliability in Perspective", *IEE J. Electronics Powe*r, 30, 1984, pp. 231-236.

[3] R. Billinton, Y. Gao, and R. Karki, "Composite System Adequacy Assessment Incorporating Large-Scale Wind Energy Conversion Systems Considering Wind Speed Correlation", *IEEE Transactions on Power Systems*, Vol. 24, No. 3, 2009, pp. 1375-1382.

[4] P. Denholm, W. Short, "An Evaluation of Utility System Impacts and Benefits of Optimally Dispatched Plug-in Hybrid Electric Vehicles", *National Renewable Energy Laboratory (NREL),* 2006. [Online]. Available: *s.*

[5] "Utility Wind Integration State of the Art" prepared by Utility Wind Integration Group in cooperation with American Public Power Association (APPA), Edison Electric Institute (EEI) and National Rural Electric Cooperative Association (NRECA), May 2006. [Online]. Available: *http://www.uwig.org.*

[6] J. Taylor, A. Maitra, M. Alexander, D. Brooks, M. Duvall, "Evaluation of the Impact of Plug-in Electric Vehicle Loading on Distribution System Operations", *IEEE Power and Energy Society General Meeting*, 2009, pp. 1-6.

[7] International Energy Agency, "Electric and Plug-in Hybrid Vehicle Road Map", 2010. [Online]. Available: *https://www.iea.org.*

[8] A. Lojowska, D. Kurowicka, G. Papaefthymiou, L. Sluis, "From transportation Patterns to Power Demand: Stochastic Modeling of Uncontrolled Domestic Charging of Electric Vehicles", *IEEE Power and Energy Society General Meeting*, 2011.

[9] A. Pesaran, T. Markel, "Battery Requirements and Cost-Benefit Analysis for Plug-In Hybrid Vehicles", National Renewable Energy Laboratory, 2007. [Online]. Available: *http://www.nrel.gov.*

[10] A. Millner, "Modeling Lithium Ion Battery Degradation in Electric Vehicles", *IEEE Conference on Innovative Technologies for an Efficient and Reliable Electricity Supply (CITRES)*, 2010, pp. 349-356.

[11] R. Karki, "Reliability and Cost Evaluation of Small Isolated Power Systems Containing Photovoltaic and Wind Energy", Thesis submitted for the Degree of *Doctor of Philosophy*, *University of Saskatchewan*, 2000.

[12] R. Karki, D. Dhungana, R. Billinton, "An Appropriate Wind Model for Wind Integrated Power Systems Reliability Evaluation Considering Wind Speed Correlations", *Applied Sciences*, Vol. 3, Issue 1, 2013, pp. 107-120.

[13] Global Wind Energy Council (GWEC), "Global Wind Power Cumulative Capacity", Global Wind Statistics 2015. [Online]. Available: *http://www.gwec.net.*

[14] D. Dhungana, "Incorporating Correlation in the Adequacy Evaluation of Wind Integrated Power Systems", Thesis submitted for the Degree of Master of Science, *University of Saskatchewan*, 2013.

[15] Y. Gao, "Adequacy Assessment of Electric Power Systems Incorporating Wind and Solar Energy", Thesis submitted for the Degree of Master of Science, *University of Saskatchewan*, 2006.

[16] Reliability Test System Task Force of the IEEE Subcommittee on the Application of Probability Methods, "IEEE Reliability Test System", *IEEE Transactions*, PAS-98 No. 6, Nov/Dec 1979, pp. 2047-54.

[17] R. Billinton, D. Huang, "Incorporating Wind Power in Generating Capacity Reliability Evaluation using Different Models", *IEEE Transactions on Power Systems*, Vol. 26, No. 4, 2011, pp. 2509-2417.

[18] P. Giorsetto and K. F. Utsurogi, "Development of A New Procedure for Reliability Modeling of Wind Turbine Generators," *IEEE Transactions on Power Apparatus and Systems*, Vol. PAS-102, No. 1, 1983, pp. 134-143.

[19] R. Billinton, C. Wee, "Derated State Modeling of Generating Units," Report prepared for Saskatchewan Power Corporation, 1985.

[20] Y. Li, "Bulk System Reliability Evaluation in A Deregulated Power Industry", Thesis submitted for the Degree of Master of Science, *University of Saskatchewan*, 2003.

[21] S. Mishra, "Wind Power Capacity Credit Evaluation Using Analytical Method", Thesis submitted for the Degree of Master of Science, *University of Saskatchewan*, 2010.

[22] W. Li, "Installation Guide and User's Manual for the MECORE Program", 1998.

[23] S. W. Hadley, A. Tsvetkova, "Potential Impacts of Plug-in Hybrid Electric Vehicles on Regional Power Generation", *Oak Ridge National Laboratory, U.S. Department of Energy*, 2008.

[24] R. C. Green II, L. Wang, M. Alam, "The Impacts of Plug-in Hybrid Electric Vehicles on Distribution Networks: A Review and Outlook", *Renewable and Sustainable Energy Reviews*, Vol. 15, Issue 1, 2011, pp. 544-553, 2011.

[25] K. Yunus, H. Zelaya D. Parra, M. Reza, "Distribution Grid Impacts of Plug-in Electric Vehicles Charging at Fast Charging Stations Using Stochastic Charging Model", *Power Electronics and Applications*. Proceedings of the 2011-14th European Conference.

[26] K. Clement-Nyns, E. Haesen, J. Driesen, "The Impact of Charging Plug-in Hybrid Electric Vehicles on a Residential Distribution Grid", *IEEE Transaction on Power Systems*, Vol. 25, Issue 1, 2010, pp. 371–380.

[27] O. Hafez, K. Bhattacharya, "Optimal PHEV Charging in Coordination with Distributed Generation Operation in Distribution Systems", *IEEE Power and Energy Society General Meeting*, 2012.

[28] V. Marano, G. Rizzoni, "Energy and Economic Evaluation of PHEVs and Their Interaction with Renewable Energy Sources and the Power Grid", *Proceedings of IEEE International Conference on Vehicular Electronics and Safety*, 2008.

[29] Ye Li, "Scenario-Based Analysis on the Impacts of Plug-in Hybrid Electric Vehicles' (PHEV) Penetration into the Transportation Sector", *IEEE International Symposium on Technology and Society (*ISTAS*),* 2007.

[30] A. Elgowainy, A. Burnham, M. Wang, J. Molburg, A. Rousseau, "Well-to-Wheels Energy Use and Greenhouse Gas Emissions Analysis of Plug-in Hybrid Electric Vehicles", *Energy System Division, Argonne National Laboratory*, 2009. [Online]. Available: *http://www.afdc.energy.gov.*

[31] M. A. Kromer, J. B. Heywood, "Electric Powertrains: Opportunities and Challenges in the U.S. Light-Duty Vehicle Fleet", *Sloan Automotive Laboratory. Laboratory for Energy and the Environment Massachusetts Institute of Technology*, 2007.

[32] J. Axsen, A. Burke, K. Kurani, "Batteries for Plug-in Hybrid Electric Vehicles (PHEVs): Goals and the State of Technology Circa 2008", *Institute of Transportation Studies, University of California*, 2008.

[33] A. Pesaran, "Battery Requirements for Plug-in Hybrid Electric Vehicles- Analysis and Rationale", *National Renewable Energy Laboratory*, 2007.

[34] Ford C-MAX 2016 Hybrid electric vehicle [Online]. Available: *http://www.ford.com/cars/cmax/*

[35] Y. Xiong, D. Jayaweera, "Reliability Based Strategic Integration of Plug-in Hybrid Electric Vehicles in Power Systems", *IEEE Probabilistic Methods Applied to Power Systems (PMAPS)*, 2014.

[36] NHTS Data Center, 2009 NHTS- Version 2.1. [Online]. Available: *http://nhts.ornl.gov/download.shtml#2009*

[37] L. Tian, S. Shi, Z. Jia, "A Statistical Model for Charging Power Demand of Electric Vehicles", *Power System Technology*, Vol. 34, No. 11, 2010, pp. 126-130.

[38] M. A. Kromer, J. B. Heywood, "Electric Powertrains: Opportunities and Challenges in the U.S. Light-Duty Vehicle Fleet", *Sloan Automotive Laboratory. Laboratory for Energy and the Environment Massachusetts Institute of Technology*, 2007.

[39] U.S. Department of Transportation, Federal Highway Administration, "Summary of Travel Trends-2009 National Household Travel Survey", [Online]. Available: *http://nhts.ornl.gov*

[40] S. Huang, D. Infield, A. Zaher, "Potential of Plug-In Electric Vehicles for Supporting Regional Power Distribution System Operation with High Penetration of Wind Generation", IEEE International Conference on Sustainable Power Generation and Supply, 2012, pp. 1-6.

[41] A. Schuelke, K. Erickson, "The Potential for Compensating Wind Fluctuations with Residential Load Shifting of Electric Vehicles", IEEE International Conference on Smart Grid Communications, 2011, pp. 327-332.